UNITED STATES DEPARTMENT OF THE INTERIOR

GEOLOGICAL SURVEY

Heat flow at Zerqa Ma'in and Zara
and a geothermal reconnaissance of Jordan

by

S. Peter Galanis, Jr.[1], J. H. Sass[2]. R. J. Munroe[1], and M. Abu-Ajamieh[3]

Open File Report 86-631

[1]U.S. Geological Survey, Menlo Park, CA 94025
[2]U.S. Geological Survey, Flagstaff, AZ 86001
[3]Natural Resources Authority, Jordan

1986

Table of Contents

Abstract

Estimated or calculated heat flow values at 18 sites in Jordan are presented in this study. These are the first heat flow measurements on the east flank of the Dead Sea Rift. The data are divided into three groups:

1) High heat flow values adjacent to the Dead Sea Rift, near the Zerqa Ma'in and Zara geothermal areas, range from 91 to ~472 mW/m².

2) High heat flow values within and adjacent to Azraq Basin range from 70 to 135 mW/m².

3) Normal heat flow values in other parts of Jordan range from 42 to 65 mW/m².

The mechanism for heat transfer in the first two groups is attributed to rapid ascent of hot water along deep faults. Near the surface, the water's heat is dissipated either by mixing with cooler waters from shallow aquifers, by direct discharge at thermal springs, or by conduction into surrounding country rock. The source of the waters are believed to be deeply buried, confined beds of Lower Paleozoic sandstones. Further study is needed to determine if the Zerqa Ma'in - Zara and the Azraq Basin anomalies are separate or part of one larger anomaly.

The mechanism of heat transfer in the third group is primarily conductive. These conductive values probably represent the regional "background" heat flow. The results of this study are similar to findings on the west flank of the Dead Sea Rift.

INTRODUCTION

This report presents estimates of heat flow based on data collected in Jordan during a six-week period in mid-1983. These are the first estimates of heat flow on the east flank of the Dead Sea Rift. The study began as one part of a joint effort between the U.S. Geological Survey (USGS) and the Natural Resource Authority or NRA (Jordanian counterpart of the USGS) to assess the geothermal potential of the Zerqa Ma'in and Zara areas, and was later expanded to a reconnaissance heat flow study of Jordan.

The results are presented in two parts:

1. Reconnaissance Heat Flow of Jordan (data from holes drilled for purposes other than heat flow)

2. Heat Flow of Zerqa Ma'in and Zara Geothermal Areas (data from holes drilled specifically for heat flow).

Preceding the two parts are a brief explanatory note on heat flow terms and concepts, and a short description of Jordan's geology. Raw data pertinent to the report are tabulated as appendices.

Scales vary among the temperature-depth profiles illustrated in the appendices and in the body of the report. However, the aspect ratio is equal for all of the profiles. The constant aspect ratio makes it possible to visually compare the thermal gradients of all the profiles.

HEAT FLOW--TERMS AND CONCEPTS

This section is designed to familiarize those less experienced with heat flow to its general principles and terms. For a more rigorous discussion, the reader is referred to Lachenbruch and Sass (1977). The terms, definitions, and applicable units are as follows (equivalent traditional c.g.s. units are in brackets):

q upward heat flux, mW/m^2
[1 HFU $(10^{-6}\ cal/cm^2\ sec)$ = 41.87 mW/m^2];

K thermal conductivity, W/m K
[1 TCU (mcal/cm sec °C) = 0.4187 W/m K];

K_f formation thermal conductivity;

K_s solid grain thermal conductivity;

Γ thermal gradient, °C/km;

Φ fractional porosity;

ρ density, g/cm^3

In the simplest case, where heat is distributed solely by conduction, heat flow is the product of two measured quantities: the rock's thermal conductivity (K) and the measured geothermal gradient (Γ),

$$q = (K)(\Gamma)$$

From this relationship, and assuming that q is a constant at any one place on the earth's surface, any change downhole in thermal conductivity will bring about an inverse change in the thermal gradient. This is an important point to remember when comparing thermal gradients from different holes; a hole with a higher thermal gradient may not necessarily have a higher heat flow, it may simply penetrate material with a lower thermal conductivity. The relationship of Γ and K is illustrated in Figure 1, where a constant quantity of heat is conducted toward the surface through media with different thermal conductivities.

Thermal Gradient.

To determine heat flow, temperature is ideally measured in near-vertical boreholes. The data are collected as temperature-depth pairs then processed to determine the thermal gradient. Our measurements were made using a four-conductor electrical cable, a thermistor probe (calibrated to ±0.01°C), and a sheave assembly (measures depth in feet with a precision of 0.1'). The equipment is a modified version of the "portable logging mode" described by Sass and others (1971b), the biggest difference being the replacement of the wheatstone bridge by a digital ohmmeter.
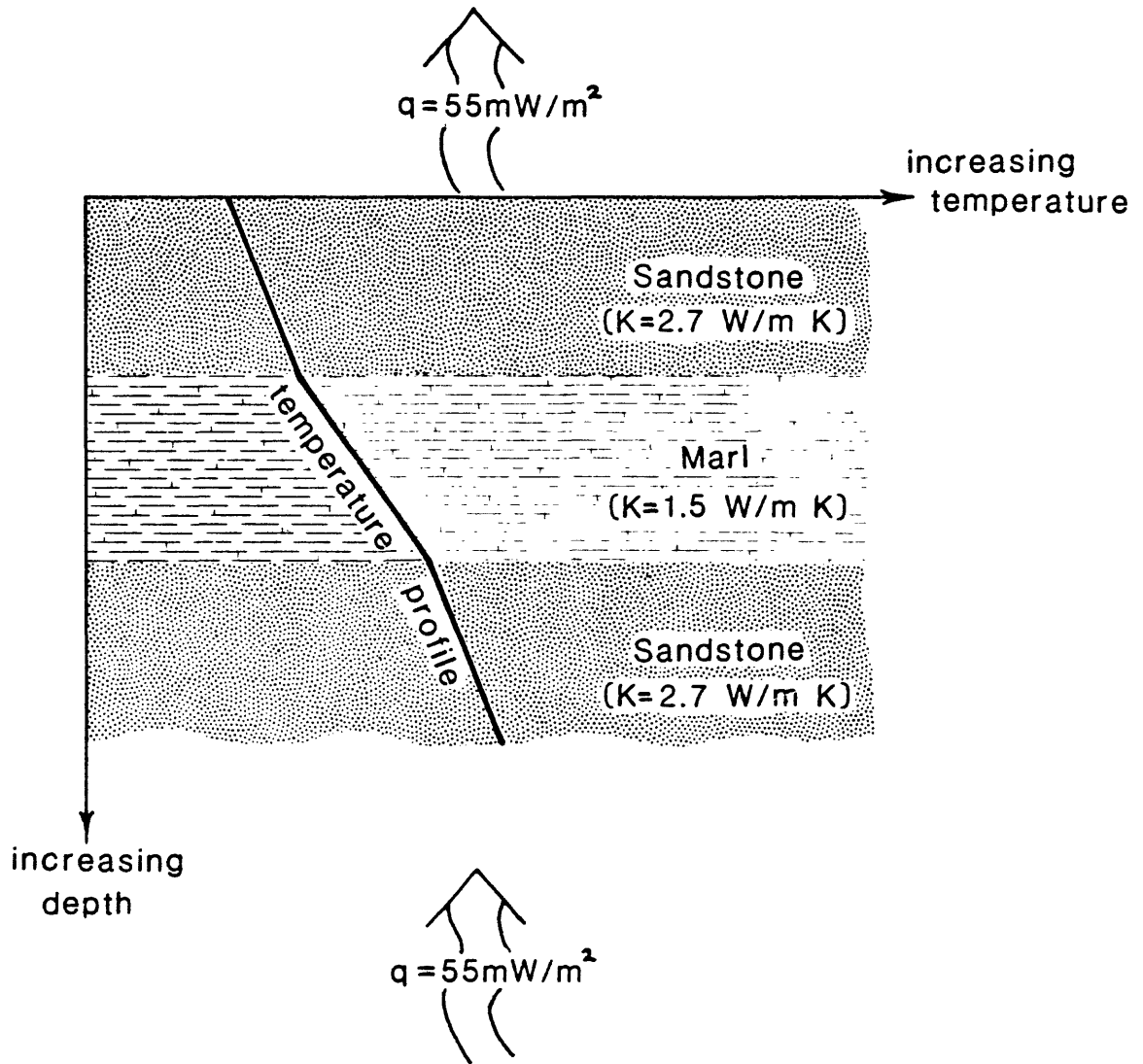
Figure 1. The inverse relationship of the temperature gradient (Γ) to thermal conductivity. When upward-flow of heat is constant, the temperature profile has a higher gradient in layers with lower thermal conductivity.

Thermal gradients may be controlled by several factors within the upper tens of meters of the earth's crust. Some of these factors are: topographic relief, local and regional hydrologic conditions, climatic and seasonal temperature changes and structural uplift and erosion. Of these, topography is the easiest to adjust for because it is readily apparent. The other factors, although their influence may be strong (especially hydrology and structure), are often complex, poorly understood, and change at rates that are unknown.

Isotherms near the surface tend to parallel topographic relief. As depth increases, the influence of surface topography decreases and the isotherms flatten. One effect is that the distance between isotherms is extended beneath hills and terraces and compressed beneath valleys and at the base of slopes. Therefore, an adjustment for relief will increase thermal gradients measured on hills and terraces and decrease those measured in valleys; the magnitude of the adjustment decreases with depth.

Thermal Conductivity.

Thermal conductivity is a quantitative measure of a substance's ability to transmit heat. In this study, owing to differences in the types of samples available, thermal conductivity was measured in two ways. Using the first and preferable technique, competent rock samples were machined into disks several centimeters in diameter and ∿1 centimeter thick, then placed in a divided-bar apparatus between two disks of known conductivity. One end of the apparatus was heated while the other was cooled. After equilibrium was reached, the thermal gradient across the stack was measured and conductivity calculated. This method is fully described in Birch (1950). An advantage to this technique is that both density and porosity can be determined reliably. The results of measurements on outcrop samples collected near Wadi Zerqa Ma'in are summarized in Table 1.

The second technique we used to measure thermal conductivity is a variant of what was just described. The difference is that instead of a solid disk-shaped sample, crushed sample is poured into a short cylinder and then measured in the divided-bar apparatus (Sass and others, 1971a). Results of measurements using this technique are summarized in Appendix IV. A disadvantage to this technique is that the sample's natural porosity cannot be determined.

Uncertainty of porosity results in uncertainty in the calculated formation conductivity (K_f). The formation conductivity can be represented as the geometric mean of the solid grain conductivity (K_s) and the conductivity of water (K_w) weighted according to the fractional porosity (ϕ):

$$K_f = K_s^{(1-\phi)} K_w^{\phi}$$

with K_w = 0.58 $Wm^{-1} K^{-1}$. When a formation is unsaturated, the conductivity of air (K_a) substitutes for (K_w) with K_a = 0.025 $Wm^{-1} K^{-1}$. In this case, the geometric mean is not an accurate estimate of formation conductivity because of the large difference between the K_a and K_s; K_s is usually on the order of 2 to 4 $Wm^{-1} K$ (see discussions by Beck, 1976; Robertson and Peck, 1974; Woodside and Messmer, 1961a, b). Another problem arises from the fact that porous rocks, even above the water table, contain some water and

TABLE 1. Thermal conductivity, density, and porosity
of representative outcrop samples collected near Wadi Zerqa Ma'in, Jordan

Rock unit	Local lithologic unit	N[†]	K* mcal cm⁻¹ sec⁻¹ °C⁻¹	K* W m⁻¹ K⁻¹	ρ** g cm⁻³	φ** %
Phosphorite member and Silicified limestone member (Amman Fm.)	B1-2	6	3.67 (.07) [.17]	1.54 (.03) [.07]	2.26 (.04) [.10]	18.88 (1.26) [3.08]
Massive limestone member (Wadi Sir Fm.)	A7	6	6.06 (.44) [1.07]	2.54 (.18) [.45]	2.50 (.06) [.15]	11.45 (3.72) [9.11]
Echinoid limestone member (Schueib and Hummar Fms.)	A4-6	7	5.21 (.32) [.86]	2.18 (.14) [.36]	2.51 (.03) [.08]	11.64 (2.13) [5.65]
Nodular limestone member (Fuheis Fm.)	A3	3	4.44 (.18) [.31]	1.86 (.07) [.13]	2.43 (.04) [.07]	17.90 (2.07) [3.59]
Kurnub Sandstone	K	5	6.42 (.93) [2.09]	2.68 (.39) [.88]	2.37 (.12) [.27]	18.12 (4.09) [9.14]

[†]Number of samples tested.
*Harmonic mean conductivity of water-saturated samples measured at ~22°C.
**Arithmetic mean
Standard error in parentheses; standard deviation in brackets.

can be nearly saturated. The geometric mean tends to overestimate the value of K_f. We thus used it in a consideration of thermal conductivity from the unsaturated portion of two wells (JD04 and JD26) as an imprecise approximation of formation conductivity, that nonetheless errs in a direction that accounts for partial saturation.

GEOLOGY OF JORDAN

Jordan is on the Nubo-Arabian Shield in the northwestern part of the Arabian Peninsula. For the purposes of this paper, the country can be divided into two physiographic provinces (generalized from Bender, 1975): The Dead Sea Rift and the Highlands and Plateaus. The Dead Sea Rift is the northward continuation of the Gulf of Aqaba depression. From south to north the rift includes, Wadi Araba, the Dead Sea, and the Jordan Valley; the floor of the rift rises from sea level at Aqaba to 250 m in Wadi Araba, falls to -800 m in the northern half of the Dead Sea, and then rises to -212 m at Lake Tiberias (Sea of Galilee) in the northern Jordan Valley (Figure 2).

The Highlands and Plateaus Province is east of the rift and includes most of the land area of Jordan. The region of highlands borders the rift and has peaks that rise to about 1700 m in the south (west of Ma'an) and 1200 m in the north (near Ajlun). In general, the highlands slope steeply toward the rift on the west and very gently toward the plateaus on the east. The land surface of most of the eastern plateau area is between 500 and 700 m above sea level. Included in the plateau area are two intracratonic basins, Al Jafr Basin in the south (near Ma'an) and Azraq Basin in the northeast (see Figure 2).

The main structural features of Jordan are summarized in Figure 2. The dominant feature is the north-south trending Dead Sea Rift, an active part of the World Rift System. Left-lateral strike-slip displacement across this transform boundary is estimated at slightly more than 100 km (Freund and others, 1970; Hatcher and others, 1981). Transform movement began in mid-Miocene time (Garfunkel, 1981) along a zone of structural weakness that had existed since the end of the Precambrian (Bender, 1975).

Several east-west faults are traceable from the border faults of the rift. Among these are the Aqaba Fault, traceable for ~40 km; the Feinan Fault, traceable for ~30 km; the Wadi el Hasa Fault, traceable for ~60 km (Bender, 1974); and the Wadi Zerqa Ma'in Fault, traceable for ~50 km (Abu-Ajamieh, 1980). Offset along the faults generally decreases eastward. These faults are associated with or merge into monoclinal flexures.

The east-west faults and several northwest-striking fracture zones have acted locally as conduits for Neogene-Pleistocene basalt dikes and flows. The volcanism is especially pronounced north of, and along the eastern side of the Azraq Basin. Here, extensive fissure-flows have formed 45,000 km^2 of plateau basalts that extend northward into Syria (Bender, 1975).

Precambrian granitic and migmatitic basement rocks crop out in southwestern Jordan. From there the basement deepens northward and northeastward along an undulatory surface. According to Bender (1975), the basement east of the rift is deepest (~5000 m below sea level) in the complexly faulted (Hatcher and others, 1981) Azraq Basin.

Jordan's stratigraphic section is summarized in Table 2 (slightly modified from Bender, 1975). Shallow marine sedimentary rocks blanket the basement.

Figure 2. Summary Map of Major Geological Features of Jordan.
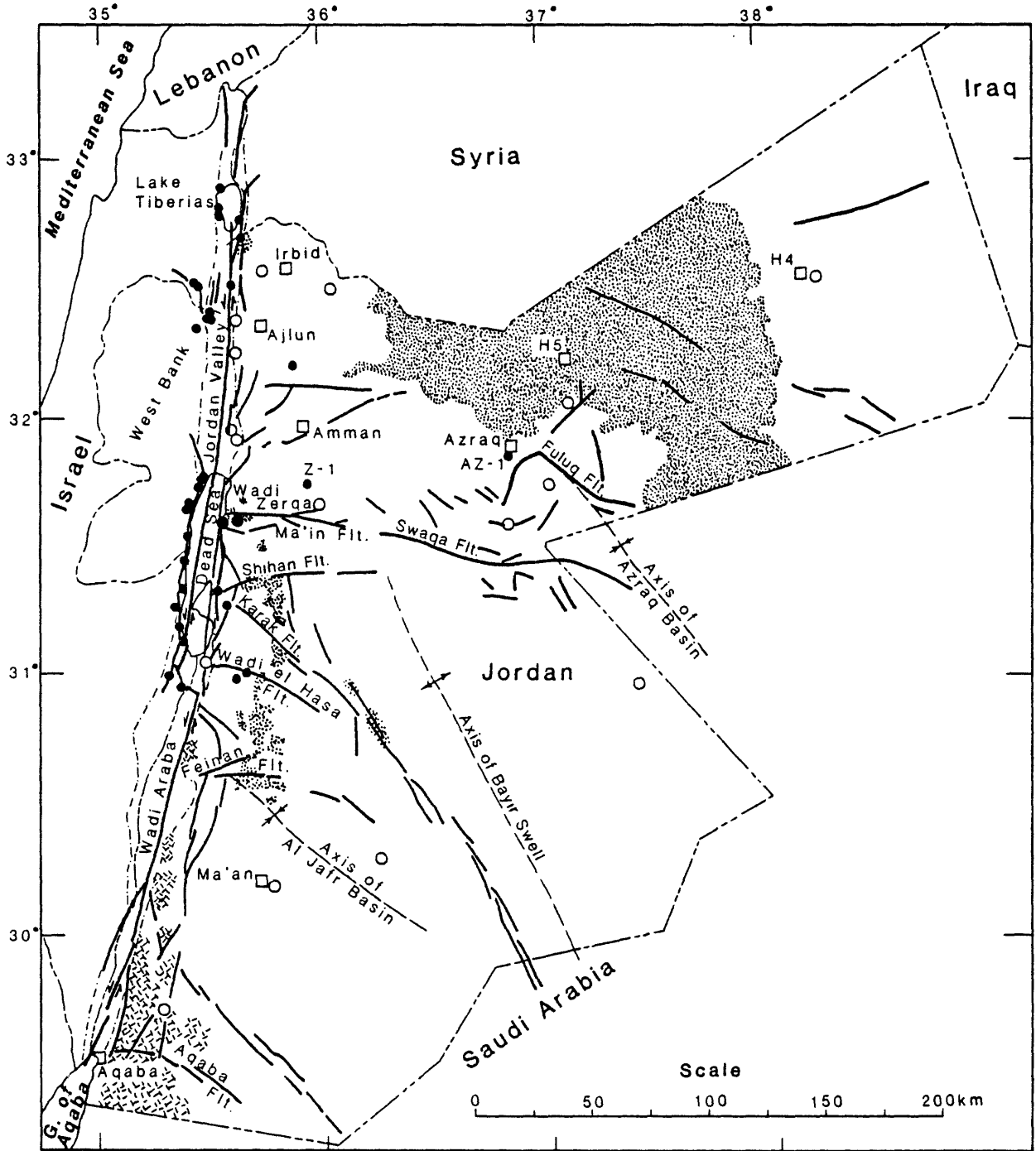
EXPLANATION

O   Geothermal Gradient/Heat Flow Site   Neogene-Pleistocene Basalt

●   Thermal Spring or Well   Granitic&Migmatitic Basement

╱   Fault   □   City or Village

╱·╱   Boundary of Dead Sea Rift

(Information compiled from: Abu-Ajamieh, 1980; Bender, 1974&1975; Eckstein, 1979;
Hatcher and others, 1981; Levitte and Eckstein, 1979; Quennell, 1982; Waring, 1965)

- 11 -

TABLE 2. Correlation Chart of Lithostratigraphic Units in Jordan

Period	Epoch/Stage	NORTHERN EAST JORDAN	Correlative Local Litologic Units	SOUTH JORDAN	SOUTHERN EAST JORDAN
QUATERNARY	Holocene	Fluviatile deposits, loess-like sediments, mantle rocks, aeolian sand, pelitic sediments in mud flats, and talus fans			Fluviatile gravels (<10 m)
	Upper Pleistocene	Mantle rocks; Basalt; Fluviatile gravels (<10m); Basalt		Fluviatile gravels (up to 40m)	Lacustrine limestone and sandy limestone (<10m)
	Middle Pleistocene	Lacustrine limestone and marl of Al Azraq (<10 m); Brackish-lacustrine and fluviolacustrine sediments of Dahukiya (<50m)			
	Lower Pleistocene				
TERTIARY	Pliocene	Sandstone, calcareous sandstone and sandy marl of Al Azraq (up to 40m); Basalt			
	Miocene	Marly limestone and glauconitic sandstone of Dahukiya (<30m); Basalt			
	Oligocene				White marly limestone member (<40m)
	Eocene	Chalky limestone and bituminous marly limestone of the Yarmuk area (<360); Barite marl and bituminous marl of Dahikiya (<25m); Limestone and chert of Thulenthuwat (<30m); Carcharodon marl (<50m); Nummulitic limestone (<20m)	B4-5	Chert limestone member (up to 70m); Nummulitic limestone member (up to 40m)	Chert limestone <=> Nummulitic limestone member (<100m)
	Paleocene	Chert-limestone member (up to 180m)	B3	Chalk-marl member (<450m)	Chalk-marl member (<20m)
	Danian	Chalk-marl member (<270m)		Phosphorite member (up to 80m)	Phosphorite member (<20m)
UPPER CRETACEOUS	Maestrichtian	Phosphorite member (up to 90m)	B1-2	Silicified limestone member (up to 100m)	Silicified limestone member (<20m)
	Campanian	Silicified limestone member (<135m)			
	Santonian	Massive limestone member (<60m)	A7	Massive limestone member <=> Sandy limestone member (up to 110m)	Sandy limestone and echinoid limestone member (up to 200m)
	Turonian	Echinoid limestone member (<210 m)	A4-6	Echinoid limestone member (up to 100m)	
	Cenomanian	Nodular limestone member (<300m)	A1-3	Nodular limestone member (<70m)	Nodular limestone member (up to 50m); Varicolored sandstone and massive white sandstone (up to 250m)
LOWER CRETACEOUS	Albian	Sandy limestone of the Albian Aptian transgression (<40m); Varicolored Sandstone (Kurnub Sandstone?) (up to 170m)	K	Varicolored sandstone (<150m); Massive white sandstone (<180m)	
	Aptian	Massive white sandstone (up to 180m)			Brown coarse grained sandstone (~90m)
	Neocomian				

Correlative Local Lithologic Units

EXPLANATION

Transgression regression
discordance, or hiatus

Major hiatus

Lateral change of facies

Thickness measured on surface
exposures or in drilled sec-
tions, may be greater in
basin

(~10 m)

Zarqa Group

Limestone, sandy marl
from the Zarqa River (up to ~200m)

Plant fossil-bearing sandstone from the
Zarqa River (up to 70m)

Thick-bedded limestone from the Zarqa River (up to 70m)

Gypsiferous sequence from the Zarqa River (~80m)
Wadi Hisban Sandstone (~100m) Muschelkalk (~70m)
and sandy marl (~40m)
Sandstone-marl sequence from Zarqa Main (~180 m)

Calcareous sandstone of SAFRA-1 (Westphalian,
Namurian, Visean, ?m)

Khreim Group

In the north
and the northeast
Silurian(?) and
Ordovician(?)

White, bedded sandstone ── Massive, brownish-weathered
(to 220m)   sandstone (up to 160m)

Massive, brownish-weathered sandstone (up to 100m)

Dolomite-limestone-shale unit (~130m)

Bedded arkosic sandstone (up to 160 m)

Basal conglomerate (~30m)

Slate-graywacke series and Saramuj
Conglomerate (~420m)

Magmatite

Graptolite sandstone (~80m)
Bedded, brownish-weathered sandstone
(~250m) - Umm Sahm Sandstone
Massive whitish-weathered sandstone
(~300m) Ram Sandstone

Subulurus sandstone
(~120m)

Tundartu
sandstone
(~250m)

Massive brownish-weathered sandstone

Dolomite-limestone── White fine-grained ═ (up to 350m)
slate unit (up to 50m) sandstone (up to 100m)   } Quweira
Bedded arkosic sandstone (up to 200m) ═ Bedded arkosic   Sandstone
Basal conglomerate (up to 50m)   sandstone (~50m)

Slate-graywacke series (~200m)
Saramuj Conglomerate (~200m)

Magmatite

Disi Group

Red-brown argillaceous sandstone

Nautiloidea sandstone (160-270 m)

(Tundartu sandstone
(500 m)

Subulurus sandstone
(200m)

Graptolite sandstone (~150m)

Bedded, brownish-weathered sandstone
(~250m)

Massive whitish-weathered sandstone (~240m)

Massive brownish-weathered
sandstone
(~350m)

Bedded arkosic sandstone (~50m)

Magmatite

JURASSIC	Portlandian to Oxfordian	
	Callovian	
	Bathonian	
	Bajocian	
	Liassic	
TRIASSIC	Rhaetian	
	Norian	
	Karnian	
	Ladinian	
	Anisian	
	Scythian	
PERMIAN TO DEVONIAN	Permian-Carboniferous Devonian	
SILURIAN	Ludlovian	
	Wenlockian	
	Llandoverian	
ORDOVICIAN	Ashgillian	
	Caradocian	
	Llandeilian	
	Llanvirnian	
	Lower Ordovician	
CAMBRIAN	Upper Cambrian	
	Middle Cambrian	
	Lower Cambrian	
PRE-CAMBRIAN	Upper "Proterozoic"	
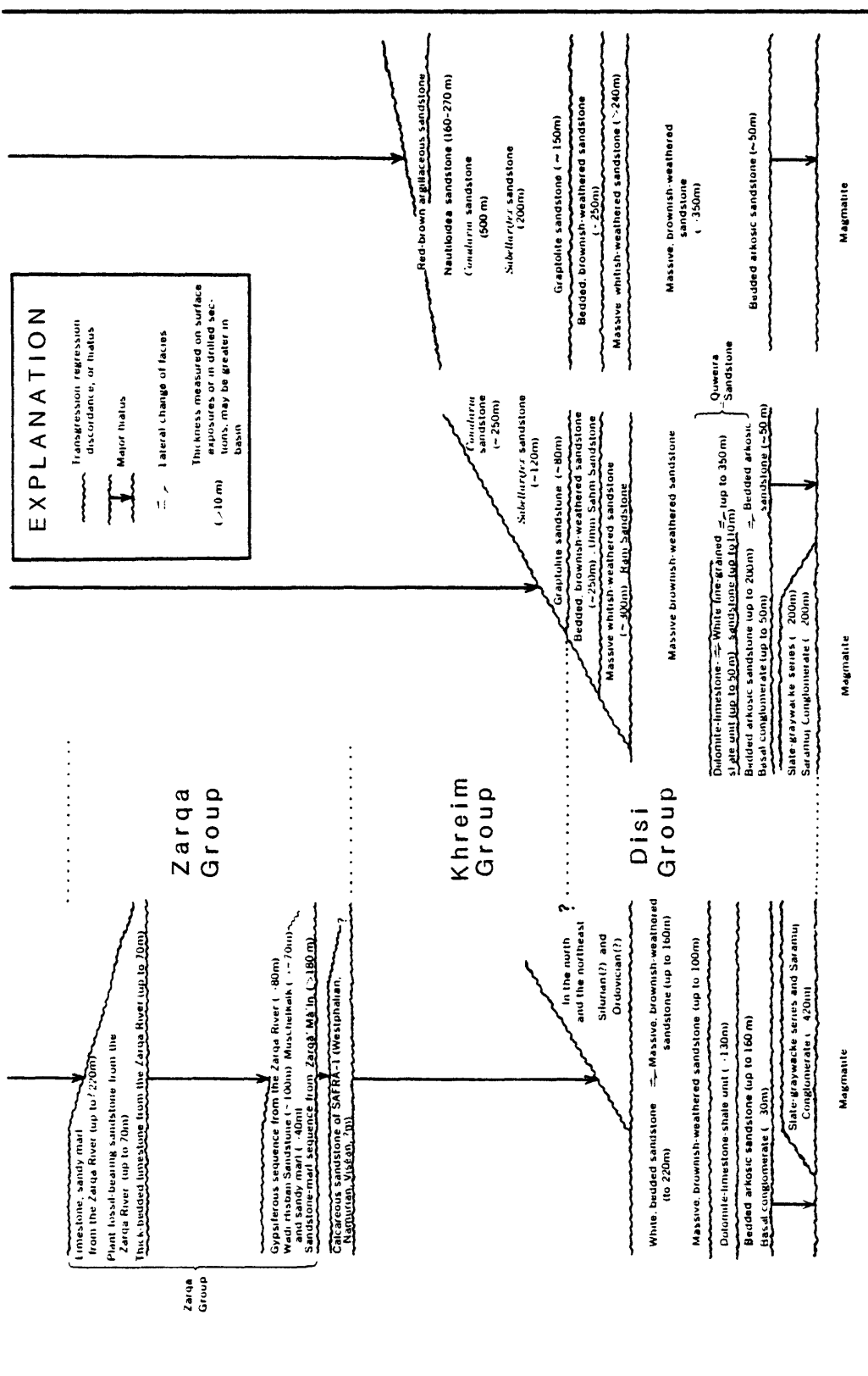
(Chart modified slightly from Bender, 1975)

- 13 -

The lowermost ∿2000 m of sedimentary rocks include sandstones of the Lower Paleozoic Disi and Khreim Groups (Lloyd, 1969), the Triassic and Jurassic Zarqa Group, and the Lower Cretaceous Kurnub Sandstone (Bender, 1975). Typically, these rocks are very porous and form complex partially interconnected regional aquifers. In most of Jordan, this aquifer complex is confined by overlying Upper Cretaceous marls and shales of lithologic units A1 through A6 (see Table 2).

Numerous thermal springs emerge along the margins of the rift, as is shown in Figure 2 (spring locations from: Waring, 1965; Abu-Ajamieh, 1980; Eckstein, 1979). The springs occur at low elevations where rift faults cut into rocks of the deep confined aquifer complex, and commonly, where east-west faults intersect the rift faults. Thermal waters are also encountered in a municipal water well near the east end of the Wadi Zerqa Ma'in Fault and in an artesian well near Azraq (Z-1 and AZ-1 respectively, Figure 2). The well near Azraq penetrates rocks of the confined aquifer (Kurnub Sandstone).

All of our temperature profiles were measured in rocks ranging in age from Early Cretaceous to Eocene. Therefore, the lithostratigraphic chart (Table 2) includes the common local names for lithologic units of this time interval (i.e., the names used in many of the drilling records). The rocks of this interval are nearly flat-lying and include sandstone, marl, limestone, and chert. As might be expected with sedimentation on a craton, many of the lithologic units are laterally continuous and recognizable over great distances; this fact has made it possible for us to, in some cases, estimate physical rock properties for our heat flow calculations.

RECONNAISSANCE HEAT FLOW OF JORDAN

Background.

While in Amman, one of us (Galanis) identified boreholes suitable for temperature-gradient measurements in other areas of Jordan. A list of boreholes was compiled, then combined with data from Zerqa Ma'in and Zara. The complete list is presented as Appendix I. Most borehole locations are shown (where space was available) on Figure 3.

An attempt was made to log many of the boreholes. However, time did not permit a visit to all of the sites, so this list could serve as a starting point for further study. Additional work could include logging the holes we were unable to visit. Also, holes where pumping prevented logging could be measured, provided pumping ceases and the hole is idle for a period long enough to reach thermal equilibrium.

A problem encountered with the majority of these boreholes is the absence of drill core and/or chip samples for conductivity measurements. The holes were drilled for purposes other than heat flow during the past ∿30 years and samples either were not saved or could not be located in the short period of this study.

We tried to mitigate the sample problem by using either of two methods. The first method was used for boreholes where our logged-depth approached the drilled-depth and where the temperature profile had a uniform gradient. Here, conductivity measurements were made on mixed chip samples collected from the drilling-waste piles at each of the boreholes. Since each site had a uniform temperature gradient, we assumed each hole penetrated material of fairly constant conductivity. We obtained conductivities for holes JD10, JD11, JD21, and JD26 using this method.

The second method was used for boreholes that lacked drilling-waste piles, or where our logged-depth was much less than the drilled-depth, or where the temperature profile was not linear. Here we compared lithologic logs of each borehole to our temperature logs, matching lithologic units to intervals of uniform temperature gradient. By correlating the lithologic units to like-units where we have conductivity measurements (see Table 1), we were able to estimate the formation conductivity at each site and then estimate heat flow.

Thermal Gradients and Estimated Heat Flows.

JD12: Located west of Irbid in northwest Jordan (Figure 3) and drilled by NRA in 1966 as stratigraphic test hole S-18. The top part of the temperature profile is slightly concave upward (see Figure 4 and Appendix Figure IIB-1); this may indicate slow downward water-flow. Although its thermal gradient is similar, the temperatures in this borehole are systematically cooler than those of the other temperature profiles shown in Figure 4. This reinforces the evidence for hydrologic transport of heat and makes the heat flow estimate suspect. The temperature gradient used in the

Figure 3. Map of Heat Flow and Geothermal Gradient Sites, Jordan.
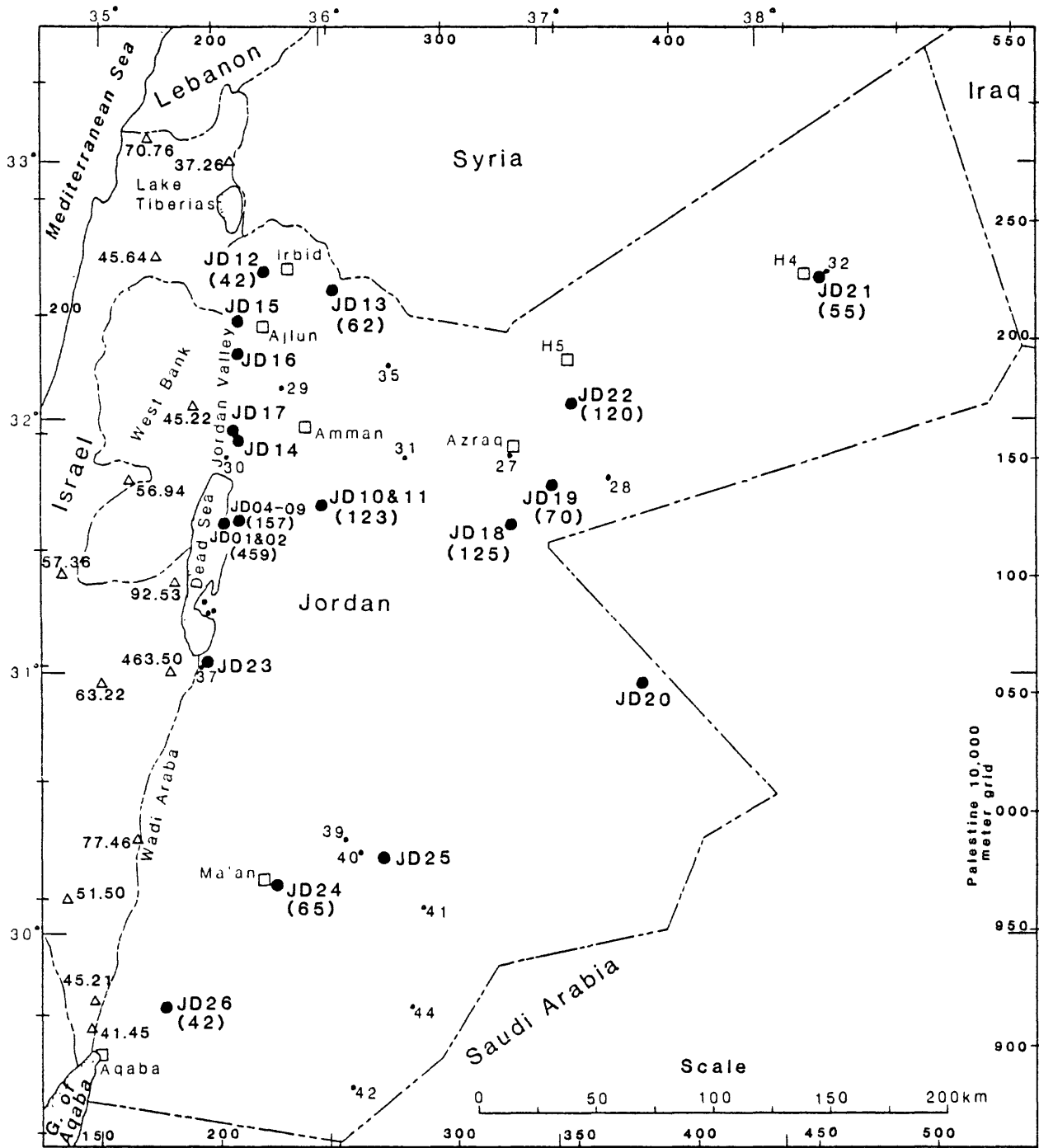
EXPLANATION

JD17 ●   Heat Flow/Geothermal Gradient Site (heat flow in parentheses, mW/m²)
(55)

36●   Borehole Listed in Appendix Table I (shown where space permits)

52.30△   Published Heat Flow, mW/m² (Eckstein & Simmons, 1978)

heat flow calculation was for the depth interval 314-384 m. According to an unpublished lithologic log prepared for NRA, rocks of this interval are limestones of the Turonian age Wadi Sir formation (locally known as lithologic unit A7). We had no samples from the borehole for conductivity, so we used the A7 measurement from Table 1 to arrive at our heat flow estimate of 42 mW/m² (Table 3).

JD13: This hole is east of Irbid in northwest Jordan (Figure 3). Drilled in the search for petroleum, it was completed by NRA in 1970 as hole S-90. We had no samples for conductivity measurements, so we used K values from Table 1 by correlating with the hole's lithologic log (see Figure 4 and Appendix Figure IIB-2). The depth interval 299-500 m is comprised of Turonian age, massive, well-bedded, dolomitic limestone (probably lithologic unit A7). Estimated heat flow in this interval is 62 mW/m². The interval 500-917 m is through Cenomanian age, gray shale, marl, and marly limestone (probably lithologic units A3 through A6). Estimated heat flow for this interval is also 62 mW/m² (Table 3).

JD14, 15, 16, and 17: These holes were drilled by the Jordan Valley Water Authority and brought to our attention by M. Teimeh (NRA). All of the holes are either on or close to the eastern escarpment of the Jordan Valley (Figure 3). For completeness, temperature profiles for each hole are included in Appendix II. However, all the temperature profiles are strongly influenced by hydrology and/or large local topographic relief, precluding any meaningful heat-flow estimates. Most of the measured thermal gradients are low, which may indicate that they are in an area of hydrologic recharge.

JD18: This hole is south of Azraq and is also known as Wadi Ghadaf #1 (WG-1). It was drilled in 1970 by INA (Industrija Nafte of Zagreb, Yugoslavia) as a petroleum wildcat well. The temperature profile is irregular, caused either by layered sediments of contrasting conductivity or by water-flow between different aquifers. The temperature gradient is from the depth interval 64 to 232 m. Rocks in this interval include marl, marly limestone, and cherty shale (probably correlative with lithologic units B4 and B5). We used the conductivity from measurements on B4-5 samples from hole JD21, for calculations at this site. Heat flow estimated here is 125 mW/m².

JD19: This is a petroleum wildcat well drilled by INA in 1971. It is located southeast of Azraq and is also known as Wadi Rajil #1 (WR-1). The hole penetrates middle Eocene marl at depths of 95 to 295 m (probably correlative with lithologic units B4 and B5). We used the conductivity value of B4-5 from hole JD21 for an estimated heat flow of 70 mW/m² at this site.

JD20: Drilled as a petroleum wildcat well by INA, this hole is also known as Wadi Sirhan #1 (WS-1). The temperature profile we measured is too shallow for a heat flow estimate but is included in Appendix II for completeness.

JD21: This hole is in northeastern Jordan, near the village of H-4 (Figure 3). It was drilled by NRA as a water well (Wadi Ruweishid #1) but is now idle. The hole penetrates Eocene sediments of lithologic units B4 and B5 (Table 2). Conductivity samples were collected from the drilling-waste pile at this site, and the K value we obtained was correlated to several other
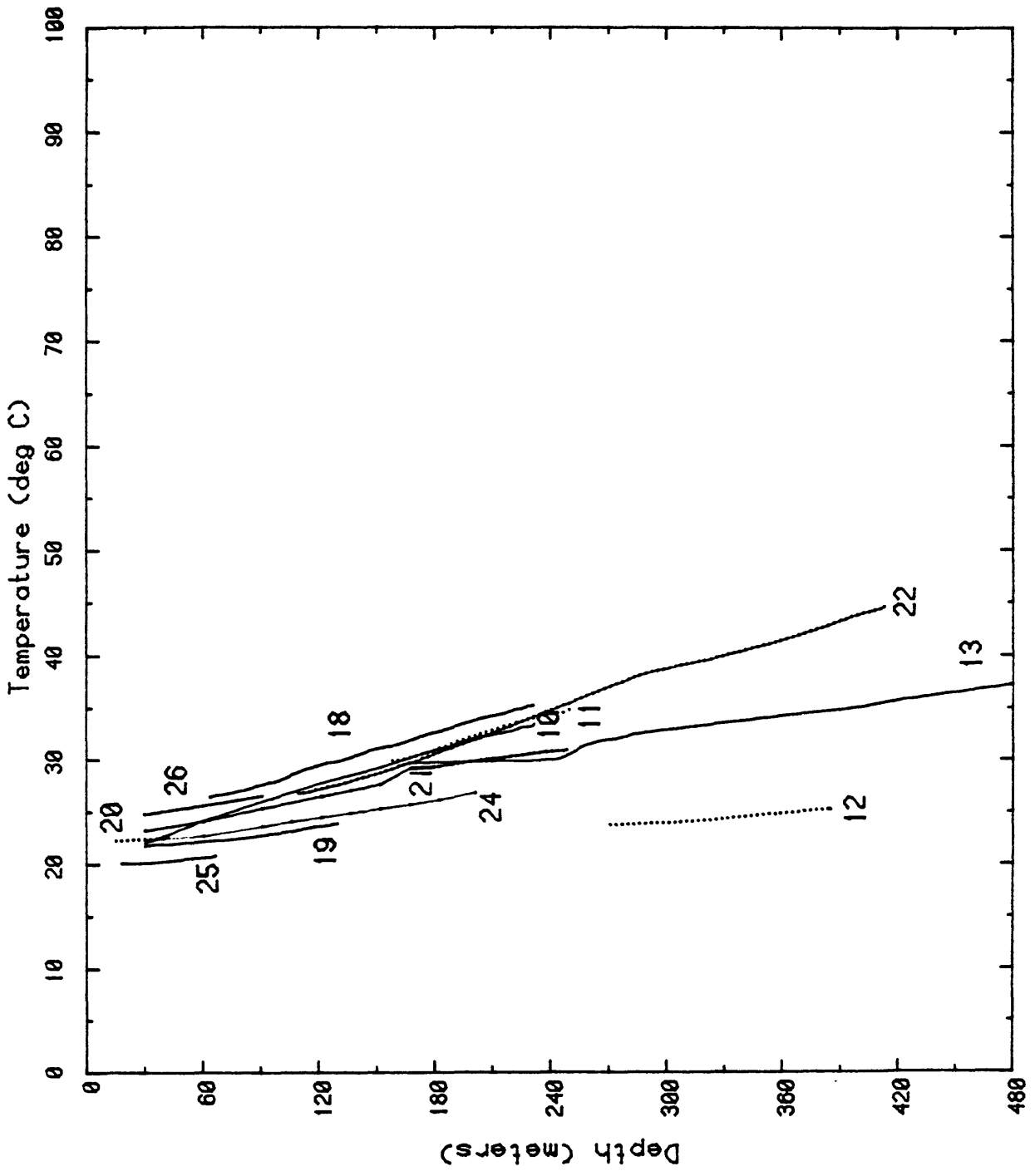
Figure 4. HIGHLANDS AND PLATEAU GEOTHERMAL GRADIENT HOLES

TABLE 3. Reconnaissance heat-flow estimates and geothermal gradients of Jordan

Hole	N. Lat.	E. Long.	Elev. m	Depth interval m	Thermal gradient* Γ_m °C km⁻¹	Surface intercept °C	Lithologic unit	Thermal conductivity** Wm⁻¹ K⁻¹ N	$\langle K_s \rangle$	φ corr.	K_f	Estimated Heat flow mW m⁻²
JD12	32° 33.9'	35° 44.6'	375	314-384	16.62 (.10)	18.9	A7	6†		12	2.54	42
JD13	32° 29.7'	36° 02.9'	570	299-500	24.58 (.17)	25.4	A7	6†		12	2.54	62
				500-917	30.53 (.12)	22.0	A3-6	10†		15	2.02	62
JD14	31° 55.0'	35° 37.3'	-120	15-61	~16	~27		7	2.47 (.04)			--
JD15	32° 22.6'	35° 37.4'	100	131-174	<-200	--						--
JD16	32° 15.0'	35° 37.4'	-140	49-93	12.70 (.44)	24.9		7	2.59 (.02)			--
JD17	31° 57.3'	35° 36.0'	-140	91-159	10.42 (3.1)	21.8						--
				159-189	156.1 (1.7)	-0.6						--
JD18	31° 35.2'	36° 50.6'	578	64-232	54.65 (.26)	22.8	B4-5	5††		14	2.30	125
JD19	31° 44.4'	37° 01.4'	545	95-131	30.28 (.47)	20.0	B4-5	5††		14	2.30	70
JD20	30° 57.9'	37° 25.1'	560	15-40	11.18 (.23)	22.1						--
JD21	32° 32.8'	38° 15.9'	700	174-247	24.05 (.29)	24.9	B4-5	5	2.83 (.09)	14	2.30	55
JD22	32° 03'	37° 07'	623	110-204	58.55 (.89)	20.0	B4-5	5††		14	2.30	135
				204-280	73.59 (.15)	17.1	B1-3	6†		19	1.54	113
				280-335	43.42 (.65)	25.7	A7	6†		12	2.54	110
				335-396	55.73 (.71)	21.4	A4-6	7†		12	2.18	121
											Mean	120
JD23	31° 02.5'	35° 28.6'	-370	15-49	-6.6 (.83)	25.6						--
JD24	30° 11.1'	35° 46.6'	1060	61-201	28.24 (.46)	21.0	B4-5	5††		14	2.30	65
JD25	30° 17.5'	36° 15.0'	850	18-67	15.85 (.82)	19.7						--
JD26	29° 43.0	35° 16.8'	750	30-91	29.31 (.56)	23.8		3	3.12 (.08)	16§	1.44	42

*Γ_m, gradient calculated over depth interval (standard error in parentheses).

**N, number of samples; $\langle K_s \rangle$, harmonic mean solid grain conductivity; φ, porosity (saturated unless otherwise noted); K_f, formation conductivity.

†Thermal conductivity from Table 1.

††Thermal conductivity of lithologic unit B4-5 from JD 21 measurements.

§Air-filled pore space (thermal conductivity of air, .025 Wm⁻¹ K⁻¹).

sites for heat-flow calculations (JD18, 19, 22, and 24). Our heat flow estimate is 55 mW/m^2 for the saturated interval 174 to 247 m; using a K_f with air-filled porosity, we obtain an identical heat flow estimate in the unsaturated interval 31 to 152 m.

JD22: This hole is located south of the village of H-5 in eastern Jordan. It was drilled by NRA as a stratigraphic test hole (hole SH-5). According to a lithologic log prepared for NRA, the hole penetrates several lithologic units (see Appendix Figure IIB-11). We have no samples from the borehole, so we used K values from Table 1 and from hole JD21 in the calculations for our heat flow estimates. The estimates are summarized in Table 3. The mean heat flow at this site is 120 mW/m^2.

JD23: This hole is in Wadi Araba, ∿20 km south of the Dead Sea. It was logged as an alternative when we found that a nearby deep hole (GS-1) was no longer open. The temperature profile is too shallow for a heat-flow estimate but is included in Appendix II for completeness.

JD24: The hole is located several kilometers east of the old Mahattat Ma'an (Ma'an railway station) in southern Jordan. It was drilled to 1383 m by NRA in 1965 as stratigraphic test hole S-1. Blockage has since reduced the hole depth and prevented our logging below ∿200 m. The temperature gradient in the interval 61-201 m is 28°C/km. A geologic cross section drawn through the site (Enclosure 2 of Lloyd, 1969) indicates that the rocks are cherty marls and limestones of the Belqa Group (Eocene). These rocks are similar in age and composition to our unit B4-5 samples from JD21. Using the conductivity from JD21, we estimate a heat flow of 65 mWm^2 at this site.

JD25: This hole is located east of Ma'an in southern Jordan. We did not estimate heat flow at this site because the hole is too shallow. The temperature profile is included in Appendix II for completeness.

JD26: Southernmost of our heat flow estimates, this hole is located 35 km northeast of Aqaba. The hole penetrates unsaturated Pleistocene sediments of the Wadi Utam basin (Lloyd, 1969). Using a K value from chip samples collected from the drilling-waste pile next to the borehole, we estimate a heat flow of 42 mWm^2 at this site.

HEAT FLOW OF ZERQA MA'IN AND ZARA GEOTHERMAL AREAS

Background and Geologic Setting.

The Zerqa Ma'in and Zara geothermal areas are the site of more than 100 moderate-temperature thermal springs (Figures 5 and 6). The area is on the eastern escarpment of the north-south trending Dead Sea Rift. Although the principal tectonism associated with the rift is horizontal, vertical motion in the Zerqa Ma'in - Zara area is indicated by great differences in local elevation; i.e., 700 m at Makawir village and -700 m at the floor of the adjacent Dead Sea (Hall, 1974), a horizontal distance of 8 km. Vertical disequilibrium is also implied by the escarpment's youthful morphology, its apparently rapid incision by streams to form wadis (gorges), and the thick accumulation of young sediments in the rift.

The geology of the study area was mapped at scales of 1:10,000 and 1:50,000 by members of the NRA Geology Division and its geohydrology was described in a 1980 report by M. Abu-Ajamieh. In ascending stratigraphic order, the rock units of immediate interest are: shales and sandstones of the Lower Zerqa Group (exposed near Zara, at the base of the escarpment); Kurnub Sandstone (a major regional aquifer and the unit from which the thermal springs issue); impermeable marls, shales, and marly limestones (locally known as units A-1 through A-6); permeable limestones of the Wadi Sir Formation (unit A-7); the bituminous and chalky marls and cherty limestones of the Amman Formation (units B-1 and B-2) cap the surrounding highlands.

A small volume (<1 km³) of late Cenozoic basalt that was emplaced from six nearby vents caps the sedimentary sequence and in part occupies a "paleowadi" that parallels but is not as deeply incised as the present Wadi Zerqa Ma'in (W. A. Duffield, 1982, written communcation; Truesdell and others, 1983).

The two main structural features of the area are the East Dead Sea fault (Quennell, 1982) near the base of the escarpment (paralleling the rift) and the east-west trending Wadi Zerqa Ma'in fault (roughly coincident with the present Wadi). The Wadi Zerqa Ma'in fault zone can be traced eastward a distance of 50 km from the Dead Sea (Abu-Ajamieh, 1980). The gross distribution of the basalt vents and flows parallel the Wadi Zerqa Ma'in fault zone.

The present study was undertaken to help assess the geothermal potential of the area and ultimately to identify the source of the heat. Bender (1974) believed that a magmatic heat source related to the nearby basaltic volcanism was a possibility, while Truesdell and others (1983) favored heating by deep circulation of ground water through crust with a normal geothermal gradient.

In this study, nine geothermal gradient holes were drilled and cased by members of the NRA, Geology Division; temperature logs and thermal properties of rock samples and drill cuttings were measured by members of the USGS, Geothermal Studies Project. In addition to the nine holes drilled
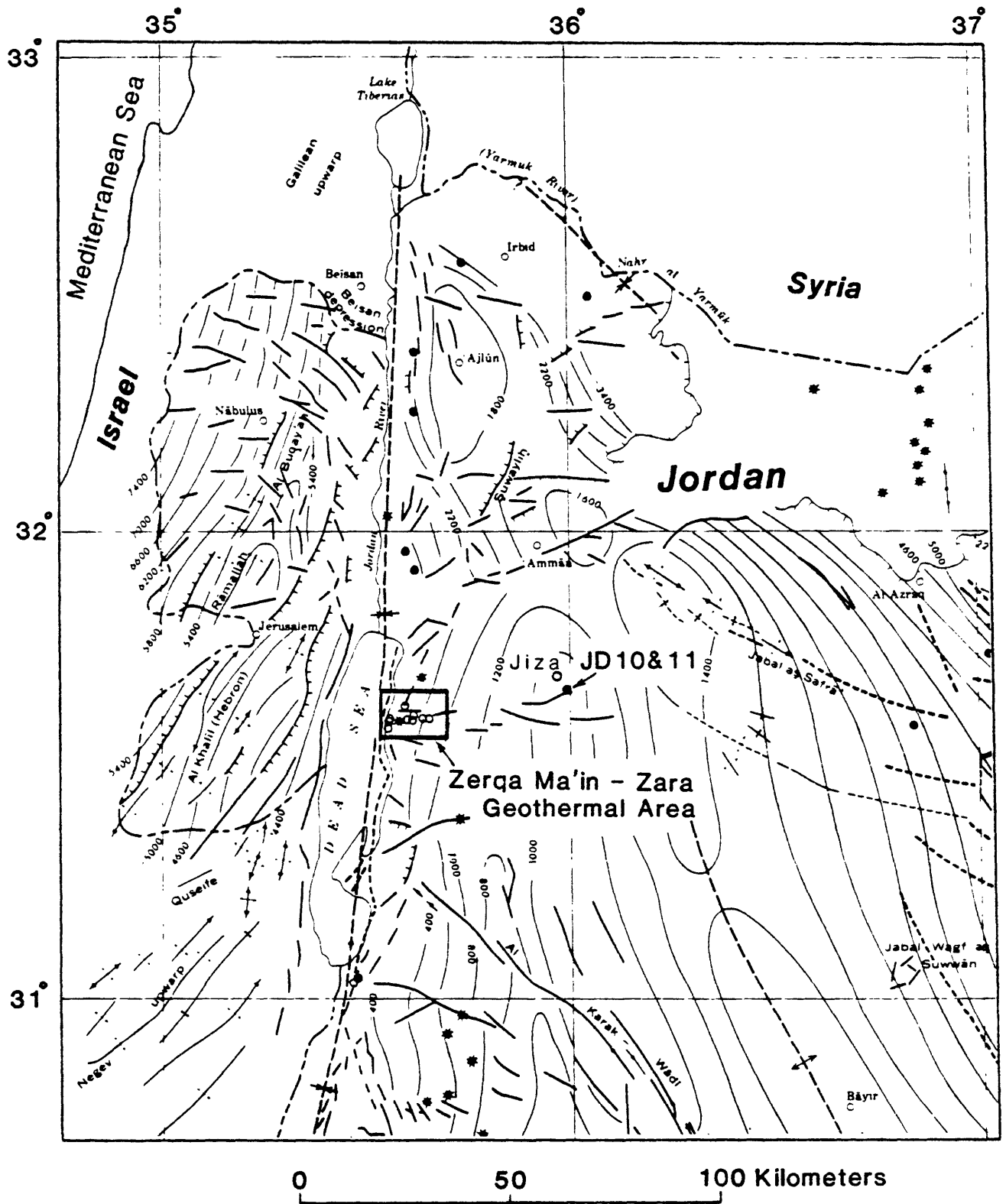
Figure 5. Index map of Northwest Jordan, with locations of Zerqa Ma'in -
Zara Geothermal Area (detailed in Figure 6) and Boreholes JD10 and 11. Map
adapted from Plate 3 of Bender (1975).

Figure 6.
Geologic Sketch Map of the Zara and Wadi Zerqa Ma'in Geothermal Areas.
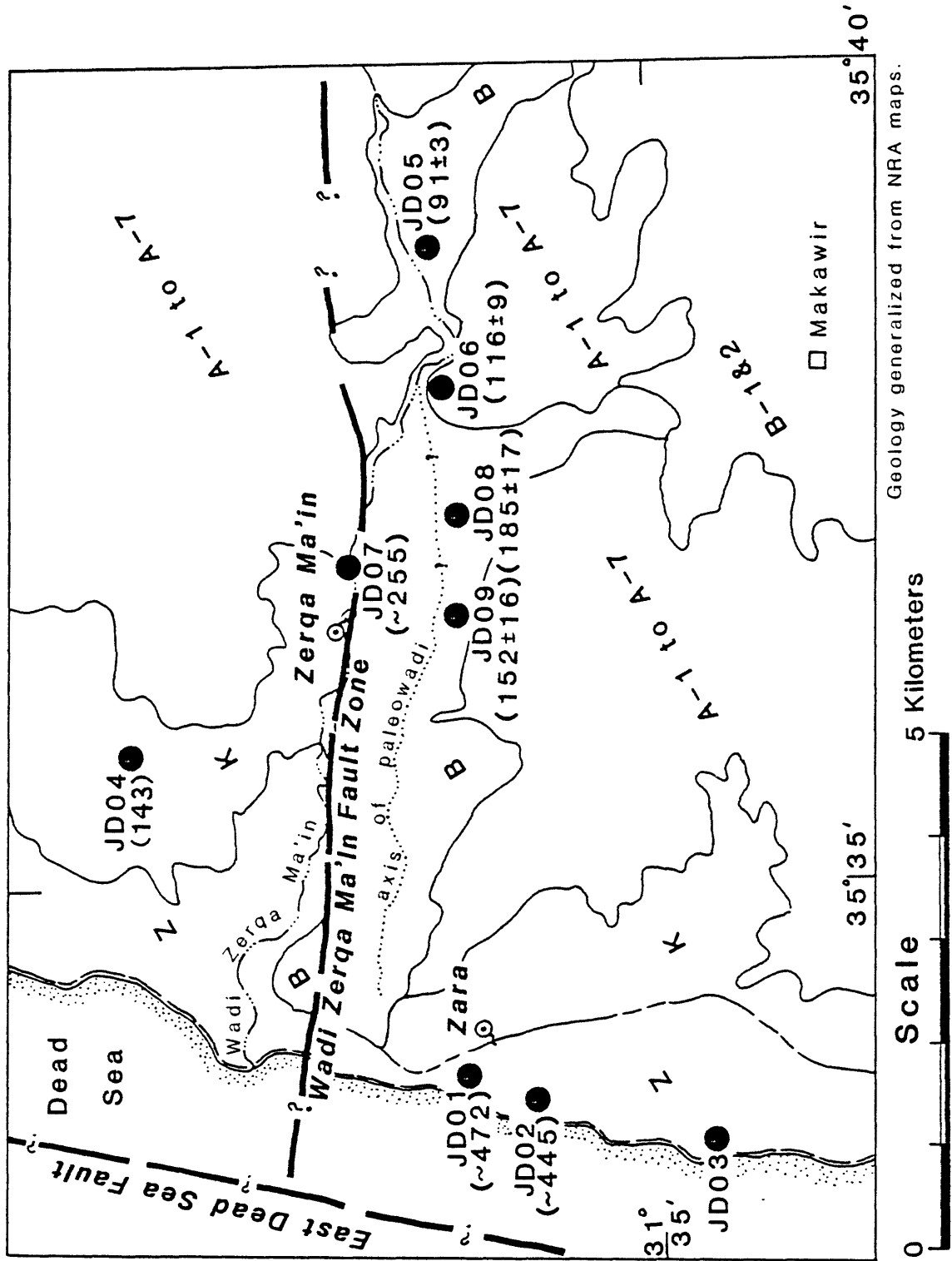
- Heat flow site (mW/m²)

$\odot$ Thermal spring area

Geology generalized from NRA maps.

Lithologic units: Z, Zarqa Group; K, Kurnub Sandstone; Units A-1 to A-7; Units B-1 & 2; B, Basalt.

specifically for heat-flow measurements, data from two unused water wells (JD10 and 11, Figure 5) are included in this section because of their proximity to the eastern end of the Wadi Zerqa Ma'in fault zone. Temperature and gradient profiles and lithologic logs for individual boreholes are presented in Appendix II.

Convective Temperature Profiles.

The holes with temperature profiles disturbed by strong convective water flow are JD01, JD02, and JD03 near the Zara thermal springs and JD07 near the Zerqa Ma'in hot springs (Figure 6).

JD01: This is the hole closest to the junction of the Wadi Zerqa Ma'in and East Dead Sea faults. The hole was drilled through a terrace of travertine spring deposits, 20 m of marly cap rock, then into Triassic sandstone of the Lower Zerqa Group (see Appendix Figure IIA-1). Strong artesian water-flow around and through the casing forms a rivulet, then a small waterfall where it cascades off of the travertine terrace. The measured temperature profile is isothermal (Figure 7).

JD02: This hole is approximately 1 km south of JD01 and also penetrates sandstone of the Lower Zerqa Group (see Appendix Figure IIA-2). Water discharges around and from the casing but the artesian flow is weaker than that from JD01. Water flows up from the bottom of the borehole then mixes with warmer water flowing in at about 70 m.

JD03: Curvature in the temperature profile is caused by lateral as well as vertical water flow. No thermal gradient was estimated for this well.

JD07: This hole is located 5 km east of Zara, near the Zerqa Ma'in springs. Water flows up the borehole then mixes with cooler water from a fracture or fault zone at 90 m. The water then continues up the borehole and exits out of a crack or joint at 17 m. During the drilling of this hole, it was noted that new springs just below the drill site began discharging into the adjacent stream.

The measured temperature profiles for these holes were nearly isothermal, so assuming that: 1) the water-flow originated at the "total-drilled-depth" of each borehole, and 2) the aquifer is nearly horizontal and very thin in relation to the drilled-depth; the thermal gradient is defined by the line joining the mean annual surface temperature with the bottom-hole temperature. This is shown graphically in Figure 7. Note that the lower surface temperature for JD07 is due to its greater elevation (an adiabatic adjustment with a lapse rate of 5°C/km). The resultant gradients range from 165 to 175 °C/km and the calculated heat flows from 255 to 472 mW/m^2 (Table 4). Our maximum of 472 mW/m^2 is remarkably close to the high of 464 mW/m^2 observed in a geothermal area on the west side of the Dead Sea Rift (Eckstein, 1979).

Conductive Temperature Profiles.

JD04: Located on a plateau 2 km north of the Zerqa Ma'in hot springs, the hole is drilled entirely in rocks of the Kurnub Sandstone. The high
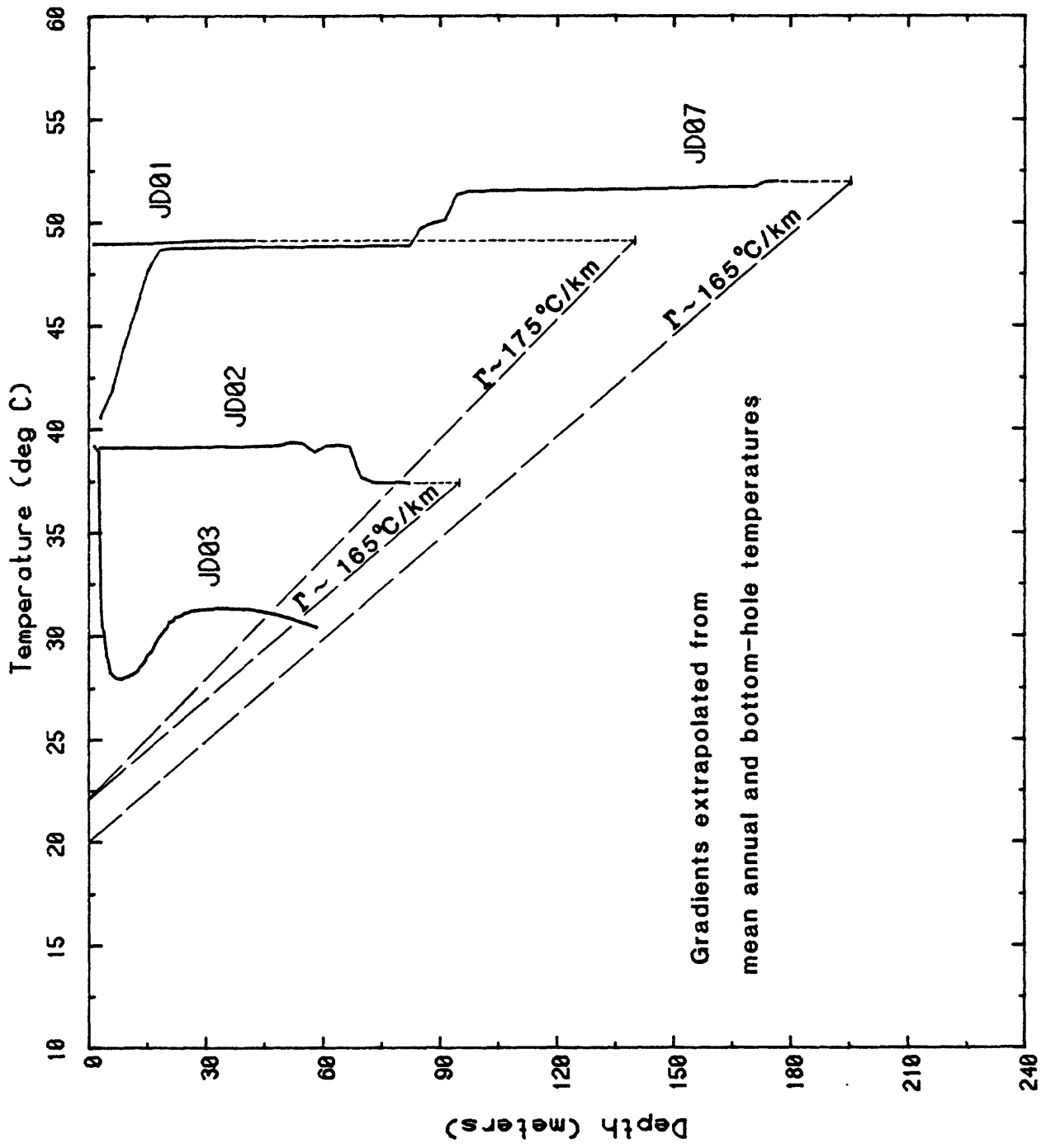
Figure 7.   Holes disturbed by convective water flow, Zerqa Ma'in – Zara

TABLE 4. Summary of heat-flow determinations for the Zerqa Ma'in and Zara Geothermal Areas, Jordan

Hole	N. Lat.	E. Long.	Elev. m	Thermal gradient*			Thermal conductivity** , Wm⁻¹ K⁻¹				Heat flow mW m⁻²
				Depth interval m	Γ_m	Γ_c	N	$\langle K_s \rangle$	φ corr.	K_f	
JD01	31° 36.0'	35° 33.8'	-365	0-140	175†	--	5††		18	2.7	~472
JD02	31° 35.7'	35° 33.6'	-360	0-95	165†	--	5††		18	2.7	~445
JD03	31° 34.7'	35° 33.4'	-380	---	---	--	-		--	--	---
JD04	31° 37.7'	35° 35.8'	160	23-61	69.06 (0.45)	73.84	3	6.26 (.35)	18§	2.32	171±27
				79-119	13.46 (0.49)	18.77	3	6.82 (.39)	18	4.38	82±9
				131-160	25.79 (0.75)	31.17	2	5.24 (.03)	18	3.53	110±4
				158-203	77.62 (2.64)	83.24	9	3.50 (.25)	18	2.54	211±29
										Mean	143
JD05	31° 36.1'	35° 38.9'	260	150-210	72.78 (0.62)	58.19	11	1.80 (.03)	12	1.57	91±3
JD06	31° 36.1'	35° 38.0'	210	100-155	88.62 (0.47)	66.40	6	2.03 (.13)	12	1.75	116±9
JD07	31° 36.6'	35° 36.9'	-60	0-195	165†	--	6††		19	1.5	~255
JD08	31° 36.0'	35° 37.3'	230	37-215	94.70 (2.45)	89.90	10	2.44 (.13)	12	2.06	185±17
JD09	31° 36.0'	35° 36.6'	210	53-203	94.16 (1.40)	86.67	6	2.04 (.16)	12	1.75	152±16
JD10	31° 39.8'	35° 59.3'	712	61-198	55.85 (0.34)	--	5	2.54 (.11)	12	2.13	119±7
JD11	31° 39.9'	35° 59.3'	708	158-250	56.88 (0.79)	--	5	2.67 (.03)	12	2.22	126±3
									JD10 & 11 Mean		123

*Γ_m, gradient calculated over depth interval (standard error in parentheses); Γ_c, corrected for two-dimensional topography.

**N, number of samples; $\langle K_s \rangle$, harmonic mean solid grain conductivity; φ, porosity correction (saturated; thermal conductivity of water, 0.58 Wm⁻¹ K⁻¹); K_f, formation conductivity.

†Gradient defined by slope of line joining mean annual temperature with temperature at total depth drilled; measured isothermal gradient caused by vertical water flow from bottom of borehole.

††Thermal conductivity from Table 1.

§Air-filled pore space (thermal conductivity of air, 0.025 Wm⁻¹ K⁻¹).

temperature gradient in the upper 75 m (see Figure 8 and Appendix Figure IIA-4) is caused by the relatively low thermal conductivity of porous unsaturated sandstone above the water table. Below the water table, the temperature profile is concave upward, caused in part by strata of different thermal conductivity and permeability coupled with vertical water movement (in this case, probably downward flow toward the escarpment and the Wadi Zerqa Ma'in). The mean heat flow calculated for this site is 143 mW/m^2 (Table 4).

JD05: Easternmost of the holes drilled for this study, JD05 is 4 km east of the Zerqa Ma'in springs. The hole penetrates 40 m of basalt and ash before encountering marl, limestone, and shale (Appendix Figure IIA-5). Rocks of the uppermost 135 m are highly permeable. Flowing water in this interval causes an isothermal temperature profile. An impermeable sequence of shale below 135 m yields a linear temperature profile and conductive gradient; a heat flow of 91 mW/m^2 is calculated for the interval 150-210 m.

Both JD05 and JD06 are in an upstream "hanging valley" portion of the Wadi Zerqa Ma'in, ∿160 m higher than the floor of the modern incised gorge. A consequence of their locations is that in each hole, permeable intervals below the water table have nearly isothermal temperature profiles caused by water-flow toward the gorge. The hanging valley is a remnant of an older land surface: The surviving part of a "paleowadi" that was clogged by basalt flows before erosion of the modern gorge.

JD06: This hole is located near the mouth of the "hanging valley." A linear temperature profile and conductive gradient in the interval 100-155 m yields a calculated heat flow of 116 mW/m^2. The decreased temperature gradient below 155 m is probably due to heat transfer by water-flow.

JD08: Located 2 km southeast of the Zerqa Ma'in springs, on a high terrace that forms the south rim of the gorge, this hole penetrates 97 m of "paleowadi fill" before encountering marl, shale, and limestone (Appendix Figure IIA-8). The temperature profile, measured by members of the NRA Geophysics Group, is linear and shows conductive heat transport. The jog in the temperature profile at ∿186 m may be due to water leaking out of the casing into the dry hole. Heat flow calculated for this site is 185 mW/m^2.

JD09: This site, located on the same terrace, is approximately 1 km west of JD08. The "paleowadi fill" at this point is 87 m thick. The linear temperature profile measured by members of the NRA yields a calculated heat flow of 152 mW/m^2.

Although both holes, JD08 and JD09, are above the saturated zone, the fine-grained nature of the rock warranted that a K_f with saturated porosity be used in the heat flow calculation.

JD10 and JD11: These holes are located near the village of Jiza, ∿40 km east of the Zerqa Ma'in springs (Figure 5). Their existence was brought to our attention by M. Teimeh (NRA) and included in this section because of their proximity to the eastern end of the Wadi Zerqa Ma'in fault zone. The holes are approximately 300 m apart and both have nearly linear conductive temperature profiles (Figure 8 and Appendix Figure IIA-10). The mean heat flow calculated for these sites is 123 mW/m^2.
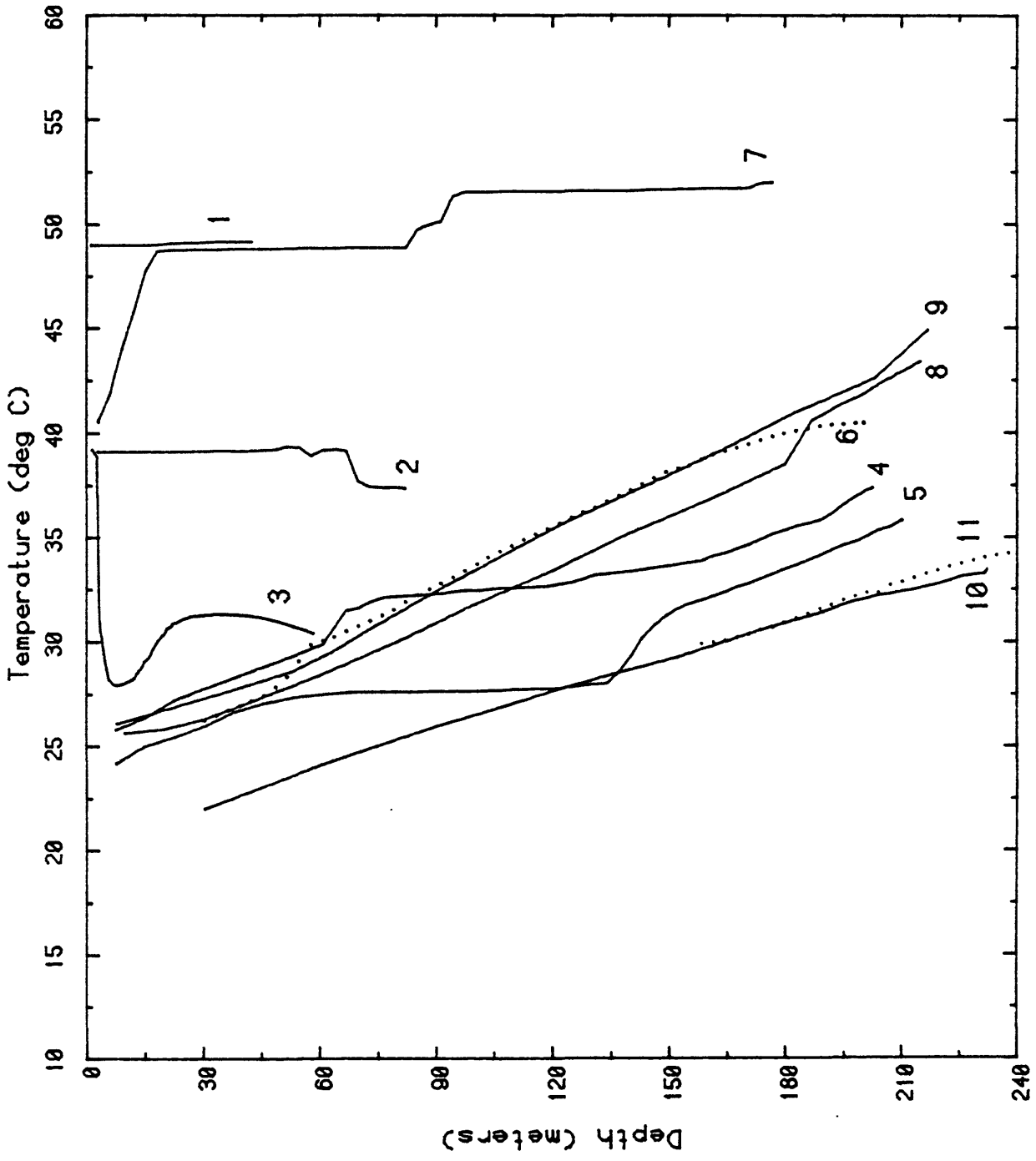
Figure 8. ZERQA MA'IN -- ZARA GEOTHERMAL GRADIENT HOLES

DISCUSSION AND CONCLUSIONS

Until recently, little was known about the surface pattern of heat flow in the Middle East. Several regional studies within the past few years have helped to rectify this situation (Eckstein and Simmons in Israel, 1978; Morgan and others in Egypt, 1983; Girdler and Evans in the Red Sea, 1977; Gettings in the southwestern Arabian Shield, 1981). In this study, we were able to either estimate or calculate heat flow for 18 of the 37 sites we visited. These are the first heat flow values reported for the east flank of the Dead Sea Rift, and only the second data set for the Arabian Peninsula. After comparing the distribution of heat flow values (Figure 3) with the geologic structures (Figure 2), we divided our data into three groups. The groups are: Zerqa Ma'in and Zara data, Azraq Basin data, and regional data.

The first group consists of the high heat flow values near the Zerqa Ma'in and Zara geothermal areas, adjacent to the Dead Sea Rift (includes sites JD01 through JD11). Heat flow in this area is high, ranging from 91 to ~472 mW/m^2 (see Table 4). The average heat flow is 133 mW/m^2, excluding our three exceptional estimated values (~472 mW/m^2, JD01; ~455 mW/m^2, JD02; ~255 mW/m^2, JD07). The area of high heat flow is associated with the Wadi Zerqa Ma'in fault zone, and probably, with the East Dead fault (Figure 6). Though the distribution of data is sparce along the Wadi Zerqa Ma'in fault zone's 50 km length, heat flow is high near its eastern end (mean of 123 mW/m^2 at sites JD10 and JD11) and peaks at its western end (~472 mW/m^2 at JD01), near the intersection with the East Dead Sea fault.

Lack of volcanism near the eastern end of the fault and small infrequent basaltic eruptions near Zara and Zerqa Ma'in on the western end (Truesdell and others, 1983) make a magmatic heat source for the anomaly seem unlikely. On the other hand, high heat flow associated with the fault is consistent with the hypothesis that waters, heated by deep circulation, are the source of heat.

Deep faults may act as conduits for the rapid ascent of hot waters from deep confined aquifers. The water is driven toward the surface by hydraulically induced forced-convection. Near the surface, the water's heat is dissipated either by mixing with cooler waters from shallow aquifers, by direct discharge at thermal springs, or by conduction into surrounding country rock.

A similar hypothesis was used to explain anomalously high heat flow on the west side of the Dead Sea Rift (Eckstein and Simmons, 1978; Levitte and Eckstein, 1979). There, faults associated with the rift act as conduits for waters from deep aquifers. Heat flow on the west side of the rift is as high as 463.5 mW/m^2 (very close to what we've estimated at Zara), but typically, it is between 52 and 146 mW/m^2 (Eckstein and Simmons, 1978).

Based on an isotopic study, Truesdell and others (1983) believed that the thermal waters at Zerqa Ma'in and Zara are ascending from the lower Paleozoic aquifers. These aquifers may be 8 to 9 km below the surface on the west side of the East Dead Sea fault (Folkman, 1980), and are 3 to 5 km

below the surface further east, beneath the Jordanian plateau. Depths of this magnitude are more than sufficient to warm the waters to their discharge temperature, and indeed, are great enough to warm them to their estimated reservoir temperature of ~100°C (Truesdell and others, 1983).

Our second group consists of the high heat flow values within and adjacent to the Azraq Basin (includes sites JD18, JD19, and JD22). Heat flow in this area is high but variable (70 to 135 mW/m^2). More data are needed to delineate this anomaly. The anomaly may be restricted to the Azraq area, or it may continue westward to the Wadi Zerqa Ma'in anomaly. We believe the mechanism of heat transfer producing this anomaly is similar to what was described for the preceding group. Sedimentary rocks in the Azraq Basin are deep (~5000 m) and complexly faulted (Hatcher and others, 1981).

Our third group consists of the normal heat flow values measured in all of the other parts of Jordan (includes sites, JD12, JD13, JD21, JD24, and JD26). The heat flow values range from 42 to 65 mW/m^2. The average heat flow is 53 mW/m^2. The mode of transfer responsible for these heat flow values is primarily conductive, as opposed to the convective heat transfer controlling heat flow at Zerqa Ma'in - Zara and Azraq Basin.

On the west side of the Dead Sea Rift, Eckstein and Simmons (1978) described a data set analogous to our third group. They believed that their heat flow values were not influenced by groundwater flow. Heat flow values in their group averaged 52.34 mW/m^2, virtually identical to our average of 53 mW/m^2.

References

Abu-Ajamieh, M., 1980, The geothermal resources of Zerqa Ma'in and Zara in Report of Phase I of the Geothermal Energy Project in Jordan: Jordan Natural Resources Authority, 82 p.

Beck, A. E., 1976, An improved method of computing the thermal conductivity of fluid-filled sedimentary rocks: Geophysics, v. 41, p. 133-144.

Bender, Friedrich., 1974, Explanatory notes on the geological map of Wadi Araba, Jordan: Geologisches Jahrbuch, Reihe B, Heft 10, 62 p.

Bender, Friedrich., 1975, Geology of the Arabian Peninsula - Jordan: U.S. Geological Survey Professional Paper 560-I, 36 p.

Birch, F., 1950, Flow of heat in the Front Range, Colorado: Geological Society of America Bulletin, v. 61, p. 567-630.

Eckstein, Y., 1979, Heat flow and the hydrologic cycle--Examples from Israel, in Terrestrial Heat Flow in Europe, edited by V. Cermak and L. Rybach: Springer-Verlag, Berlin, p. 88-97.

Eckstein, Y., and Simmons, G., 1978, Measurements and interpretation of terrestrial heat flow in Israel: Geothermics, v. 6, p. 117-142.

Folkman, Y., 1980, Magnetic and gravity investigations of the Dead Sea rift and adjacent areas in northern Israel: Journal of Geophysics, v. 48, p. 34-39.

Freund, R., Garfunkel, Z., Zak, I., Goldberg, M., Weissbrod, T., and Derin, B., 1970, The shear along the Dead Sea rift: Royal Soc. London Philos. Trans., v. A267, p. 107-130.

Garfunkel, Z., 1981, Internal structure of the Dead Sea leaky transform (rift) in relation to plate kinematics: Tectonophysics, v. 80, p. 81-108.

Gettings, M. E., 1981, A heat flow profile across the Arabian Shield and Red Sea (abstract): EOS Transactions, AGU, v. 62, p. 407.

Girdler, R. W., and Evans, T. R., 1977, Red Sea heat flow: Geophysical Journal of the Royal Astronomical Society, v. 51, p. 245-251.

Hall, J. K., 1974, Dead Sea geophysical survey--Bathymetric Chart: Marine Geology Division, Geological Survey of Israel, 1 sheet.

Hatcher, R. D., Jr., Zietz, I., Regan, R. D., Abu-Ajamieh, M., 1981, Sinistral strike-slip motion on the Dead Sea Rift--Confirmation from new magnetic data: Geology, v. 9, p. 458-462.

Jaeger, J. C., and Sass, J. H., 1963, Lees's topographic correction in heat flow and geothermal flux in Tasmania: Geofisica Pura E Applicata - Milano, v. 54, p. 53-63.

Lachenbruch, A. H., and Sass, J. H., 1977, Heat flow in the United States and the thermal regime of the crust, in The Earth's Crust--Its Nature and Physical Properties, Geophysical Monograph Series, v. 20, edited by J. G. Heacock, p. 626-675: American Geophysical Union, Washington, D. C.

Lees, C. H., 1910, On the shapes of the isogeotherms under mountain ranges in radioactive districts: Proceedings of the Royal Astronomical Society, v. A83, p. 339-346.

Levitte, D., and Eckstein, Y., 1979, Correlation between the silica concentration and the orifice temperature in the warm springs along the Jordan - Dead Sea Rift Valley: Geothermics, v. 7, p. 1-8.

Lloyd, J. W., 1969, Investigation of the sandstone aquifers of east Jordan: Food and Agricultural Organization of the U.N., LA:SF/JOR9, Technical Report 1, 207 p.

Morgan, P., Boulos, F. K., and Swanberg, C. A., 1983, Regional geothermal exploration in Egypt: Geophysical Prospecting, v. 31, p. 361-376.

Quennell, A. M., 1982, Tectonics of the Dead Sea rift, in Rift Valleys, Afro-Arabian, Benchmark Papers in Geology, v. 20, edited by A. M. Quennell, p. 365-383: Hutchinson Ross Publishing Company, Stroudsburg, Pennsylvania.

Robertson, E. C., and Peck, D. L., 1974, Thermal conductivity of vesicular basalt from Hawaii: Journal of Geophysical Research, v. 79, p. 4875-4888.

Sass, J. H., Lachenbruch, A. H., and Munroe, R. J., 1971a, Thermal conductivity of rocks from measurements on fragments and its application to heat-flow determinations: Journal of Geophysical Research, v. 76, p. 3391-3401.

Sass, J. H., Lachenbruch, A. H., Munroe, R. J., Greene, G. W., and Moses, T. H., Jr., 1971b, Heat flow in the western United States: Journal of Geophysical Research, v. 76, p. 6376-6413.

Truesdell, A. H., Duffield, W. A., and Abu-Ajamieh, M., 1983, Origin and heat source of thermal waters at Zerqa Ma'in and Zara, Jordan (abstract): Fourth International Symposium on Water-rock Interactions, August 29 - September 8, 1983, Misasa, Japan.

Waring, G. A., 1965, Thermal springs of the United States and other countries of the world: U.S. Geological Survey Professional Paper 492, 383 p.

Woodside, W., and Messmer, J. H., 1961a, Thermal conductivity of porous media, I. Unconsolidated sands: Journal of Applied Physics, v. 32, p. 1688-1699.

Woodside, W., and Messmer, J. H., 1961b, Thermal conductivity of porous media, II. Consolidated rock: Journal of Applied Physics, v. 32, p. 1699-1706.

APPENDIX I. Jordan borehole data

TABLE 1. Jordan borehole data

USGS Hole* Designation	Location	N. Lat.	E. Long.	Palestine 10,000-Meter Grid (East/North)	Type of† Hole	Hole Number	Completion Date	Depth Drilled m	Elev. m	Thermal Log** Date	Thermal Log** Depth of log m	Thermal Log** S.W.L. m
JD01	Zara	31° 36.0'	35° 33.8'	203.6/112.1	G.G.	GTZ-1	7-82	140	-365	8-7-83	43.3	F
JD02	Zara	31° 35.7'	35° 33.6'	203.4/111.4	G.G.	GTZ-2	7-82	95	-360	8-7-83	82.6	F
JD03	Zara	31° 34.7'	35° 33.4'	203.0/109.7	G.G.	GTZ-3	8-82	150	-380	8-7-83	58.5	~30
JD04	Zerqa Ma'in	31° 37.7'	35° 35.8'	206.8/115.5	G.G.	GTZ-4	11-82	225	160	8-20-83	202.8	75
JD05	Zerqa Ma'in	31° 36.1'	35° 38.9'	211.7/112.3	G.G.	GTZ-5	2-83	220	260	8-19-83	210.6	70
JD06	Zerqa Ma'in	31° 36.1'	35° 38.0'	210.4/112.2	G.G.	GTZ-6	5-83	204	210	8-6-83	200.3	~100
JD07	Zerqa Ma'in	31° 36.6'	35° 36.9'	208.6/113.0	G.G.	GTZ-7	8-83	195	-60	8-20-83	177.3	~17
JD08	Zerqa Ma'in	31° 36.0'	35° 37.3'	209.0/112.0	G.G.	GTZ-8	9-83	232	230	11-13-83	215††	D
JD09	Zerqa Ma'in	31° 36.0'	35° 36.6'	208.0/111.9	G.G.	GTZ-9	9-83	242	210	11-13-83	217††	D
JD10	Jiza	31° 39.8'	35° 59.3'	243.9/119.0	W.W.	Zizya #1	---	~720	712	8-10-83	232.3	163.1
JD11	Jiza	31° 39.9'	35° 59.3'	243.9/119.2	W.W.	Zizya #2	---	~720	708	8-10-83	250.0	157.0
JD12	Qumein	32° 33.9'	35° 44.6'	220 /219	S.T.	S-18	9-66	895	375	8-11-83	385.3	268.2
JD13	Ramtha	32° 29.7'	36° 02.9'	248.7/211.5	P.T.	S-90	3-70	2192	570	8-11-83	917.4	158.5
JD14	Jordan Valley	31° 55.0'	35° 37.3'	209.0/147.5	W.W.	JRV-12	---	61.3	-120	8-8-83	61.0	D
JD15	Jordan Valley	32° 22.6'	35° 37.4'	208.8/198.1	W.W.	JRV-5	---	---	100	8-9-83	175.3	68.6
JD16	Jordan Valley	32° 15.0'	35° 37.4'	209.0/184.0	W.W.	JRV-6	---	---	-140	8-9-83	93.0	47.2
JD17	Jordan Valley	31° 57.3'	35° 36.0'	206.9/151.2	W.W.	JRV-7	---	---	-140	8-9-83	189.0	<90
JD18	Wadi Ghadaf	31° 35.2'	36° 50.6'	325.0/111.4	P.T.	WG-1	4-70	3081	578	8-16-83	231.6	61.6
JD19	Wadi Rajil	31° 44.4'	37° 01.4'	341.8/128.8	P.T.	WR-1	4-71	3076	545	8-16-83	130.5	27.7
JD20	Wadi Sirhan	30° 57.9'	37° 25.1'	381.0/043.6	P.T.	WS-1	7-71	1800	560	8-18-83	42.1	13.7
JD21	Wadi Ruweishid	32° 32.8'	38° 15.9'	---	W.W.	WR-1	---	250	700	8-17-83	248.4	167.3
JD22	H-5	32° 03'	37° 07'	350 /163	S.T.	SH-5	12-71	1405	623	8-21-83	413.2	108.2
JD23	Es Safi	31° 02.5'	35° 28.6'	195.4/050.1	W.W.	---	---	---	-370	8-23-83	49.1	16.1
JD24	Ma'an	30° 11.1'	35° 46.6'	225.0/955.0	S.T.	S-1	10-65	1386	1060	8-25-83	201.2	D
JD25	Al Jafr	30° 17.5'	36° 15'	270 /967	W.W.	#7	---	---	850	8-24-83	66.4	17.7
JD26	Wadi Utam	29° 43.0'	35° 16.8'	176.7/903.1	W.W.	S-20	---	100	750	8-25-83	96.5	D

TABLE I. Jordan borehole data (continued)

USGS Hole* Designation	Location	N. Lat.	E. Long.	Palestine 10,000-Meter Grid (East/North)	Type of† Hole	Hole Number	Completion Date	Depth Drilled m	Elev. m	Thermal Log** Date	Depth of log m	S.W.L. m
27	Azrak	---	---	321.1/142.1	W.W.	AZ-1	63	1299	513	7-27-83	---	F
28	Wadi Hazim	---	---	361.8/123.1	P.T.	WH-1	10-71	1861	530	N.V.	---	
29	Suweileh	32° 05'	35° 50'	---	P.T.	SW-1	---	2329		8-11-83	---	P
30	Jordan Valley	---	---	207.0/137.1	P.T.	JV-1	6-59	1097	-290	8-1-83	---	P
31	Safra	---	---	280.0/137.4	P.T.	SA-1	12-57	2584	745	8-14-83	---	Z
32	Wadi Ruweishid	32° 33.2'	38° 17.2'	459.1/221.8	W.W.	WR-2	---	315	700	8-17-83	---	P
33	H-4	---	---	466.2/248.4	W.W.	S-92	---	600	---	8-17-83	---	P
34	H-4	---	---	435.5/210.2	W.W.	Mougat-7	---	308	760	8-17-83	---	P
35	Khalida	---	---	272.0/174.8	S.T.	KH-1	3-71	1333	605	8-21-83	---	Z
36	Er Ramtha	---	---	246.5/208.8	P.T.	ER-1	---	1130	---	N.V.	---	
37	Ghor es Safi	31° 02.1'	35° 28.1'	194.5/049.2	P.T.	GS-1	3-72	2785	-365	8-23-83	---	Z
38	Lisan	---	---	194.3/074.3	P.T.	L-1	---	3673	---	8-23-83	---	Z
39	Al Jafr	---	---	254.8/977.0	W.W.	#4	---	515	897	8-24-83	---	Z
40	Al Jafr	---	---	260.7/967.3	S.T.	S-15	2-66	1383		N.V.	---	330
41	Wadi Jadaniya	---	---	286.0/943.0	S.T.	S-57	4-68	1243		N.V.	---	234
42	Wadi Tabilah	---	---	256.0/866.8	W.W.	S-43		663		N.V.	---	71
43	Wadi Harad	---	---	231.7/888.3	W.W.	S-33		455		N.V.	---	242
44	Auja	---	---	281.3/899.7	W.W.	S-46		1092		N.V.	---	218
45	Lisan	31° 17'	35° 35'	---	S.T.	NRA-2	2-68	1014		N.V.	---	
46	Lisan	31° 11'	35° 34'	---	S.T.	NRA-3	5-68	1000		N.V.	---	

*Holes with "JD" prefix have thermal logs; hole locations shown on Figure 3.

†Type of hole: GG, geothermal gradient; WW, water well; ST, stratigraphic test; PT, petroleum test.

**Date of log; NV, hole not visited; S.W.L., depth below ground surface (m) of water table; F, flowing artesian water; D, dry hole; P, hole not logged due to active pumping; Z, hole destroyed.

††Thermal log by NRA, Geophysics Group.
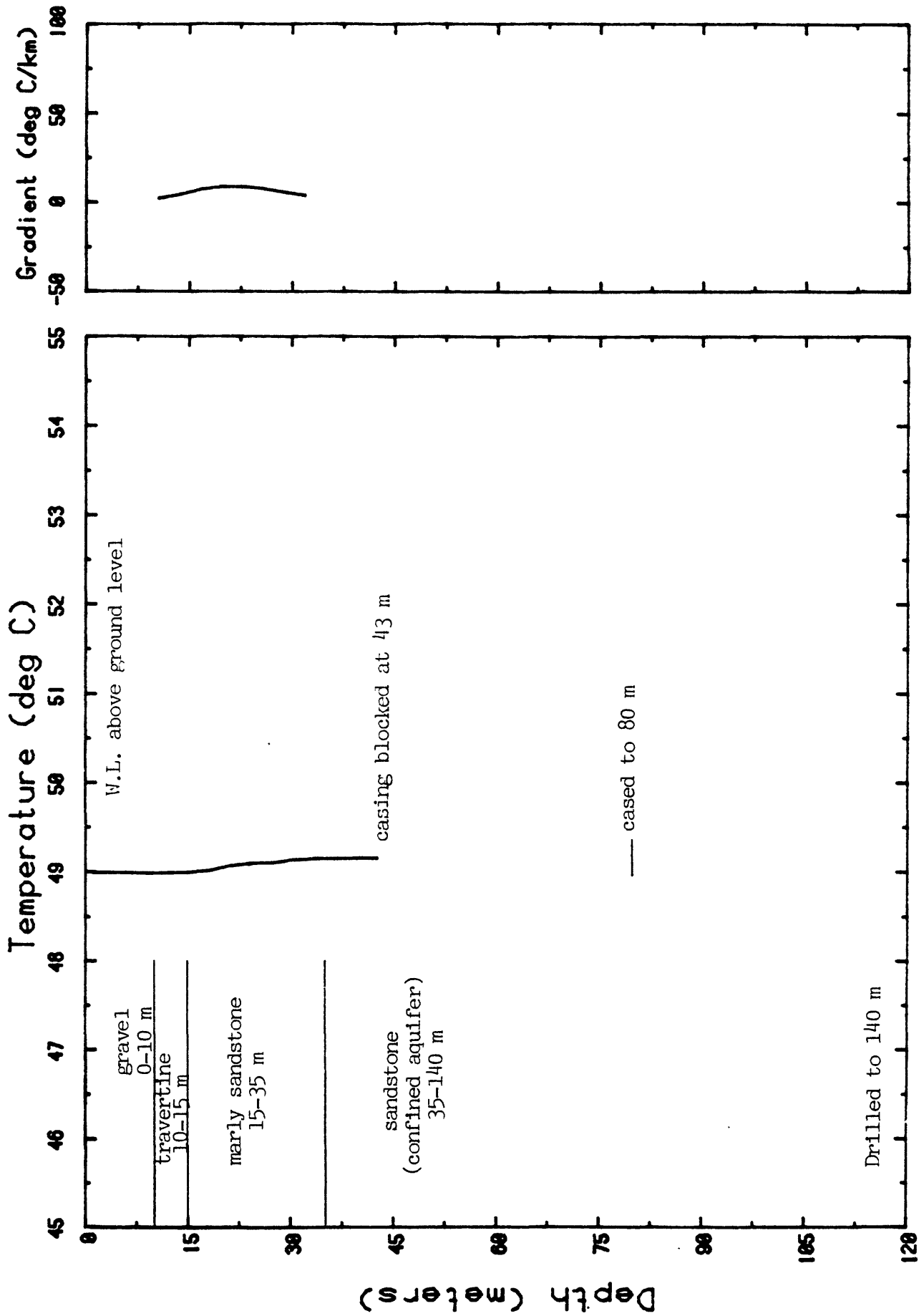
Figure IIA-1. Temperature profile, geothermal gradient, and lithology of borehole JD01, Jordan. W.L. represents the standing-water level in the borehole.

APPENDIX IIA.   Individual borehole logs and tabulated temperatures,

Zerqa Ma'in and Zara areas, Jordan

(Lithologic logs generalized from descriptions by M. Teimeh and M. Assaf,
N.R.A.)

Figure IIA-2. Temperature profile, geothermal gradient, and lithology of borehole JD02, Jordan. W.L. represents the standing-water level in the borehole.

TABLE IIA-1

JD01/AUG0783

Depth (m)	Temp. (°C)	Depth (m)	Temp. (°C)
1.21	48.98	3.04	48.98
6.09	48.98	9.144	48.98
12.19	48.99	15.24	48.99
18.28	49.01	21.33	49.06
24.38	49.10	27.43	49.10
30.48	49.14	33.52	49.14
36.57	49.15	39.62	49.15
42.67	49.15		

@JD02/AUG0783

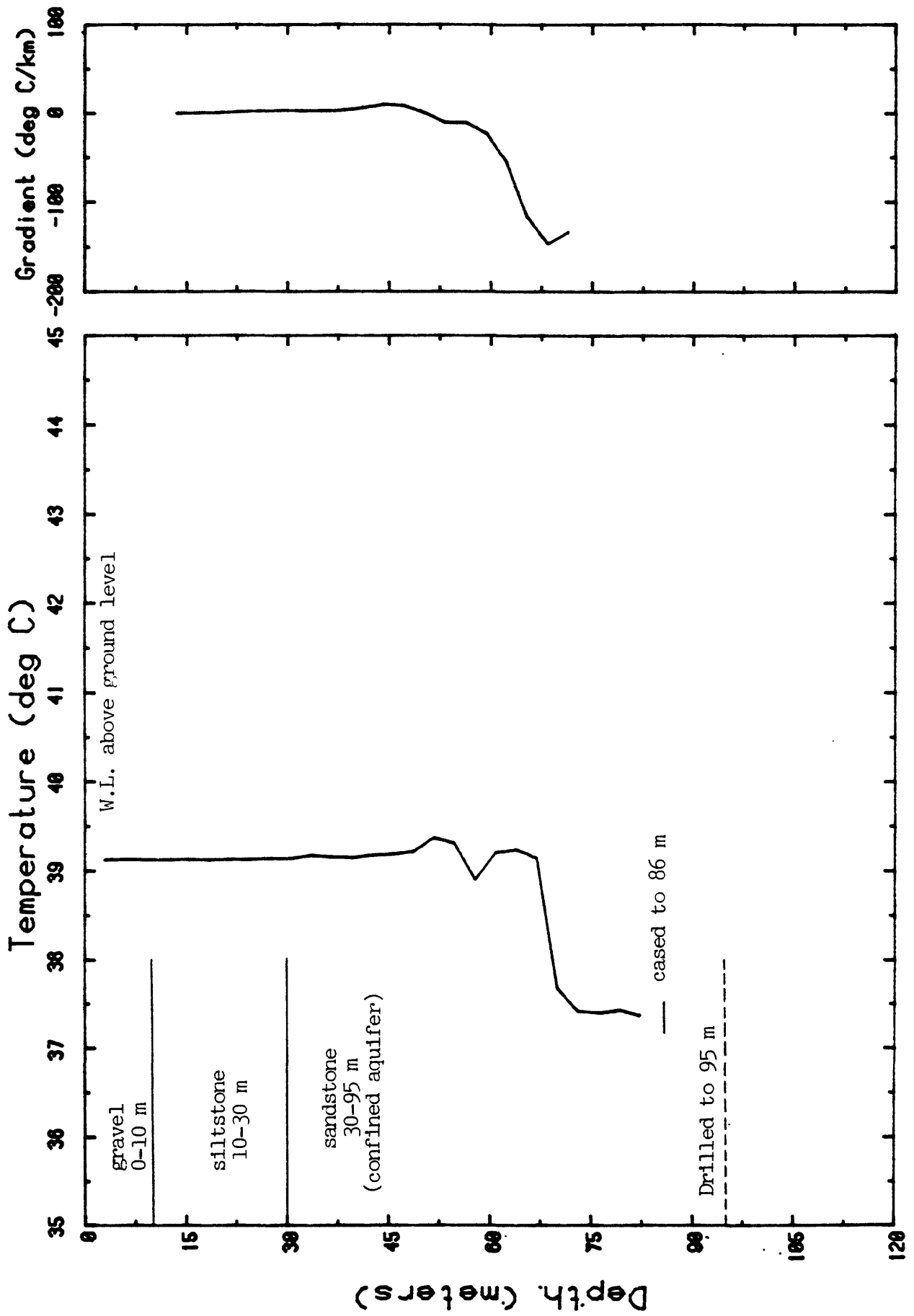| Depth (m)	Temp. (°C)	Depth (m)	Temp. (°C)
3.04	39.11	6.09	39.12
9.14	39.11	12.19	39.11
15.24	39.12	18.28	39.11
21.33	39.12	24.38	39.12
27.43	39.13	30.48	39.13
33.52	39.17	36.57	39.15
39.62	39.15	42.67	39.17
45.72	39.19	48.76	39.21
51.81	39.37	54.86	39.30
57.91	38.9	60.96	39.20
64.00	39.23	67.05	39.14
70.10	37.66	73.15	37.40
76.2	37.39	79.24	37.42
82.29	37.36		

JD03 AUG0783

Figure IIA-3. Temperature profile, geothermal gradient, and lithology of borehole JD03, Jordan. W.L. represents the standing-water level in the borehole.

@JD3 /AUG0783

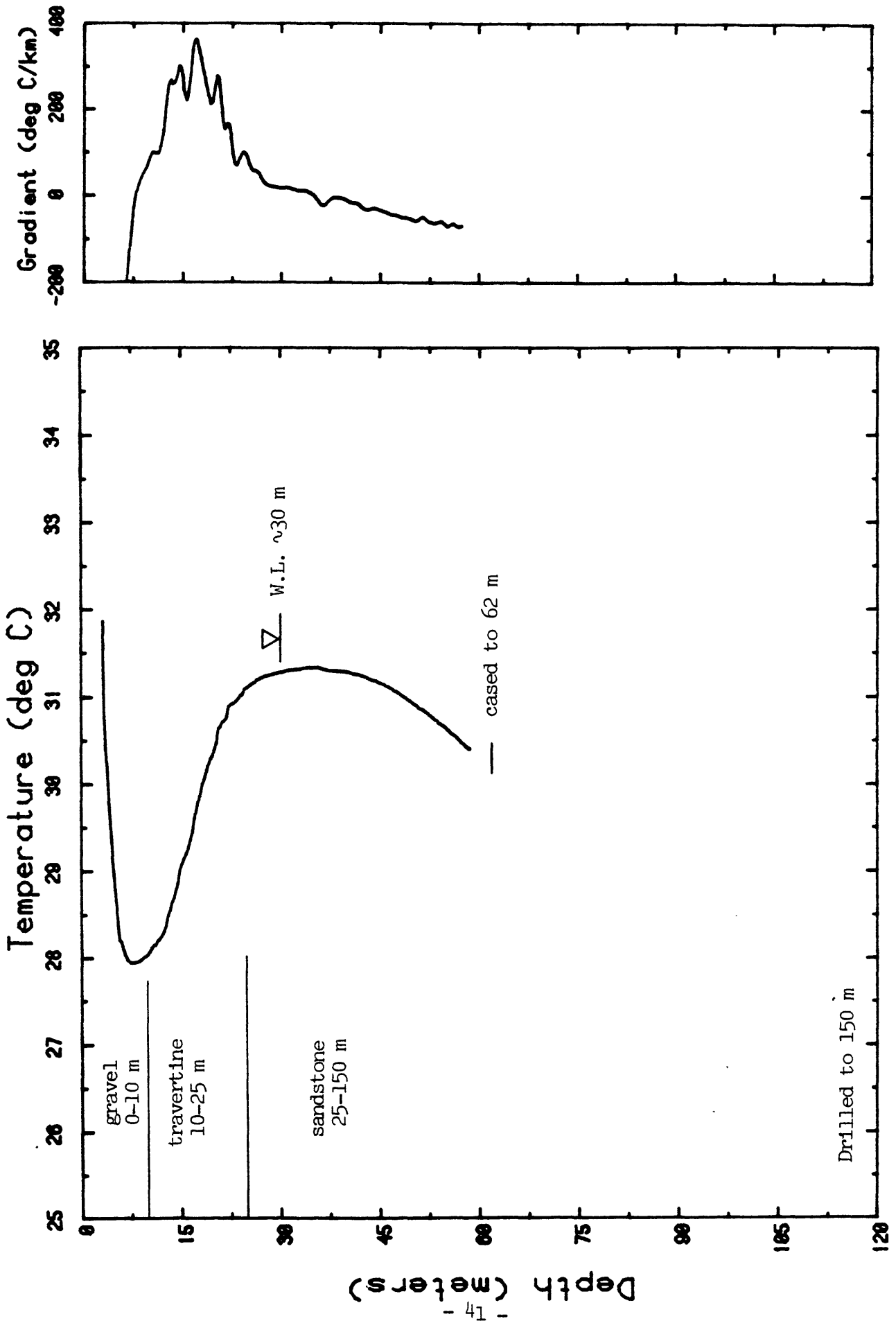| Depth (m)	Temp. (°C)	Depth (m)	Temp. (°C)
1.52	39.20	1.82	39.10
2.13	39.05	2.43	38.97
2.74	38.91	3.04	34.13
3.35	31.19	3.65	30.47
3.96	30.19	4.26	29.75
4.57	29.40	4.87	29.00
5.18	28.74	5.48	28.46
5.79	28.20	6.09	28.17
6.40	28.09	6.70	28.02
7.01	27.97	7.31	27.94
7.62	27.94	7.92	27.94
8.22	27.95	8.53	27.95
8.83	27.97	9.14	27.98
9.44	28.00	9.75	28.02
10.05	28.04	10.36	28.07
10.66	28.11	10.97	28.14
11.27	28.15	11.58	28.20
11.88	28.22	12.19	28.26
12.49	28.31	12.80	28.37
13.10	28.48	13.41	28.55
13.71	28.64	14.02	28.70
14.32	28.79	14.63	28.86
14.93	29.01	15.24	29.08
15.54	29.14	15.84	29.19
16.15	29.26	16.45	29.34
16.76	29.44	17.06	29.60
17.37	29.69	17.67	29.80
17.98	29.88	18.28	30.00
18.59	30.06	18.89	30.13
19.20	30.22	19.50	30.28
19.81	30.32	20.11	30.38
20.42	30.47	20.72	30.64
21.03	30.66	21.33	30.71
21.64	30.73	21.94	30.76
22.25	30.88	22.55	30.91
22.86	30.92	23.16	30.93
23.46	30.95	23.77	30.98
24.07	31.01	24.38	31.03
24.68	31.08	24.99	31.11
25.29	31.12	25.60	31.14
25.90	31.16	26.21	31.17
26.51	31.2	26.82	31.20
27.12	31.22	27.43	31.23
27.73	31.23	28.04	31.24
28.34	31.25	28.65	31.25
28.95	31.26	29.26	31.26
29.56	31.27	29.87	31.27
30.17	31.28	30.48	31.28

@JD3 /AUG0783

Depth (m)	Temp. (°C)	Depth (m)	Temp. (°C)
30.78	31.29	31.08	31.3
31.39	31.30	31.69	31.30
32.00	31.31	32.30	31.31
32.61	31.32	32.91	31.32
33.22	31.32	33.52	31.32
33.83	31.33	34.13	31.33
34.44	31.33	34.74	31.33
35.05	31.33	35.35	31.33
35.66	31.33	35.96	31.32
36.27	31.32	36.57	31.31
36.88	31.30	37.18	31.3
37.49	31.29	37.79	31.29
38.1	31.29	38.40	31.29
38.70	31.29	39.01	31.29
39.31	31.28	39.62	31.28
39.92	31.28	40.23	31.28
40.53	31.27	40.84	31.26
41.14	31.26	41.45	31.25
41.75	31.25	42.06	31.24
42.36	31.23	42.67	31.22
42.97	31.22	43.28	31.20
43.58	31.19	43.89	31.18
44.19	31.18	44.50	31.17
44.80	31.16	45.11	31.15
45.41	31.14	45.72	31.13
46.02	31.11	46.32	31.10
46.63	31.09	46.93	31.07
47.24	31.06	47.54	31.05
47.85	31.04	48.15	31.02
48.46	31.00	48.76	30.99
49.07	30.97	49.37	30.96
49.68	30.94	49.98	30.93
50.29	30.91	50.59	30.89
50.90	30.87	51.20	30.85
51.51	30.84	51.81	30.83
52.12	30.81	52.42	30.79
52.73	30.77	53.03	30.75
53.34	30.73	53.64	30.72
53.94	30.69	54.25	30.68
54.55	30.66	54.86	30.65
55.16	30.62	55.47	30.60
55.77	30.57	56.08	30.56
56.38	30.54	56.69	30.52
56.99	30.5	57.30	30.47
57.60	30.46	57.91	30.43
58.21	30.41	58.52	30.4

Figure IIA-4. Temperature profile, geothermal gradient, and lithology of borehole JD04, Jordan. W.L. represents the standing-water level in the borehole.
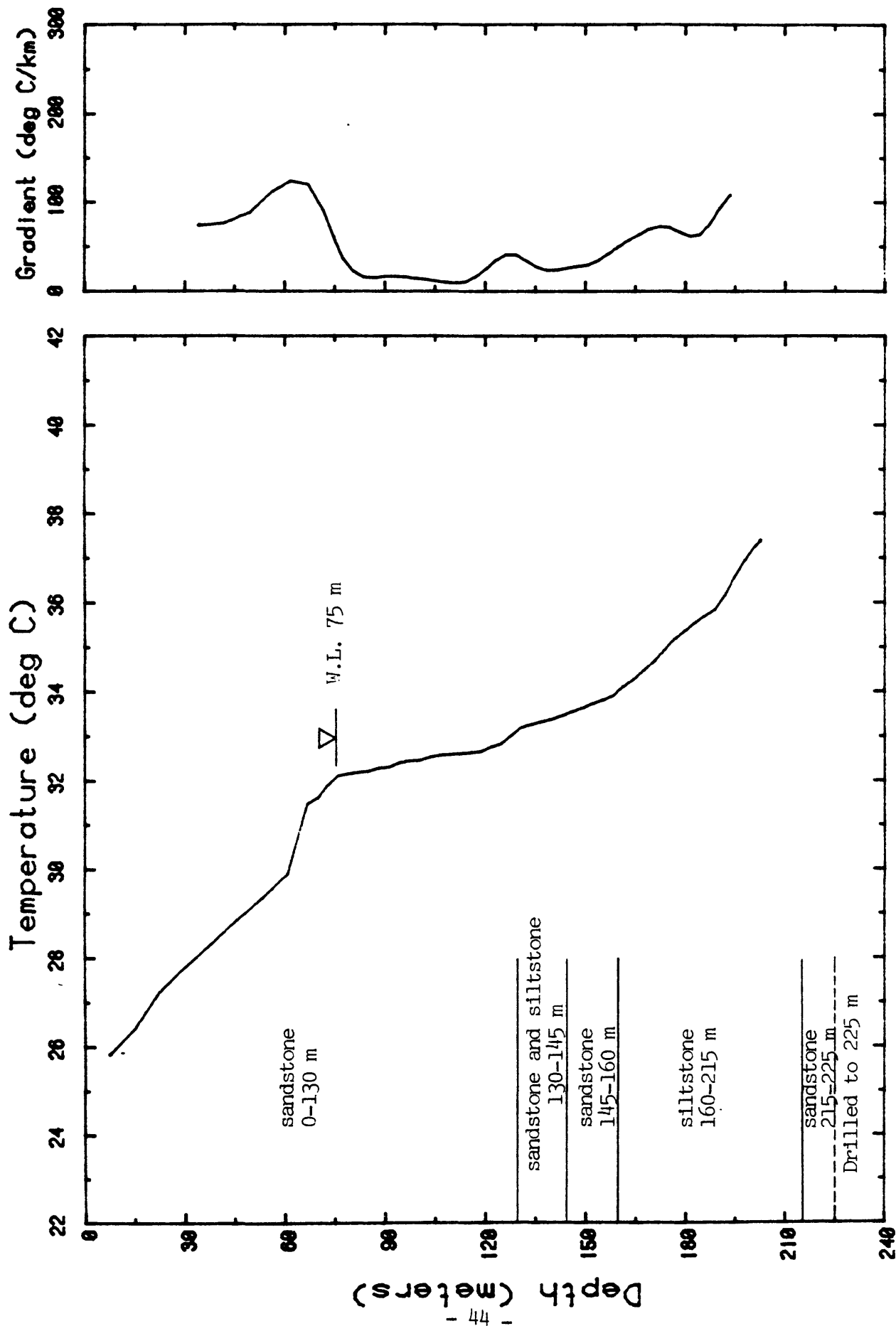
JD04 AUG2083

TABLE IIA-4

Depth (m)	Temp. (°C)	Depth (m)	Temp. (°C)
7.62	25.83	15.24	26.40
22.86	27.25	30.48	27.80
38.1	28.30	45.72	28.84
53.34	29.34	60.96	29.90
67.05	31.49	70.10	31.61
73.15	31.90	76.2	32.10
79.24	32.16	82.29	32.19
85.34	32.21	88.39	32.28
91.44	32.30	94.48	32.40
97.53	32.43	100.58	32.45
103.63	32.52	106.68	32.57
109.72	32.57	112.77	32.60
115.82	32.62	118.87	32.65
121.92	32.75	124.96	32.81
128.01	33.00	131.06	33.19
134.11	33.26	137.16	33.31
140.20	33.37	143.25	33.45
146.30	33.54	149.35	33.62
152.4	33.71	155.44	33.79
158.49	33.89	161.54	34.10
164.59	34.26	167.64	34.45
170.68	34.66	173.73	34.91
176.78	35.18	179.83	35.35
182.88	35.54	185.92	35.69
188.97	35.84	192.02	36.15
195.07	36.59	198.12	36.96
201.16	37.27	202.75	37.39

Figure IIA-5. Temperature profile, geothermal gradient, and lithology of borehole JD05, Jordan. W.L. represents standing-water level in the borehole.

TABLE IIA-5

JD05/AUG1983

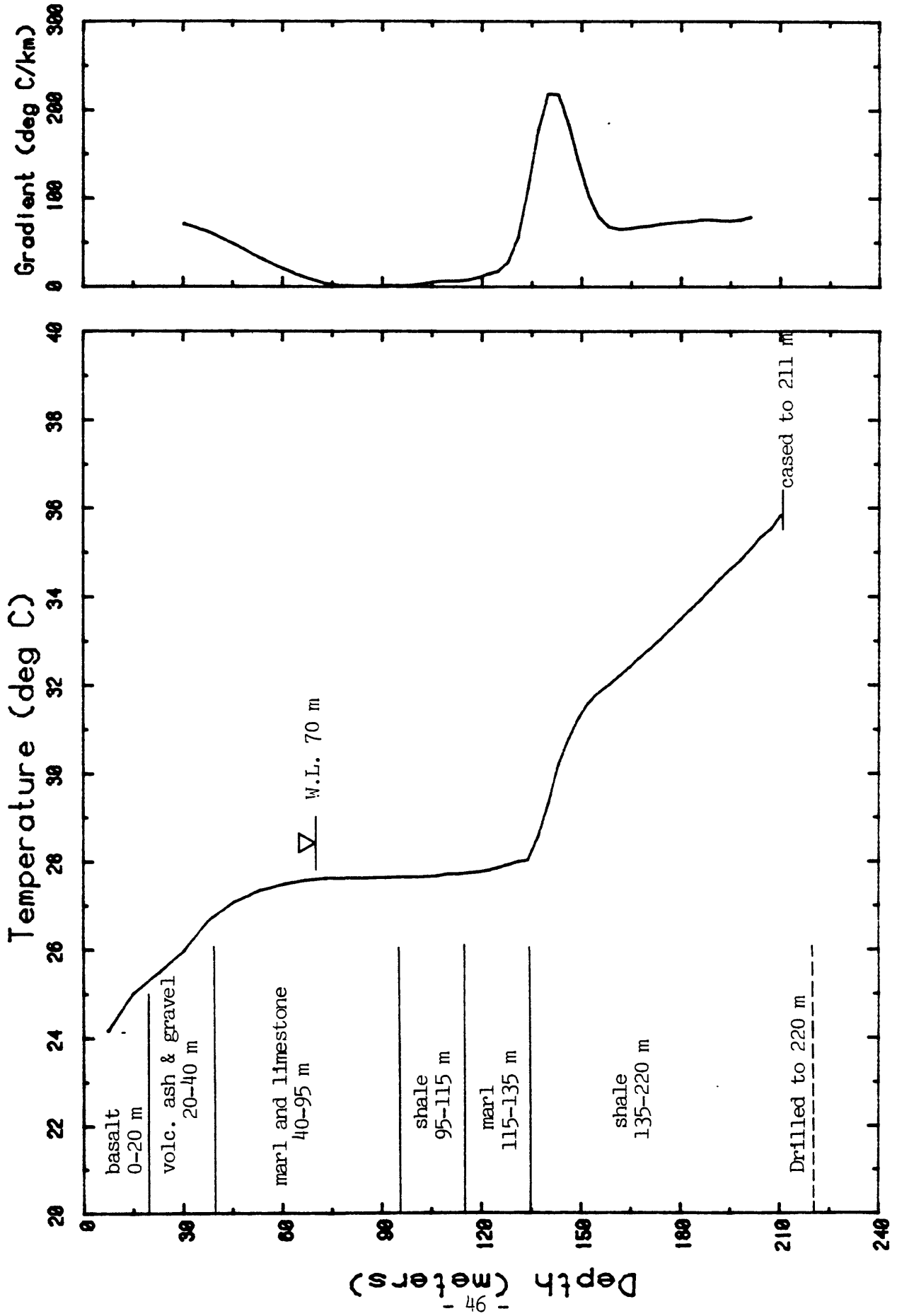| Depth (m)	Temp. (°C)	Depth (m)	Temp. (°C)
7.62	24.16	15.24	25.00
22.86	25.47	30.48	25.98
38.1	26.67	45.72	27.08
53.34	27.35	60.96	27.51
67.05	27.59	70.10	27.61
73.15	27.63	76.2	27.63
79.24	27.63	82.29	27.63
85.34	27.63	88.39	27.64
91.44	27.64	94.48	27.65
97.53	27.65	100.58	27.66
103.63	27.67	106.68	27.68
109.72	27.73	112.77	27.72
115.82	27.75	118.87	27.77
121.92	27.81	124.96	27.86
128.01	27.93	131.06	28.00
134.11	28.03	137.16	28.55
140.20	29.29	143.25	30.19
146.30	30.77	149.35	31.25
152.4	31.59	155.44	31.82
158.49	32.004	161.54	32.19
164.59	32.392	167.64	32.61
170.68	32.805	173.73	33.01
176.78	33.246	179.83	33.47
182.88	33.694	185.92	33.91
188.97	34.156	192.02	34.40
195.07	34.626	198.12	34.81
201.16	35.071	204.21	35.34
207.26	35.535	210.31	35.83

Figure IIA-6.   Temperature profile, geothermal gradient, and lithology of borehole JD06, Jordan.
W.L. represents standing-water level in the borehole.

JD06 AUG0683

9JD06/AUG0683

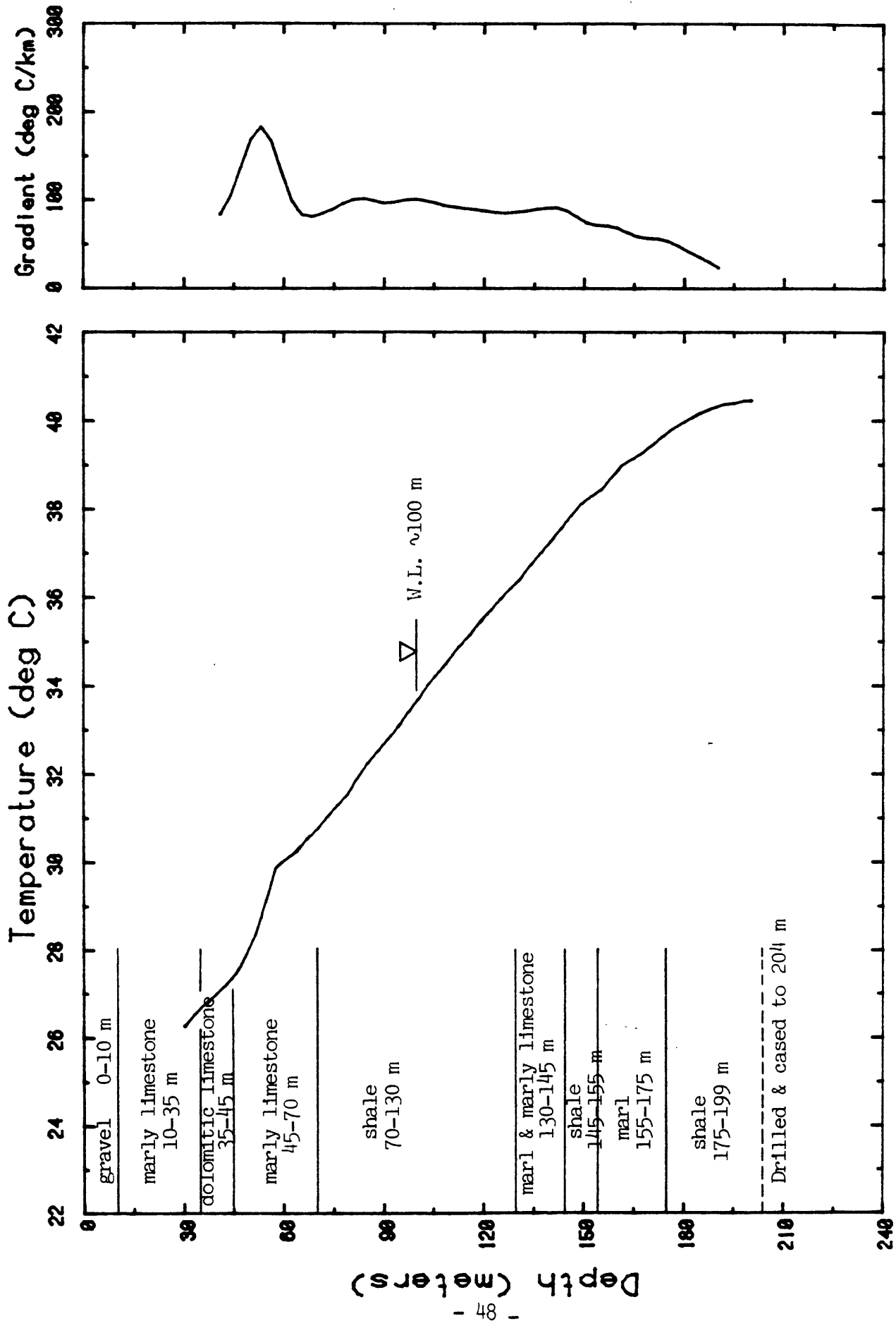| Depth (m)	Temp. (°C)	Depth (m)	Temp. (°C)
30.48	26.27	33.52	26.54
36.57	26.77	39.62	26.97
42.67	27.19	45.72	27.44
48.76	27.84	51.81	28.35
54.86	29.09	57.91	29.86
60.96	30.07	64.00	30.23
67.05	30.51	70.10	30.74
73.15	31.02	76.2	31.28
79.24	31.52	82.29	31.90
85.34	32.23	88.39	32.52
91.44	32.78	94.48	33.06
97.53	33.40	100.58	33.70
103.63	34.04	106.68	34.30
109.72	34.58	112.77	34.88
115.82	35.14	118.87	35.42
121.92	35.68	124.96	35.95
128.01	36.20	131.06	36.43
134.11	36.74	137.16	36.99
140.20	37.26	143.25	37.55
146.30	37.85	149.35	38.12
152.4	38.30	155.44	38.45
158.49	38.72	161.54	38.99
164.59	39.14	167.64	39.27
170.68	39.46	173.73	39.66
176.78	39.83	179.83	39.96
182.88	40.09	185.92	40.21
188.97	40.30	192.02	40.38
195.07	40.40	198.12	40.46
200.25	40.46		
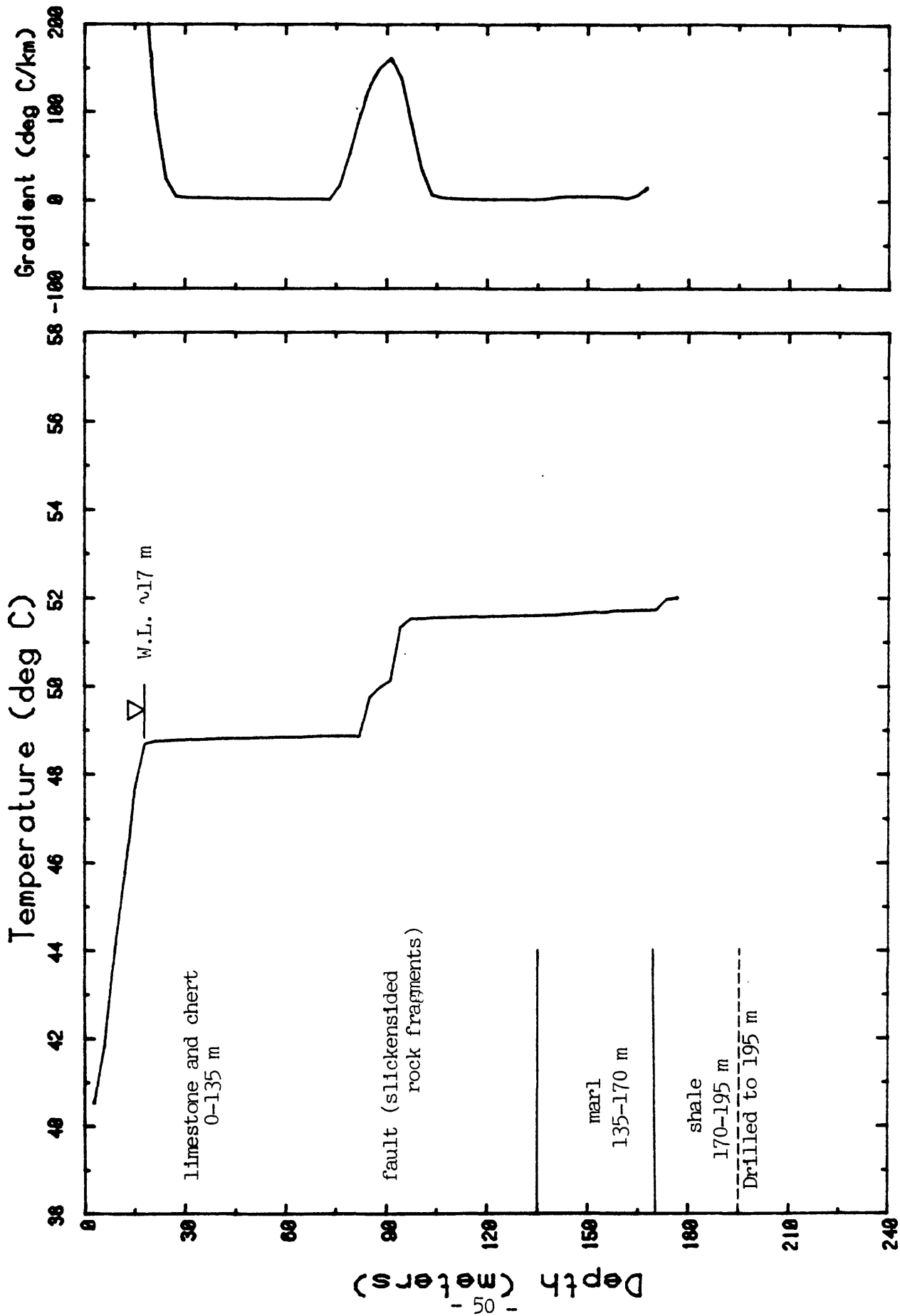
Figure IIA-7. Temperature profile, geothermal gradient, and lithology of borehole JD06, Jordan. W.L. represents standing-water level in the borehole.
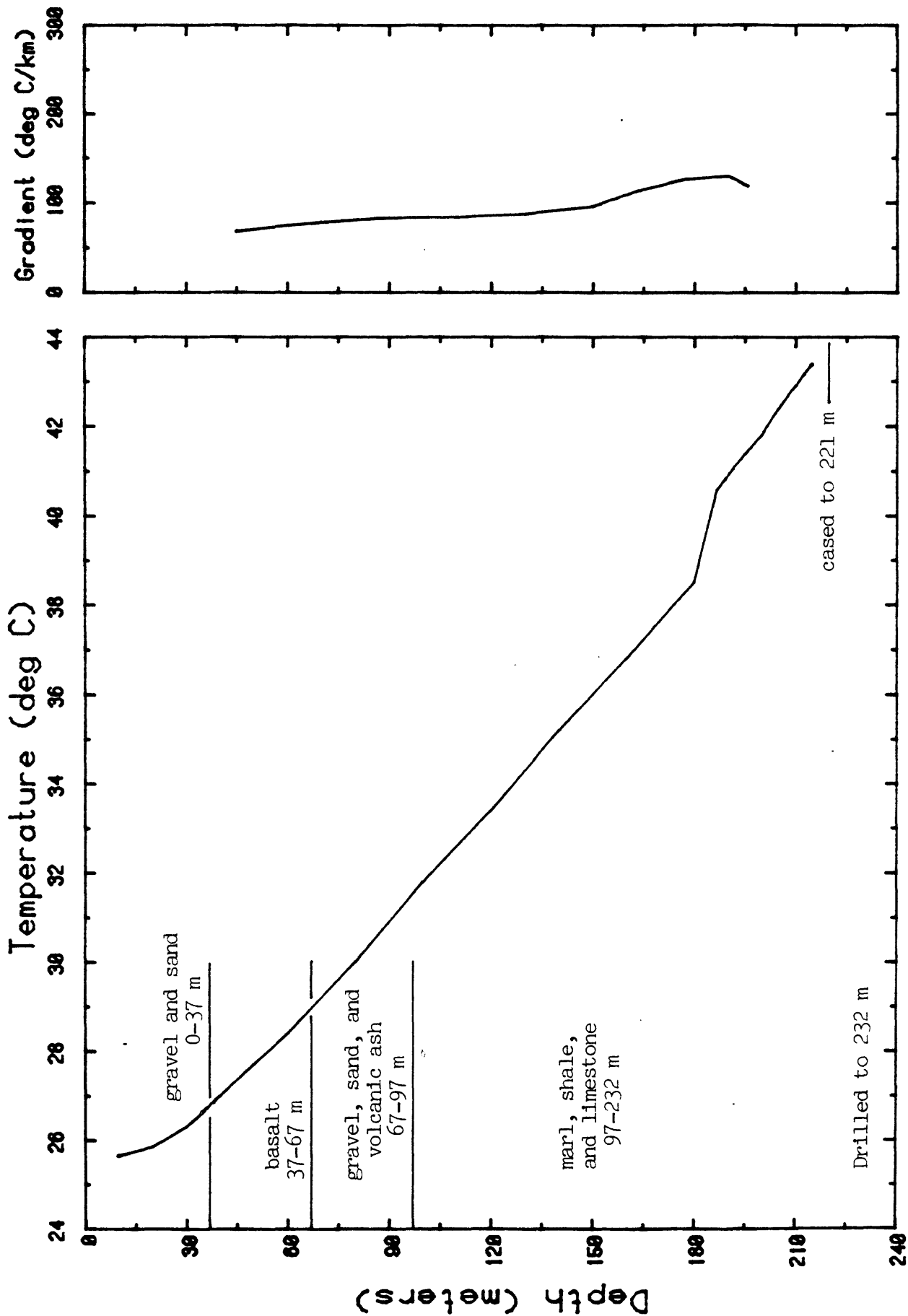
Figure IIA-8. Temperature profile and geothermal gradient of borehole JD08, Jordan.

@JD07/AUG2083

Depth (m)	Temp. (°C)	Depth (m)	Temp. (°C)
3.04	40.54	6.09	41.85
9.14	43.97	12.19	45.76
15.24	47.71	18.28	48.69
21.33	48.76	24.38	48.77
27.43	48.77	30.48	48.78
33.52	48.79	36.57	48.80
39.62	48.81	42.67	48.81
45.72	48.82	48.76	48.82
51.81	48.83	54.86	48.84
57.91	48.84	60.96	48.85
64.00	48.85	67.05	48.86
70.10	48.87	73.15	48.87
76.2	48.87	79.24	48.87
82.29	48.87	85.34	49.77
88.39	49.99	91.44	50.14
94.48	51.35	97.53	51.53
100.58	51.53	103.63	51.55
106.68	51.56	109.72	51.56
112.77	51.57	115.82	51.57
118.87	51.58	121.92	51.58
124.96	51.59	128.01	51.59
131.06	51.60	134.11	51.60
137.16	51.61	140.20	51.61
143.25	51.63	146.30	51.65
149.35	51.67	152.4	51.68
155.44	51.68	158.49	51.72
161.54	51.72	164.59	51.72
167.64	51.73	170.68	51.74
173.73	51.97	176.78	52.01
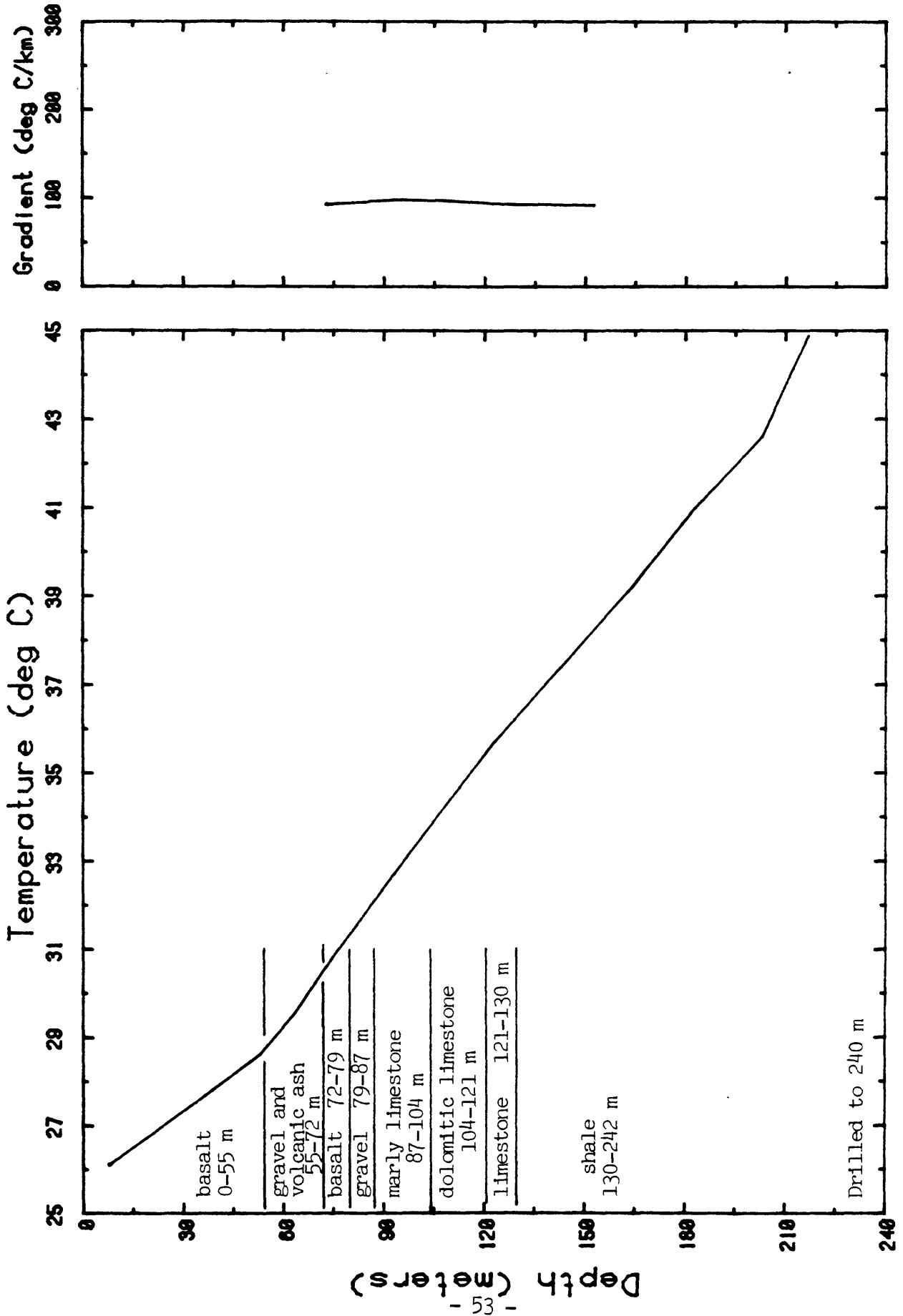
Figure IIA-9. Temperature profile and geothermal gradient of borehole JD09, Jordan.
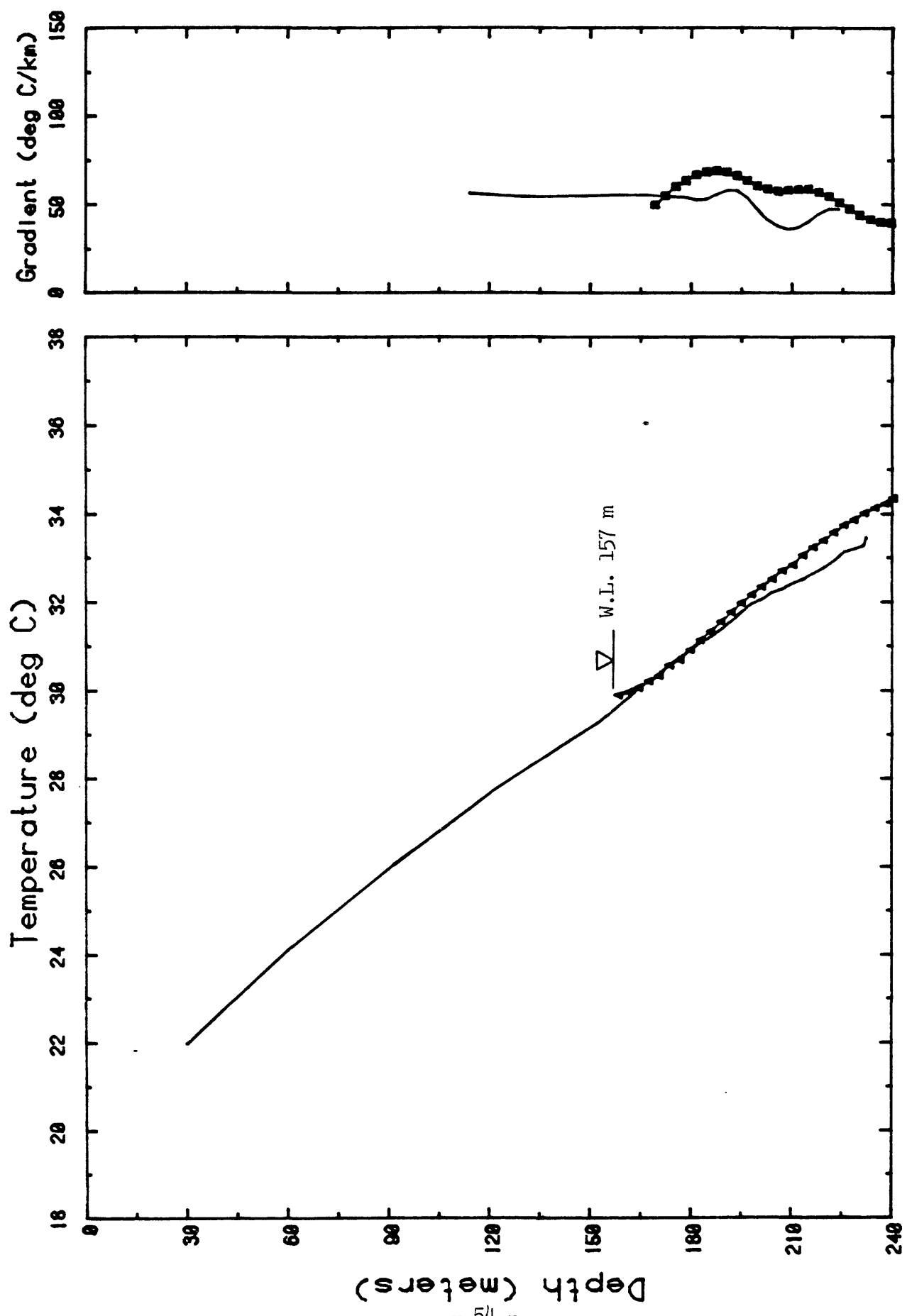
JD09 NOV1383

Figure IIA-10. Temperature profiles and geothermal gradients of boreholes JD10 and JD11, Jordan.

@JD10/AUG1083

Depth (m)	Temp. (°C)	Depth (m)	Temp. (°C)
30.48	21.99	60.96	24.16
91.44	26.03	106.68	26.88
121.92	27.76	137.16	28.53
152.4	29.28	173.73	30.58
176.78	30.76	179.83	30.91
182.88	31.07	185.92	31.21
188.97	31.39	192.02	31.56
195.07	31.77	198.12	31.96
201.16	32.07	204.21	32.21
207.26	32.30	210.31	32.42
213.36	32.51	216.40	32.64
219.45	32.77	222.50	32.93
225.55	33.14	228.6	33.21
231.64	33.29	232.25	33.46

@JD11/AUG1083

Depth (m)	Temp. (°C)	Depth (m)	Temp. (°C)
158.49	29.89	161.54	29.97
164.59	30.07	167.64	30.21
170.68	30.34	173.73	30.57
176.78	30.69	179.83	30.91
182.88	31.14	185.92	31.33
188.97	31.55	192.02	31.76
195.07	31.97	198.12	32.16
201.16	32.34	204.21	32.52
207.26	32.71	210.31	32.84
213.36	33.06	216.40	33.24
219.45	33.40	222.50	33.58
225.55	33.74	228.6	33.87
231.64	34.02	234.69	34.14
237.74	34.23	240.79	34.39
243.84	34.50	246.88	34.57
249.93	34.79		

APPENDIX IIB. Individual borehole logs and tabulated temperatures,

Jordan Reconnaissance
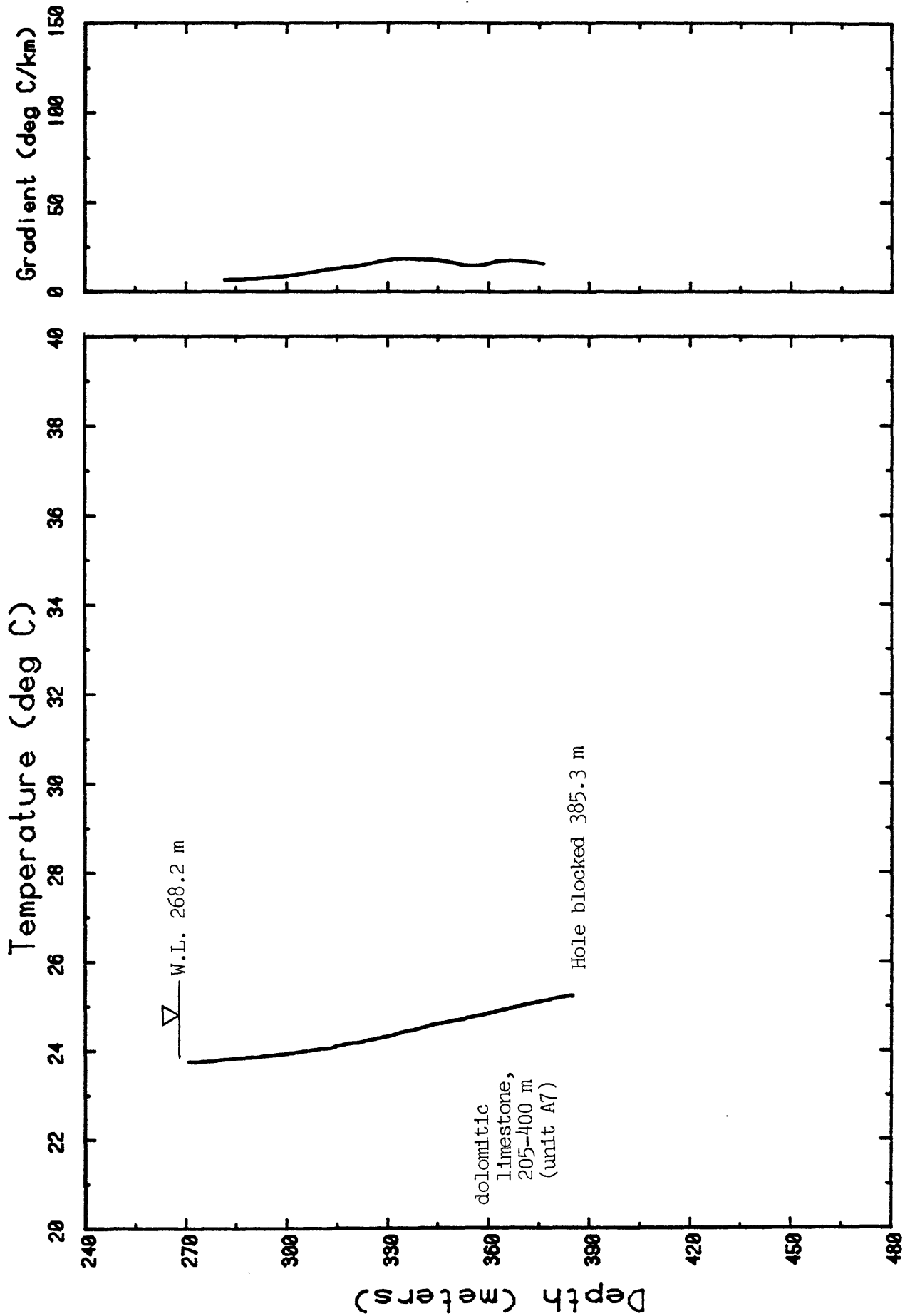
JD12 (QUMEIM S-18) AUG1183

Figure IIB-1

@JD12/AUG1183

Depth (m)	Temp. (°C)	Depth (m)	Temp. (°C)
271.27	23.74	274.32	23.76
277.36	23.77	280.41	23.79
283.46	23.81	286.51	23.83
289.56	23.85	292.60	23.87
295.65	23.9	298.70	23.92
304.8	23.98	307.84	24.01
310.89	24.04	313.94	24.08
316.99	24.13	320.04	24.16
323.08	24.21	326.13	24.25
329.18	24.31	332.23	24.36
335.28	24.43	338.32	24.48
341.37	24.54	344.42	24.59
347.47	24.64	350.52	24.70
353.56	24.74	356.61	24.77
359.66	24.82	362.71	24.87
365.76	24.93	368.80	24.98
371.85	25.04	374.90	25.08
377.95	25.13	381	25.18
384.04	25.23	385.26	25.23

Temperature (deg C) / Gradient (deg C/km) vs Depth (meters)

chalk and marl, 0-120 m
(unit B3)

W.L. 158.5 m

phosphatic marl and chert, (B2)

shale, 230-280 m (B1-2)

dolomitic limestone,
280-500 m
(unit A7)

shale and marl,
500-890 m
(units A4-6)

marly limestone,
890-1000 m
(unit A-3)

bituminous shale,
1000-1075 m
(units A1-2)

Kurnub sandstone

end of cable 917.4 m
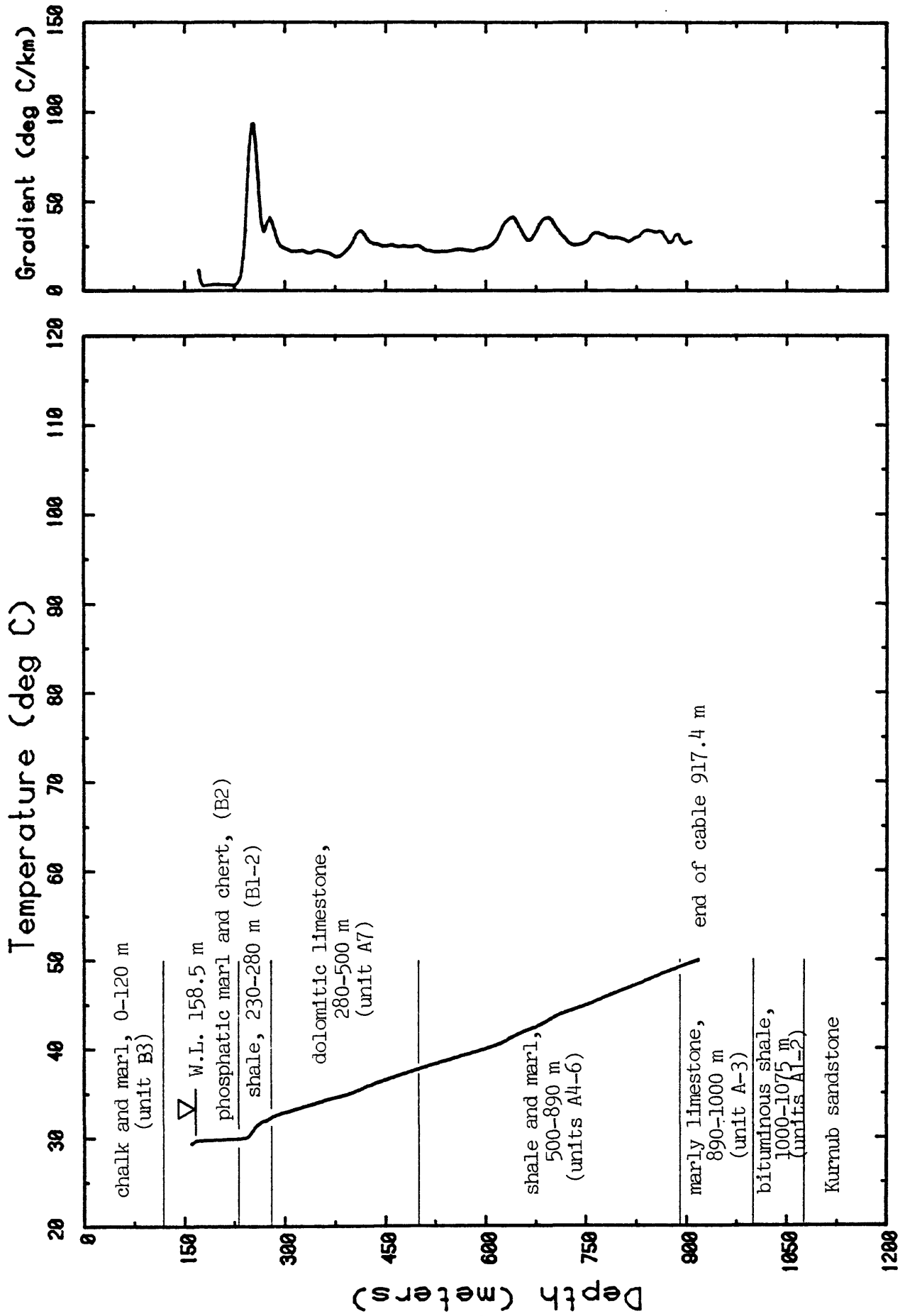
JD13 (RAMTHA S-90) AUG11183

Figure IIB-2

@JD13/AUG1183

Depth (m)	Temp. (°C)	Depth (m)	Temp. (°C)
161.54	29.37	164.59	29.53
167.64	29.72	170.68	29.74
173.73	29.75	176.78	29.74
179.83	29.76	182.88	29.77
185.92	29.78	188.97	29.78
192.02	29.79	195.07	29.81
198.12	29.82	201.16	29.83
204.21	29.84	207.26	29.85
210.31	29.86	213.36	29.87
216.40	29.88	219.45	29.89
222.50	29.90	225.55	29.91
228.6	29.91	231.64	29.92
234.69	29.93	237.74	29.98
240.79	29.99	243.84	30.01
246.88	30.22	249.93	30.50
252.98	30.83	256.03	31.20
259.08	31.43	262.12	31.62
265.17	31.79	268.22	31.87
271.27	31.94	274.32	32.01
277.36	32.18	280.41	32.31
283.46	32.44	286.51	32.53
289.56	32.63	292.60	32.70
295.65	32.78	298.70	32.85
301.75	32.92	304.8	33.00
307.84	33.06	310.89	33.13
313.94	33.20	316.99	33.27
320.04	33.33	323.08	33.40
326.13	33.47	329.18	33.54
332.23	33.60	335.28	33.67
339.32	33.73	341.37	33.80
344.42	33.86	347.47	33.93
350.52	34.01	353.56	34.07
356.61	34.13	359.66	34.21
362.71	34.27	365.76	34.33
368.80	34.40	371.85	34.46
374.90	34.52	377.95	34.57
381	34.63	384.04	34.70
387.09	34.75	390.14	34.82
393.19	34.88	396.24	34.97
399.28	35.04	402.33	35.11
405.38	35.21	408.43	35.31
411.48	35.40	414.52	35.52
417.57	35.63	420.62	35.71
423.67	35.81	426.72	35.89
429.76	35.97	432.81	36.05
435.86	36.13	438.91	36.21
441.96	36.29	445.00	36.37
448.05	36.44	451.10	36.51
454.15	36.6	457.2	36.67
460.24	36.75	463.29	36.83
466.34	36.91	469.39	36.98

Depth (m)	Temp. (°C)	Depth (m)	Temp. (°C)
472.44	37.05	475.48	37.13
478.53	37.20	481.58	37.29
484.63	37.36	487.68	37.43
490.72	37.51	493.77	37.58
496.82	37.66	499.87	37.74
502.92	37.82	505.96	37.89
509.01	37.96	512.06	38.03
515.11	38.09	518.16	38.17
521.20	38.23	524.25	38.30
527.30	38.37	530.35	38.43
533.4	38.50	536.44	38.57
539.49	38.63	542.54	38.7
545.59	38.77	548.64	38.83
551.68	38.90	554.73	38.97
557.78	39.05	560.83	39.11
563.88	39.19	566.92	39.26
569.97	39.33	573.02	39.40
576.07	39.46	579.12	39.54
582.16	39.60	585.21	39.67
588.26	39.74	591.31	39.81
594.36	39.88	597.40	39.96
600.45	40.03	603.50	40.11
606.55	40.17	609.6	40.26
612.64	40.34	615.69	40.42
618.74	40.51	621.79	40.60
624.84	40.70	627.88	40.83
630.93	40.94	633.98	41.06
637.03	41.13	640.08	41.31
643.12	41.44	646.17	41.57
649.22	41.69	652.27	41.80
655.32	41.89	658.36	42.00
661.41	42.08	664.46	42.16
667.51	42.25	670.56	42.34
673.60	42.42	676.65	42.53
679.70	42.64	682.75	42.74
685.8	42.87	688.84	42.99
691.89	43.12	694.94	43.24
697.99	43.37	701.04	43.51
704.08	43.61	707.13	43.72
710.18	43.83	713.23	43.92
716.28	44.02	719.32	44.11
722.37	44.19	725.42	44.28
728.47	44.35	731.52	44.44
734.56	44.51	737.61	44.58
740.66	44.67	743.71	44.75
746.76	44.83	749.80	44.91
752.85	45.00	755.90	45.08
758.95	45.17	762	45.28
765.04	45.38	768.09	45.48
771.14	45.58	774.19	45.67
777.24	45.77	780.28	45.87
783.33	45.96	786.38	46.05
789.43	46.13	792.48	46.23
795.52	46.32	798.57	46.42

Depth (m)	Temp. (°C)	Depth (m)	Temp. (°C)
801.62	46.50	804.67	46.59
807.72	46.68	810.76	46.77
813.81	46.85	816.86	46.93
819.91	47.02	822.96	47.11
826.00	47.20	829.05	47.30
832.10	47.39	835.15	47.47
838.2	47.60	841.24	47.70
844.29	47.78	847.34	47.91
850.39	48.00	853.44	48.10
856.48	48.21	859.53	48.29
862.58	48.41	865.63	48.53
868.68	48.61	871.72	48.69
874.77	48.78	877.82	48.86
880.87	48.94	883.92	48.99
886.96	49.17	890.01	49.24
893.06	49.32	896.11	49.4
899.16	49.48	902.20	49.56
905.25	49.64	908.30	49.72
911.35	49.83	914.4	49.9
917.44	49.99		

Temperature (deg C)

Depth (meters)

dry hole
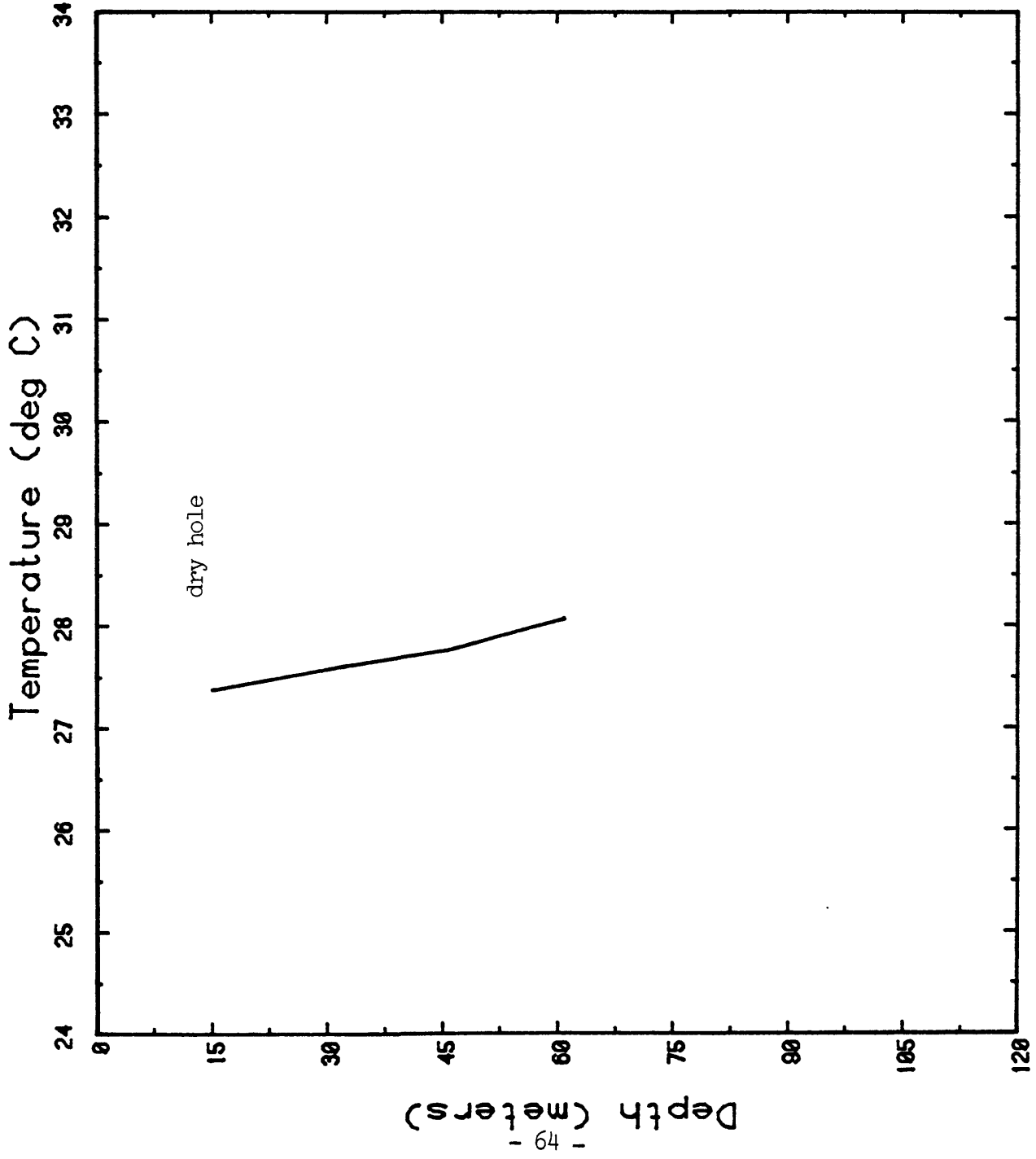
JD14 (JRV-12) AUG0883

Figure IIB-3

TABLE IIB-3

@JD14/AUG0883

Depth (m)	Temp. (^oC)	Depth (m)	Temp. (^oC)
15.24	27.37	30.48	27.58
45.72	27.76	60.96	28.07

Gradient (deg C/km)

Temperature (deg C)

Depth (meters)

W.L. 68.6 m
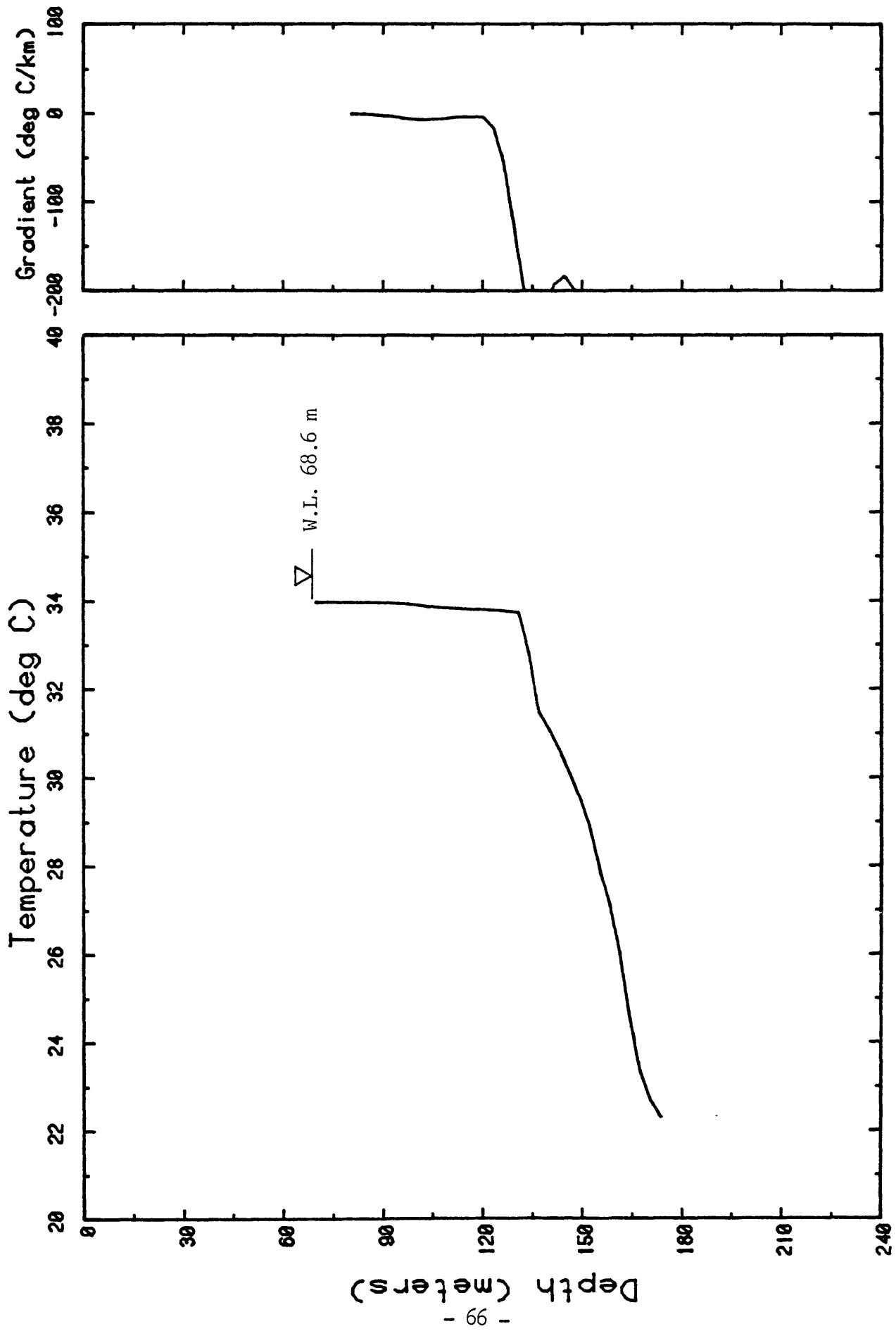
JD15 (JRV-5) AUG0983

Figure IIB-4

@JD15/AUG0983

Depth (m)	Temp. (°C)	Depth (m)	Temp. (°C)
70.10	33.96	73.15	33.97
76.2	33.97	79.24	33.96
82.29	33.96	85.34	33.96
88.39	33.95	91.44	33.95
94.488	33.93	97.53	33.92
100.58	33.90	103.63	33.87
106.68	33.85	109.72	33.83
112.77	33.82	115.82	33.81
118.87	33.80	121.92	33.79
124.96	33.77	128.01	33.75
131.06	33.72	134.11	32.81
137.16	31.47	140.20	31.08
143.25	30.64	146.30	30.10
149.35	29.57	152.4	28.90
155.44	27.93	158.49	27.13
161.54	26.03	164.59	24.52
167.64	23.33	170.68	22.67
173.73	22.3		
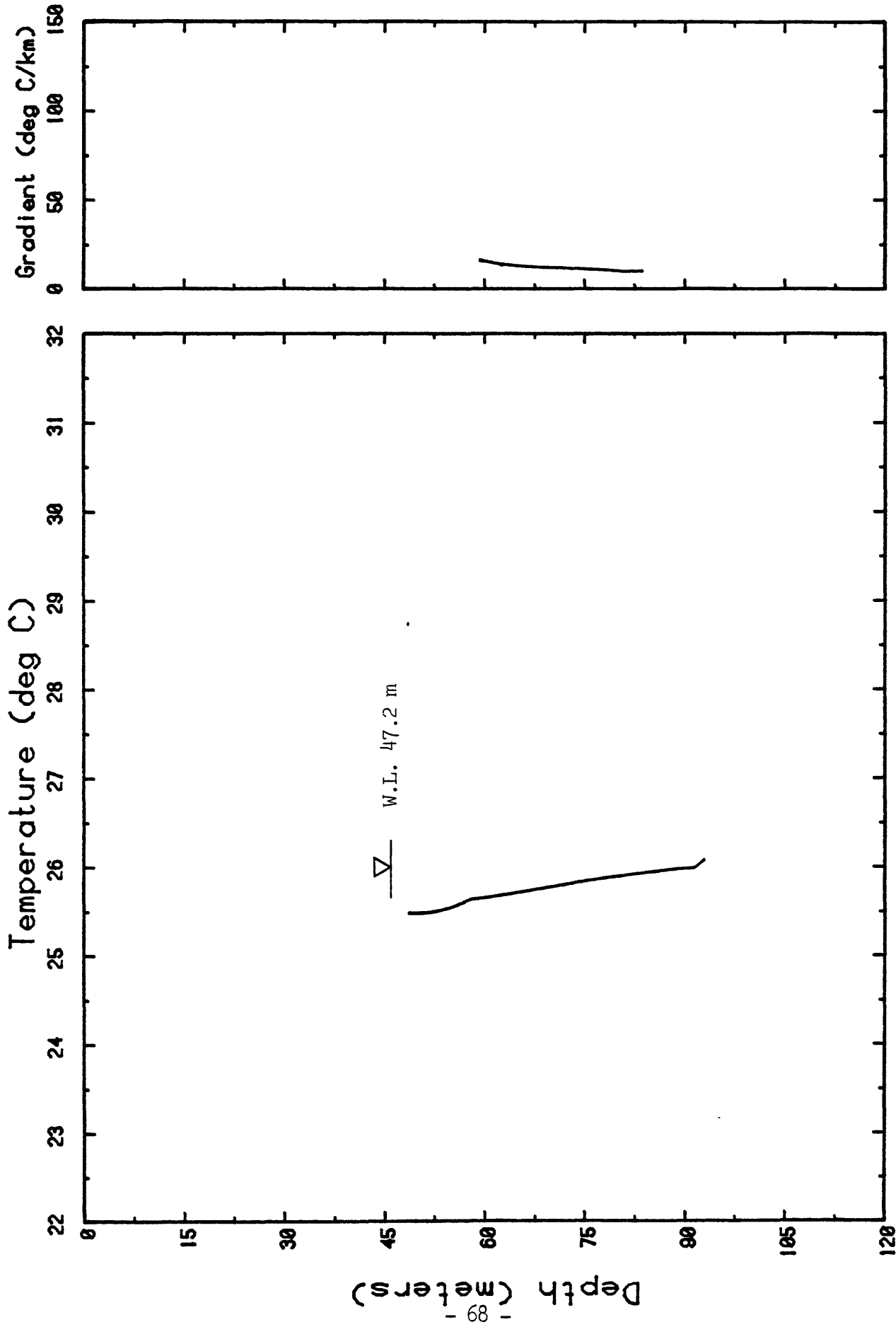
JD16 (JRV-6) AUG0983

Figure IIB-5

TABLE IIB-5

@JD16/AUG0983

Depth (m)	Temp. (°C)	Depth (m)	Temp. (°C)
48.76	25.48	51.81	25.49
54.86	25.54	57.91	25.63
60.96	25.67	64.00	25.70
67.05	25.74	70.10	25.78
73.15	25.82	76.2	25.85
79.24	25.89	82.29	25.92
85.34	25.95	88.39	25.97
91.44	25.99	92.96	26.08
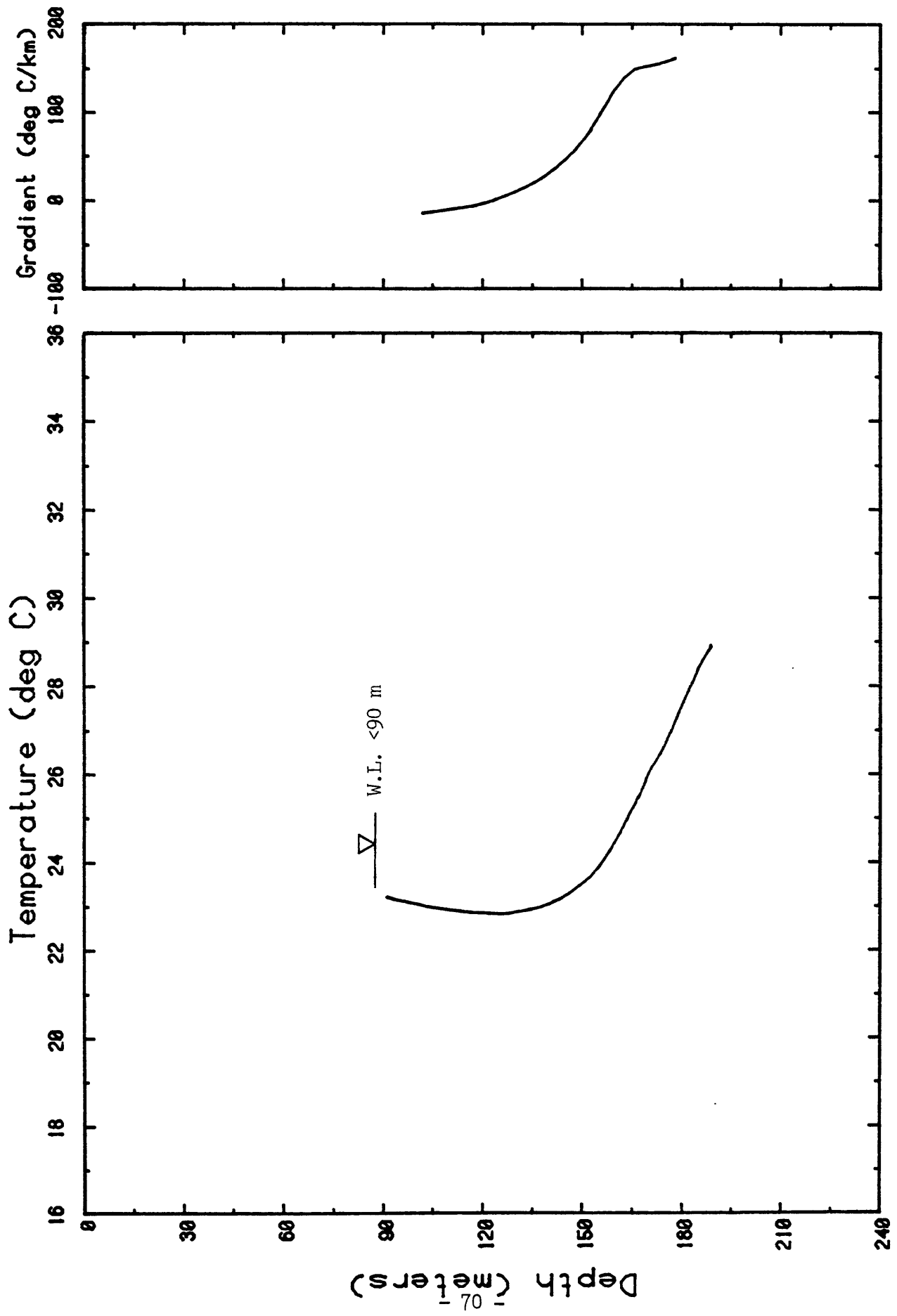
JD17 (JRV-7) AUG0983

Figure IIB-6

@JD17/AUG0983

Depth (m)	Temp. (°C)	Depth (m)	Temp. (°C)
91.44	23.20	94.488	23.14
97.53	23.08	100.58	23.04
103.63	22.99	106.68	22.95
109.72	22.91	112.77	22.89
115.82	22.86	118.87	22.84
121.92	22.83	124.96	22.83
128.01	22.84	131.06	22.88
134.11	22.91	137.16	22.97
140.20	23.05	143.25	23.16
146.30	23.29	149.35	23.47
152.4	23.65	155.44	23.91
158.49	24.23	161.54	24.64
164.59	25.10	167.64	25.53
170.68	26.10	173.73	26.47
176.78	26.94	179.83	27.50
182.88	28.00	185.92	28.50
188.97	28.90		
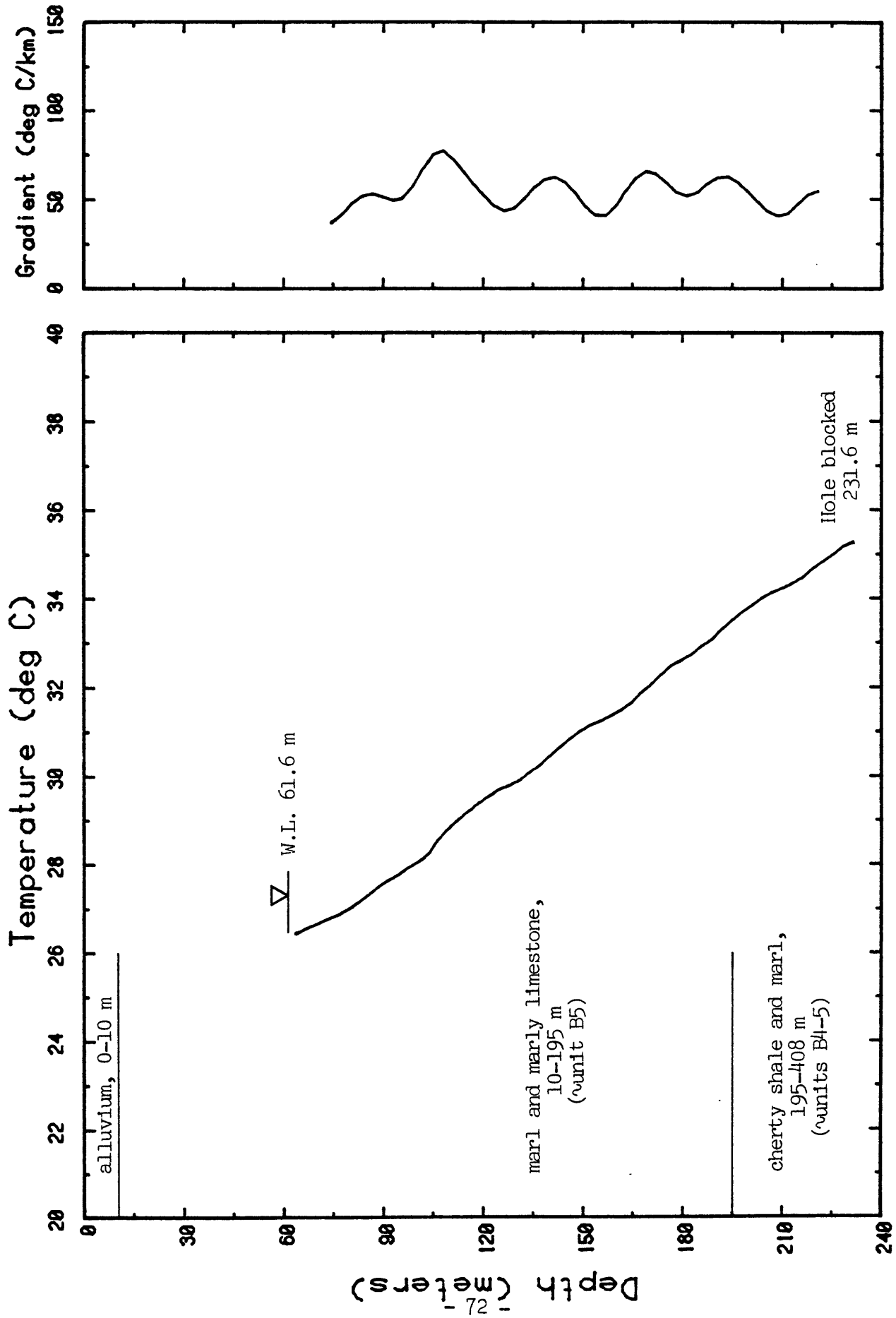
JD18 (WADI GHADAF #1) AUG1683

Figure IIB-7

TABLE IIB-7

8JD18/AUG1683

Depth (m)	Temp. (°C)	Depth (m)	Temp. (°C)
64.00	26.43	67.05	26.56
70.10	26.65	73.15	26.75
76.2	26.85	79.24	26.97
82.29	27.12	85.34	27.29
88.39	27.48	91.44	27.64
94.48	27.75	97.53	27.92
100.58	28.06	103.63	28.23
106.68	28.55	109.72	28.81
112.77	29.02	115.82	29.20
118.87	29.39	121.92	29.55
124.96	29.70	128.01	29.79
131.06	29.90	134.11	30.08
137.16	30.24	140.20	30.45
143.25	30.65	146.30	30.84
149.35	31.01	152.4	31.15
155.44	31.24	158.49	31.35
161.54	31.47	164.59	31.64
167.64	31.86	170.68	32.07
173.73	32.28	176.78	32.48
179.83	32.61	182.88	32.71
185.92	32.92	188.97	33.07
192.02	33.30	195.07	33.50
198.12	33.69	201.16	33.83
204.21	34.01	207.26	34.13
210.31	34.22	213.36	34.34
216.40	34.46	219.45	34.68
222.50	34.84	225.55	35.00
228.6	35.18	231.64	35.26
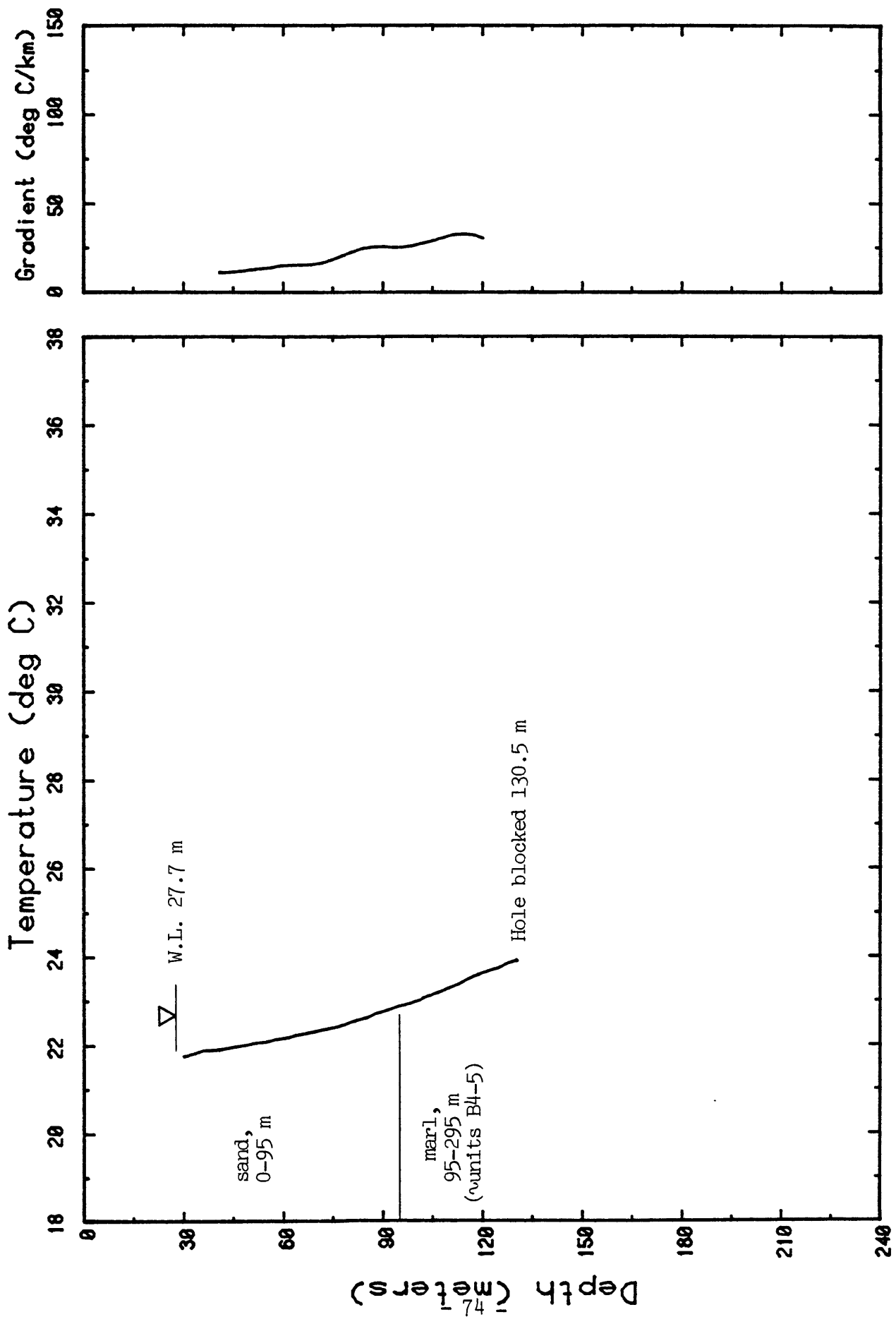
Figure IIB-8

JD19 (WADI RAJIL #1) AUG1683

TABLE IIB-8

Depth (m)	Temp. (°C)	Depth (m)	Temp. (°C)
30.48	21.76	33.52	21.82
36.57	21.89	39.62	21.90
42.67	21.93	45.72	21.97
48.76	22.01	51.81	22.05
54.86	22.08	57.91	22.13
60.96	22.17	64.00	22.22
67.05	22.27	70.10	22.31
73.15	22.36	76.2	22.41
79.24	22.48	82.29	22.55
85.34	22.61	88.39	22.71
91.44	22.78	94.48	22.87
97.53	22.92	100.5	23.01
103.63	23.10	106.68	23.18
109.72	23.28	112.77	23.36
115.82	23.49	118.87	23.59
121.92	23.68	124.96	23.74
128.01	23.86	130.45	23.91
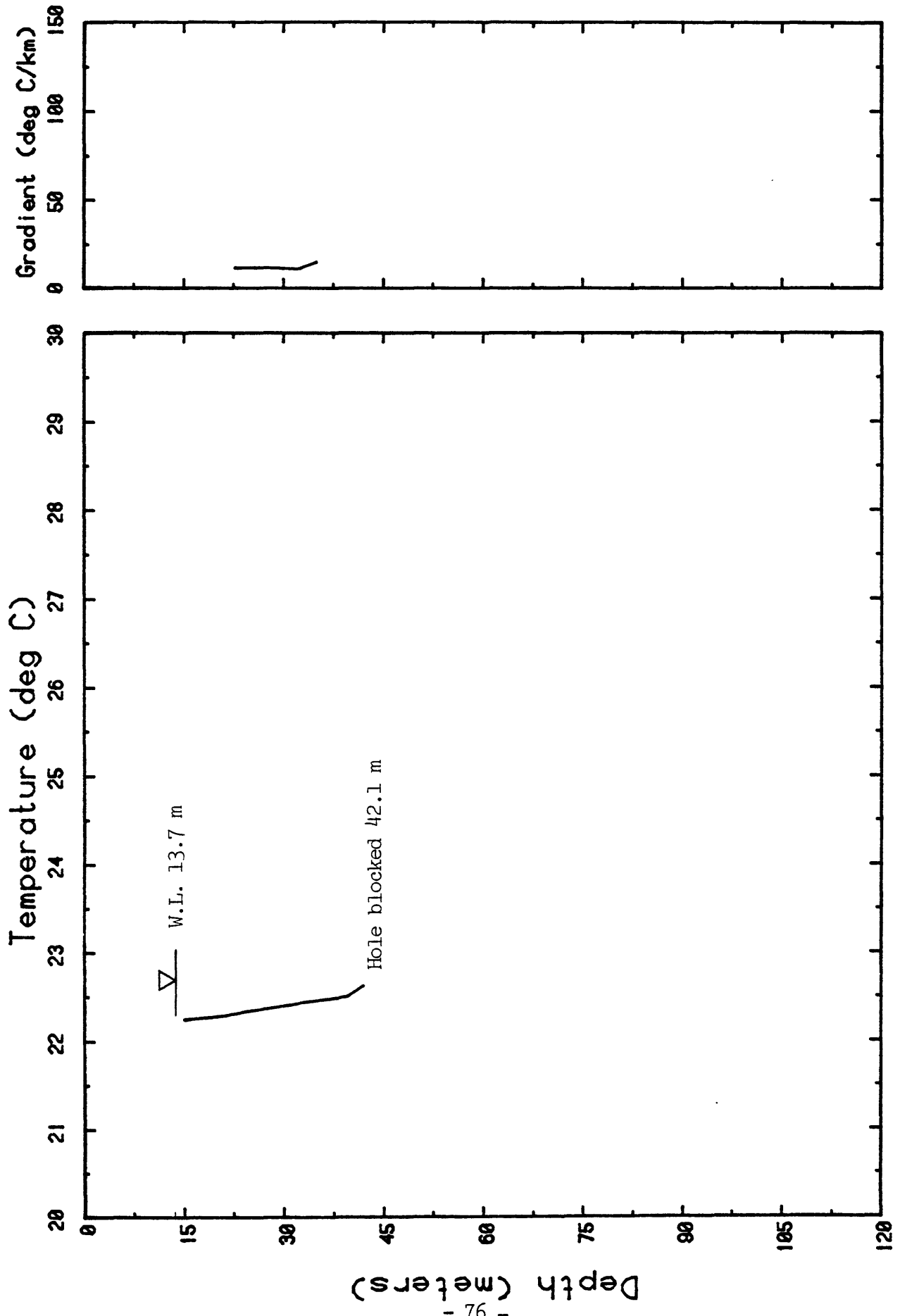
JD20 (WADI SIRHAN #1) AUG1883

Figure IIB-9

QJD20/AUG1983

Depth (m)	Temp. (°C)	Depth (m)	Temp. (°C)
15.24	22.24	18.28	22.26
21.33	22.29	24.38	22.33
27.43	22.37	30.48	22.40
33.52	22.44	36.57	22.47
39.62	22.50	42.06	22.62

Gradient (deg C/km)

Temperature (deg C)

Depth (meters)

W.L. 167.3 m

Log T.D. 248.4 m

marl with chalk and
chert interbeds
(units B4-5)
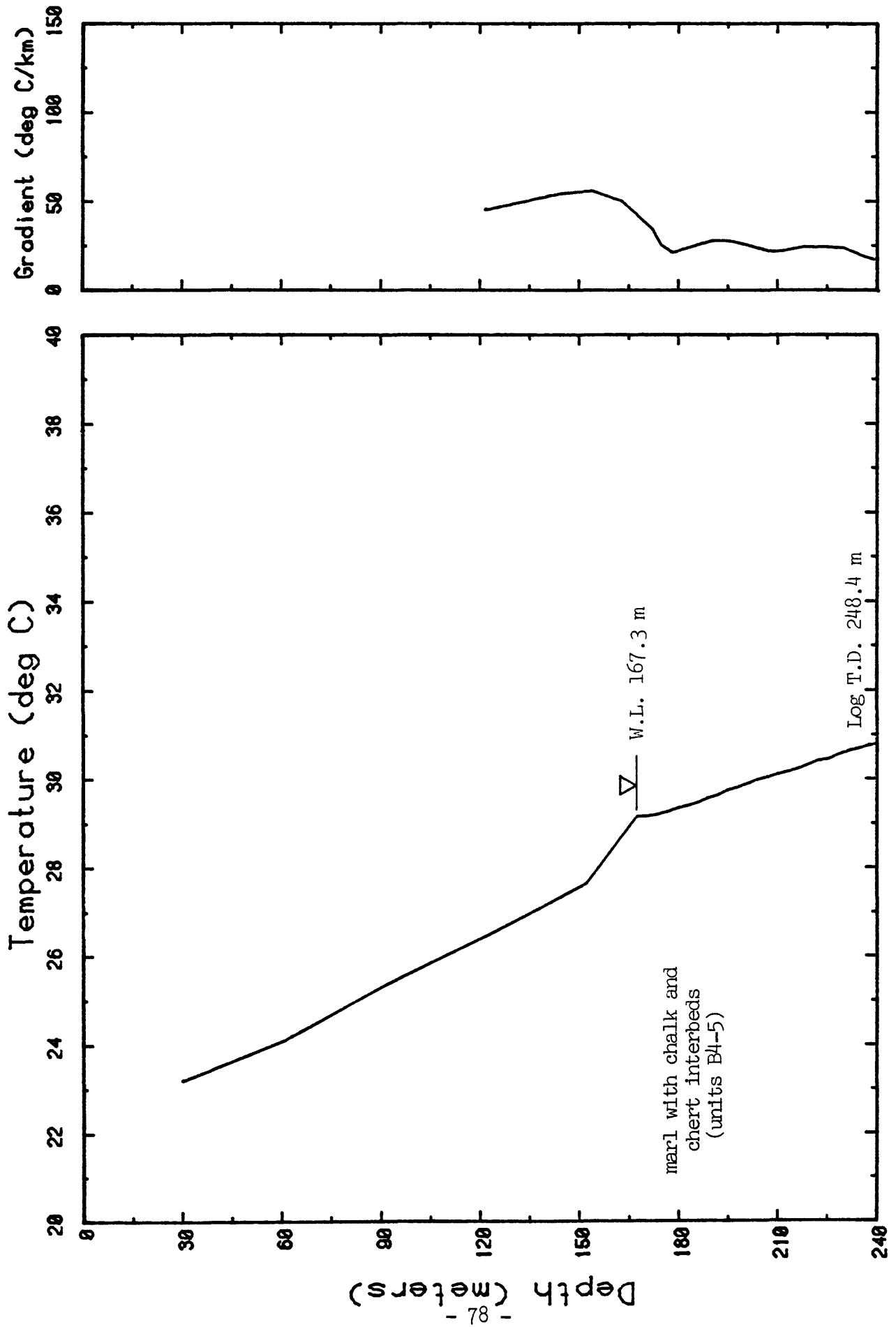
JD21 (WADI RUWEISHID #1) AUG1783

Figure IIB-10

TABLE IIB-10

Depth (m)	Temp. (°C)	Depth (m)	Temp. (°C)
30.48	23.2	60.96	24.10
91.44	25.34	121.92	26.46
137.16	27.04	152.4	27.64
167.64	29.15	170.69	29.16
173.73	29.19	176.78	29.27
179.83	29.34	182.88	29.40
185.92	29.47	188.97	29.57
192.02	29.64	195.07	29.75
198.12	29.82	201.16	29.90
204.21	29.98	207.26	30.05
210.31	30.11	213.36	30.17
216.40	30.24	219.45	30.33
222.50	30.41	225.55	30.45
228.6	30.56	231.64	30.62
234.69	30.69	237.74	30.75
240.79	30.8	243.84	30.84
246.88	30.88	248.41	30.96

Figure IIB-11

JD22 (SH-5) AUG2183

Temperature (deg C)

Gradient (deg C/km)

Depth (meters)

W.L. 108.2 m

Hole blocked 413.2 m

cherty marl, 0-204 m (units B4-5)

marl, 204-280 m (units B1-3)

limestone, 280-335 m (unit A7)

marl, limestone, and shale, 335-420 m (units A4-6)
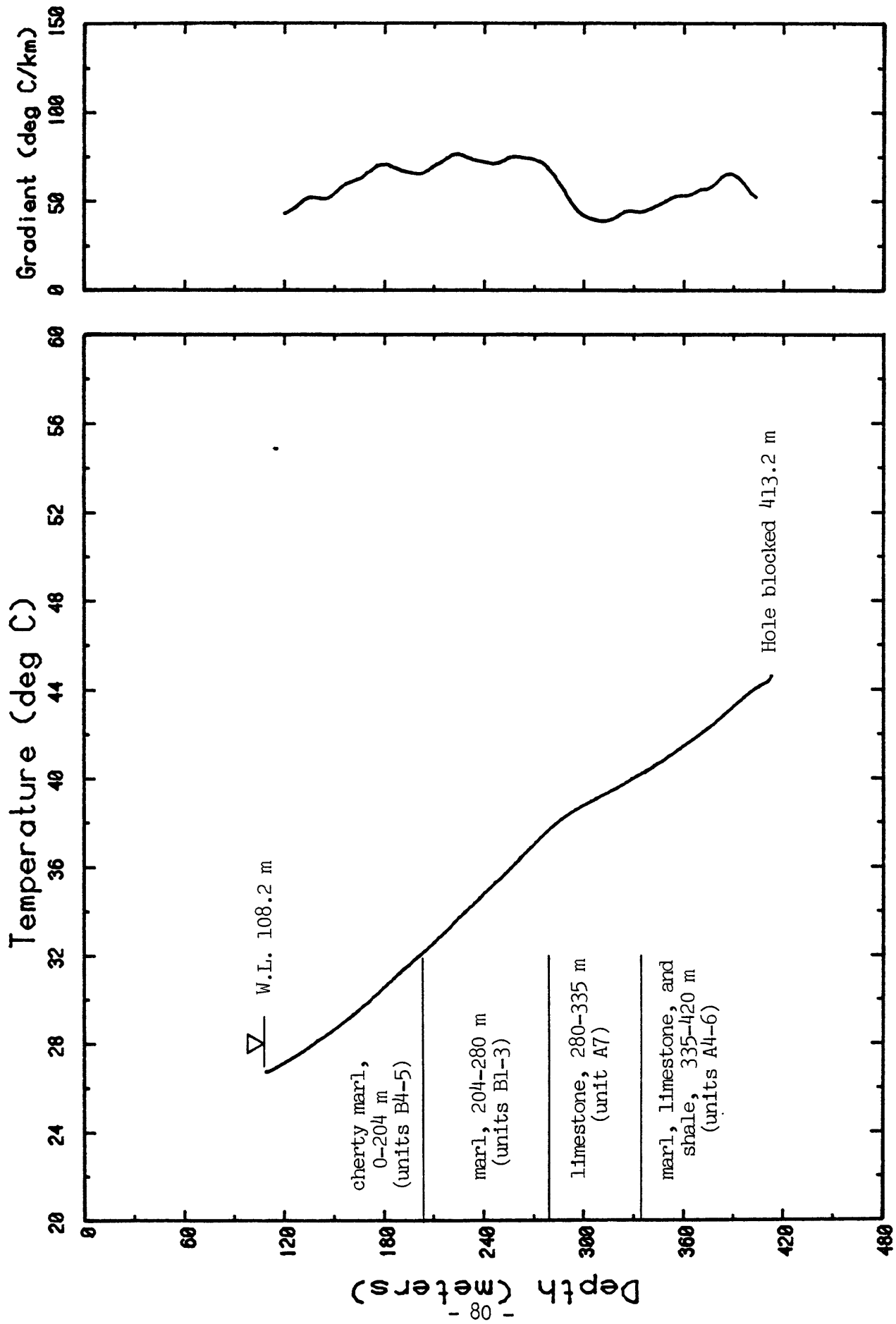
@JD22/AUG2193

Depth (m)	Temp. (°C)	Depth (m)	Temp. (°C)
109.72	26.75	112.77	26.83
115.82	26.94	118.87	27.08
121.92	27.22	124.96	27.36
128.01	27.48	131.06	27.64
134.11	27.80	137.16	27.96
140.20	28.13	143.25	28.27
146.30	28.42	149.35	28.58
152.4	28.76	155.44	28.92
158.49	29.11	161.54	29.32
164.59	29.47	167.64	29.69
170.68	29.85	173.73	30.11
176.78	30.28	179.83	30.53
182.88	30.73	185.92	30.95
188.97	31.16	192.02	31.36
195.07	31.55	198.12	31.77
201.16	31.96	204.21	32.14
207.26	32.35	210.31	32.56
213.36	32.80	216.40	33.01
219.45	33.20	222.50	33.48
225.55	33.72	228.6	33.93
231.64	34.17	234.69	34.38
237.74	34.61	240.79	34.83
243.84	35.04	246.88	35.28
249.93	35.46	252.98	35.70
256.03	35.93	259.08	36.16
262.12	36.40	265.17	36.61
268.22	36.84	271.27	37.08
274.32	37.29	277.36	37.50
280.41	37.74	283.46	37.91
286.51	38.11	289.56	38.28
292.60	38.45	295.65	38.57
298.70	38.71	301.75	38.82
304.8	38.96	307.84	39.07
310.89	39.19	313.94	39.31
316.99	39.43	320.04	39.55
323.08	39.67	326.13	39.82
329.18	39.96	332.23	40.10
335.28	40.22	338.32	40.35
341.37	40.50	344.42	40.65
347.47	40.78	350.52	40.94
353.56	41.10	356.61	41.27
359.66	41.44	362.71	41.59
365.76	41.75	368.80	41.92
371.85	42.10	374.90	42.29
377.95	42.42	381	42.62
384.04	42.82	387.09	43.03
390.14	43.24	393.19	43.42
396.24	43.63	399.28	43.79
402.33	43.97	405.38	44.11
408.43	44.26	411.48	44.37
413.18	44.59		
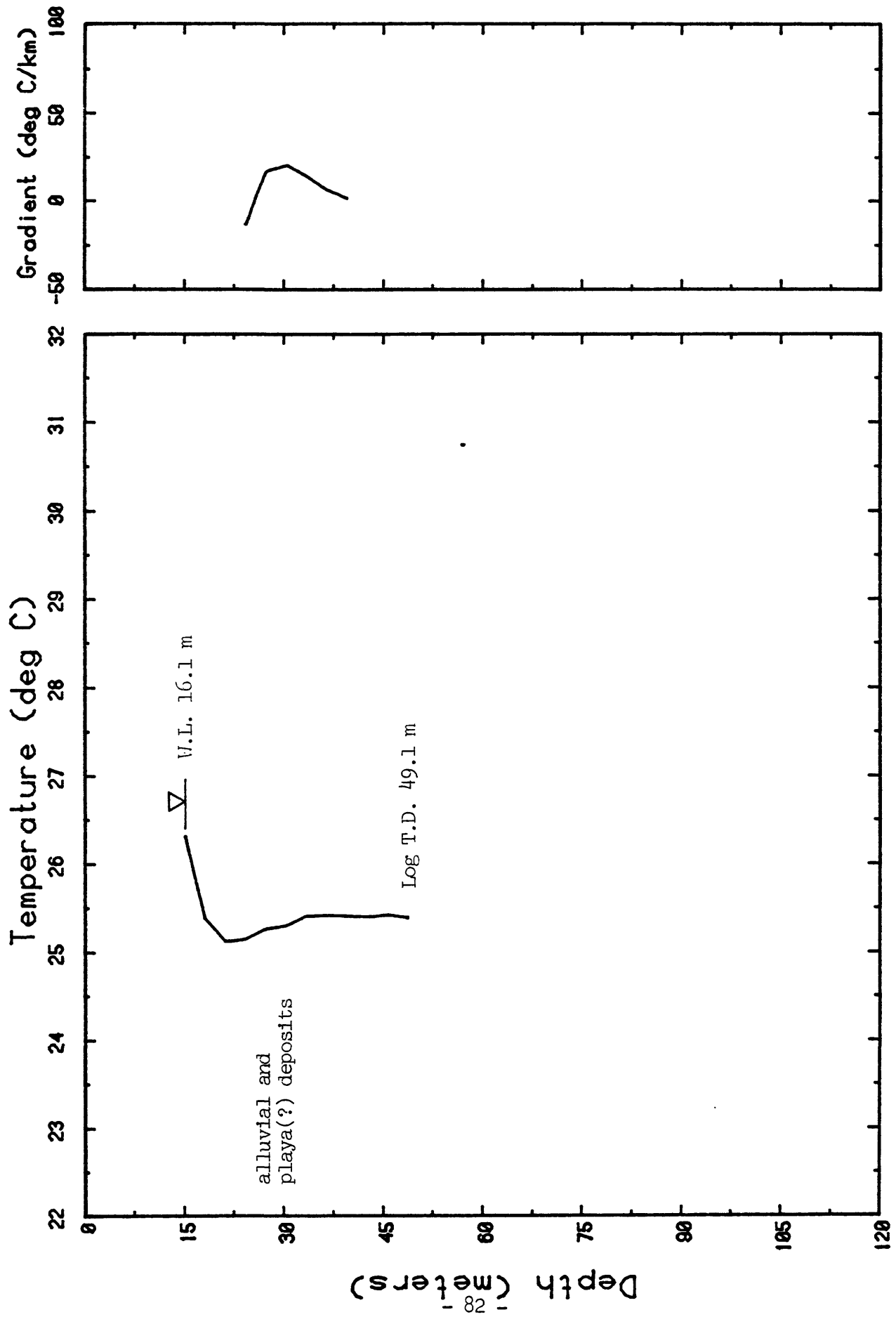
JD23 (ES SAFI WATER WELL) AUG2383

Figure IIB-12

TABLE IIB-12

@JD23/AUG2383

Depth (m)	Temp. (°C)	Depth (m)	Temp. (°C)
15.24	26.30	18.28	25.37
21.33	25.12	24.38	25.19
27.43	25.26	30.48	25.31
33.52	25.41	36.57	25.41
39.62	25.41	42.67	25.40
45.72	25.42	48.76	25.39

Gradient (deg C/km)

Temperature (deg C)

Depth (meters)

Alluvium, 0-20 m

dry hole

cherty marl, 20-200 m (units B4-5)

Hole blocked 201.2 m
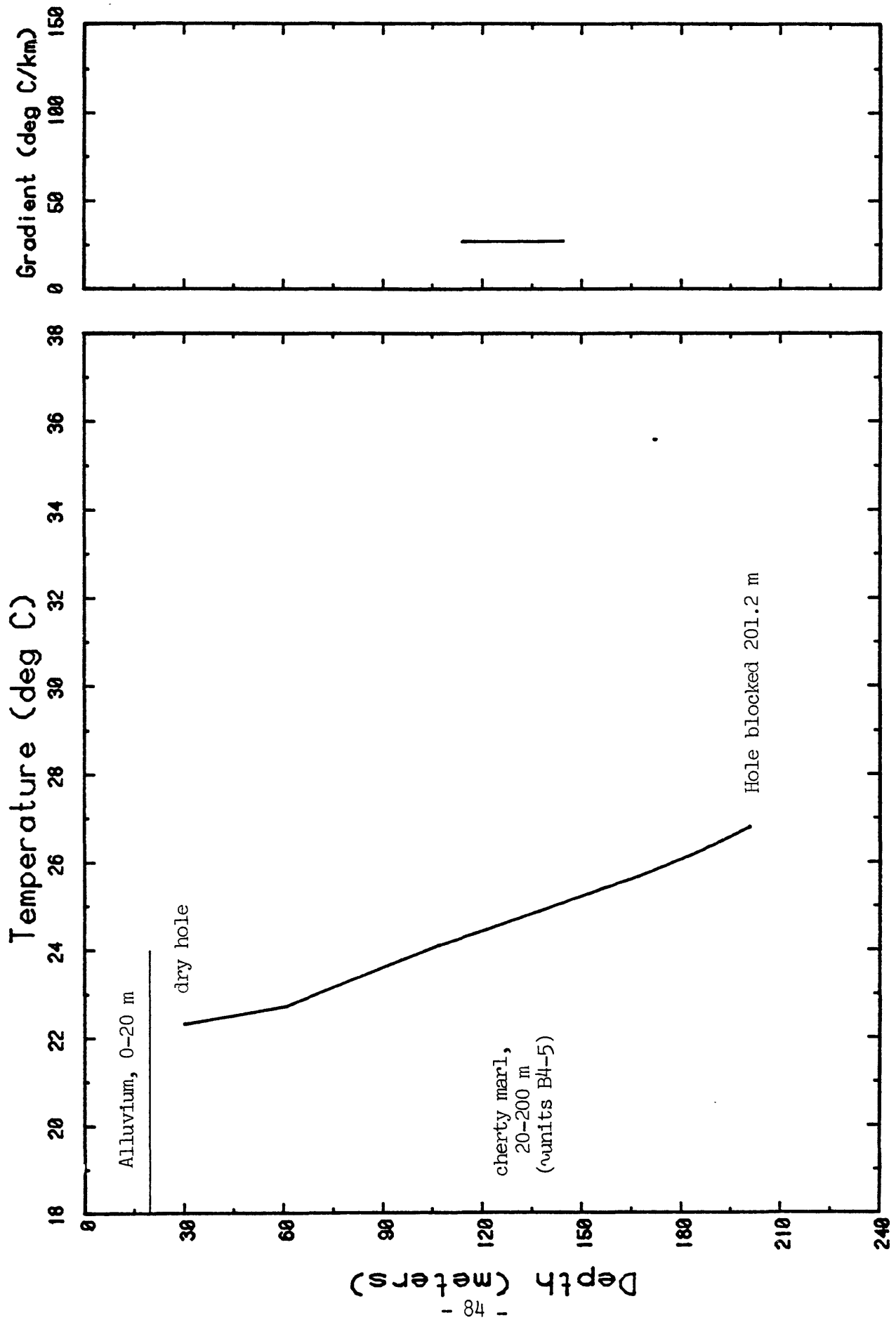
JD24 (MA'AN S-1) AUG25583

Figure IIB-13

TABLE IIB-13

@JD24/AUG2583

Depth (m)	Temp. (°C)	Depth (m)	Temp. (°C)
30.48	22.32	60.96	22.72
91.44	23.63	106.68	24.08
121.9	24.47	137.16	24.87
152.4	25.28	167.64	25.67
182.8	26.14	201.16	26.80

Gradient (deg C/km)

Temperature (deg C)

Depth (meters)

W.L. 17.7 m

log T.D. 66.4 m

playa deposits
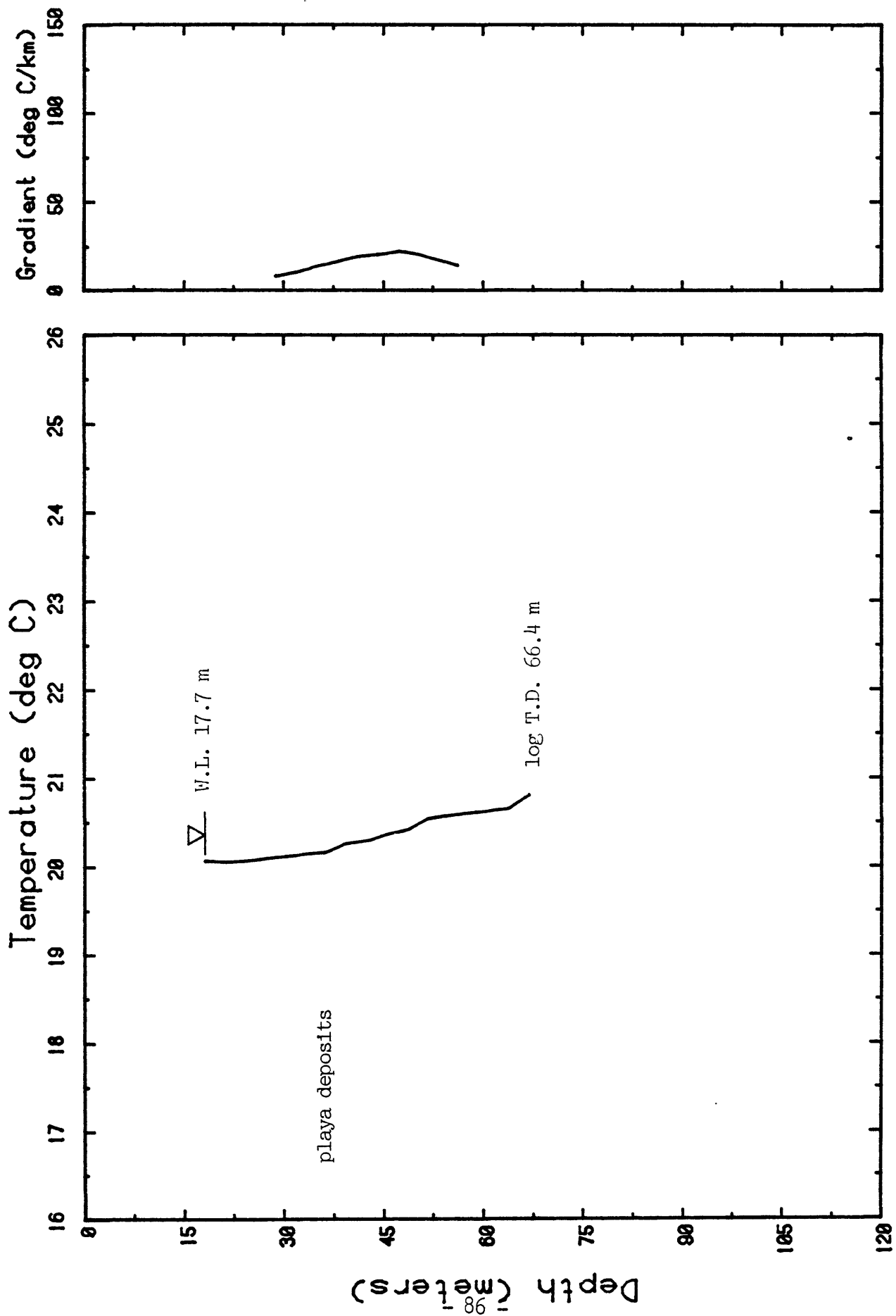
JD25 (EL JAFR #7) AUG2483

Figure IIB-14

TABLE IIB-14

@JD25/AUG2483

Depth (m)	Temp. (°C)	Depth (m)	Temp. (°C)
18.28	20.06	21.33	20.05
24.38	20.06	27.43	20.09
30.48	20.12	33.52	20.14
36.57	20.16	39.62	20.26
42.67	20.29	45.72	20.37
48.76	20.42	51.81	20.54
54.86	20.57	57.91	20.60
60.96	20.62	64.00	20.65
67.05	20.80		

Gradient (deg C/km)

Temperature (deg C)

Depth (meters)

dry hole

alluvium

log T.D. 96.5 m
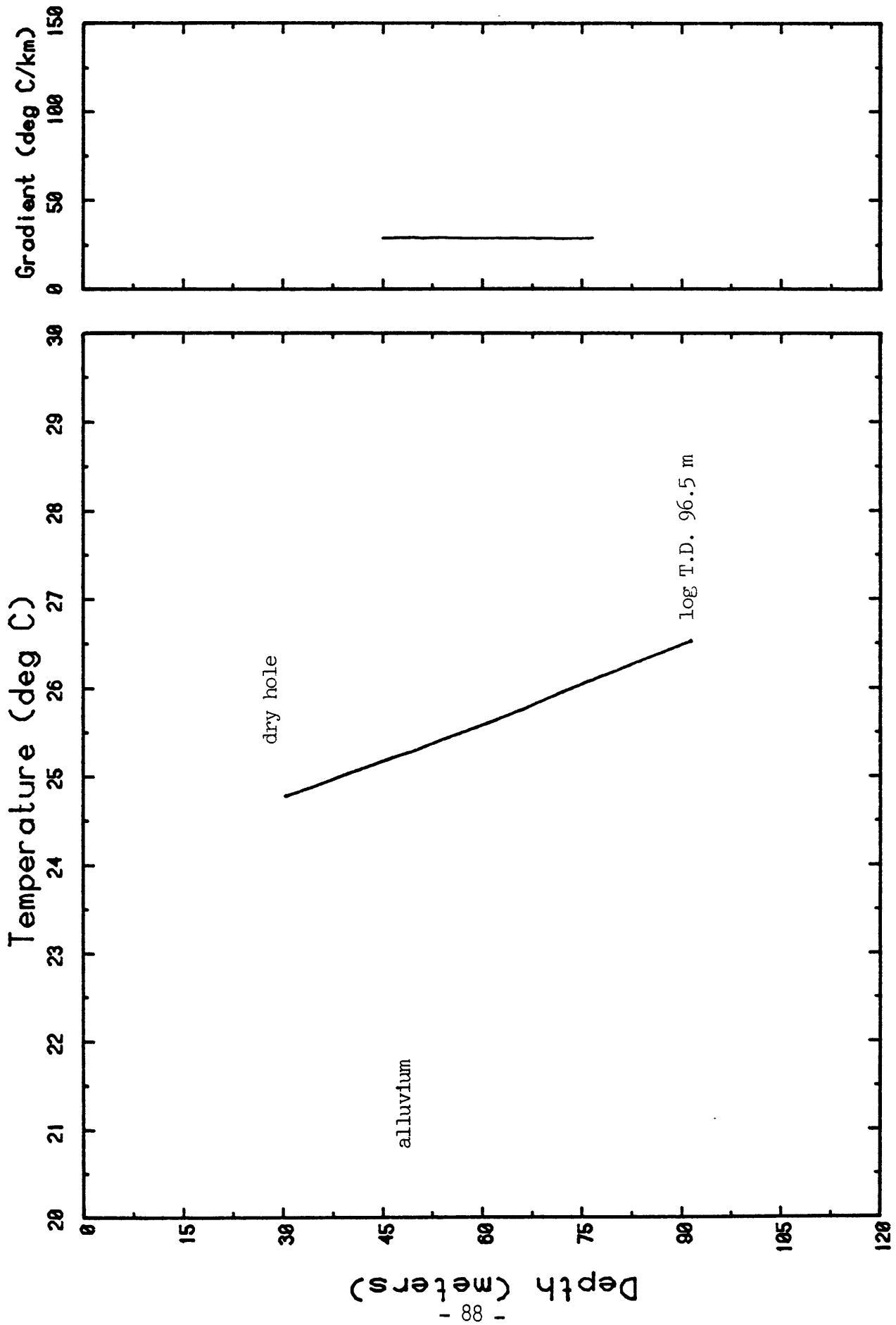
JD26 (WADI UTAM S-20) AUG2583

Figure IIB-15

⚙JD26/AUG2583

Depth (m)	Temp. (°C)	Depth (m)	Temp. (°C)
30.48	24.77	45.72	25.19
60.96	25.60	76.2	26.08
91.44	26.52		

APPENDIX III.   Topographic corrections for sites near Zerqa Ma'in

   Topography near Zerqa Ma'in is rugged, necessitating adjustment of the measured thermal gradients. Corrections were only made for sites with gradients unaffected by convective water flow (JD04, 05, 06, 08, and 09). The magnitude of each correction was assessed using a technique originally developed by Lees (1910) and later expanded by Jaeger and Sass (1963) for the effect of two-dimensional topography on thermal gradients. Corrections for each site are tabulated on the following pages. The correction factors are greatest at the surface and decrease with depth. Computer-generated topographic profiles show the model topography (solid line), actual topography (+'s), and hole location. The topographic sections were selected to maximize the two-dimensional topography. Two corrections were computed and combined for each of the three sites closest to the rift escarpment, one for close-in, and one for distant relief.

   The thermal gradients estimated at sites with convective discharge (JD01, 02, 03, and 07) were not corrected for topography because of the inherent uncertainty of the estimates. However, if corrections were made, they would lower the thermal gradients and thereby decrease the heat-flow estimate.

HOLE JD04   DEPTH 203 m   Alpha = 2.45   HT 300

BASE LEVEL = 87 m   COLLAR ELEV = 167 m

SCALE: 1 TIC MARK = 150 m   X OFFSET = 2800

GRADIENT = 77   LAPSE RATE= 5 deg C/km

West

East

JD04

Figure III-1a, close-in relief.

TABLE III-1a, Correction for close-in relief

JD04   DEPTH 203 m   alpha = 2.45   H: 300

BASE LEVEL = 87 m   COLLAR ELEV = 167 m

SCALE: 1 TIC MARK = 150 m   X OFFSET = 2800
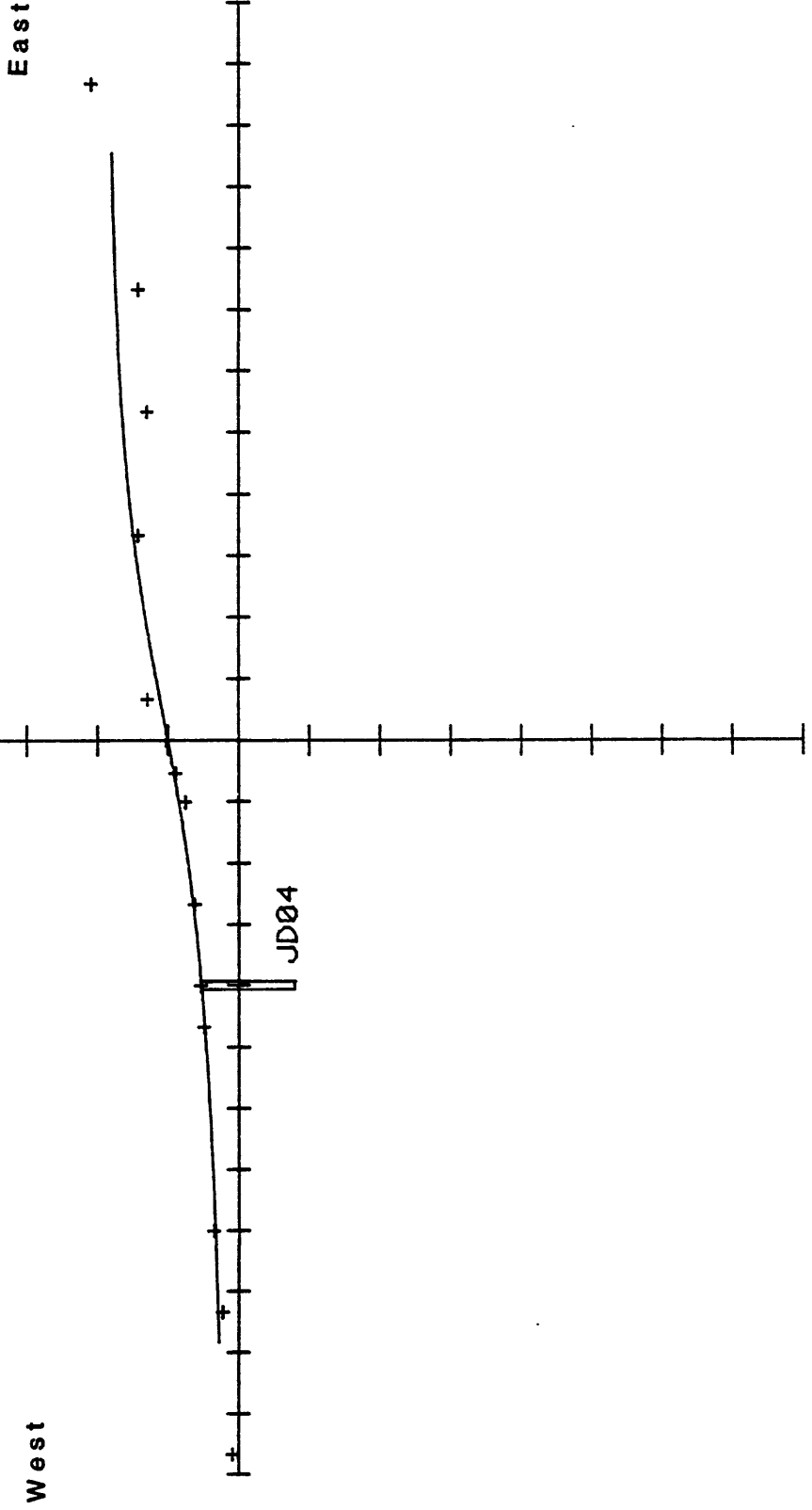
GRADIENT = 77   LAPSE RATE= 5 deg C/km

Depth,m   dG, DEG C/km

Depth,m	dG, DEG C/km
0	-5.22
10	-5.13
20	-5.05
30	-4.96
40	-4.88
50	-4.8
60	-4.72
70	-4.64
80	-4.57
90	-4.49
100	-4.42
110	-4.35
120	-4.28
130	-4.21
140	-4.14
150	-4.07
160	-4.01
170	-3.94
180	-3.88
190	-3.82
200	-3.76

HOLE JD04   DEPTH 203 m   Alpha = 1.1   HT 650

BASE LEVEL = -472.75 m   COLLAR ELEV = 167 m

SCALE: 1 TIC MARK = 325 m   X OFFSET = 700

GRADIENT = 77   LAPSE RATE= 5 deg C/km

West

East

JD04

Figure III-1b, Distant relief.

TABLE III-1b, Correction for distant relief

JD04   DEPTH 203 m   Alpha = 1.1   HT 650

BASE LEVEL = -472.75 m   COLLAR ELEV = 167 m

SCALE: 1 TIC MARK = 325 m   X OFFSET = 700
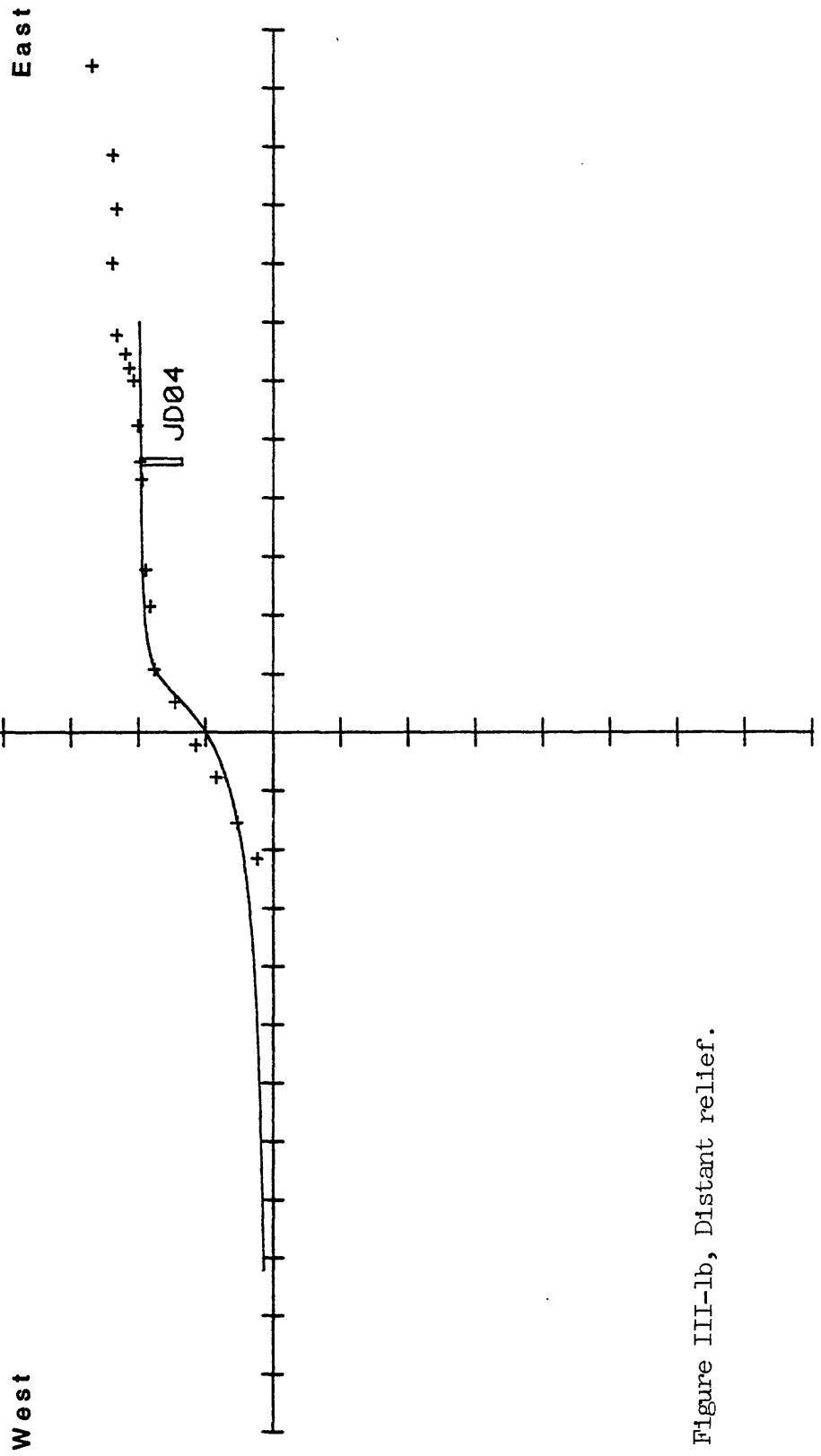
GRADIENT = 77   LAPSE RATE= 5 deg C/km

Depth,m	dG, DEG C/km
0	9.79
10	9.78
20	9.78
30	9.77
40	9.76
50	9.75
60	9.74
70	9.73
80	9.71
90	9.7
100	9.69
110	9.67
120	9.66
130	9.64
140	9.62
150	9.6
160	9.59
170	9.57
180	9.55
190	9.52
200	9.5

HOLE JD05   DEPTH 210 m   BETA = -3.55   HT 450

BASE LEVEL = 257 m   COLLAR ELEV = 260 m

SCALE: 1 TIC MARK = 225 m   X OFFSET = 2100

GRADIENT = 72.8   LAPSE RATE= 5 deg C/km
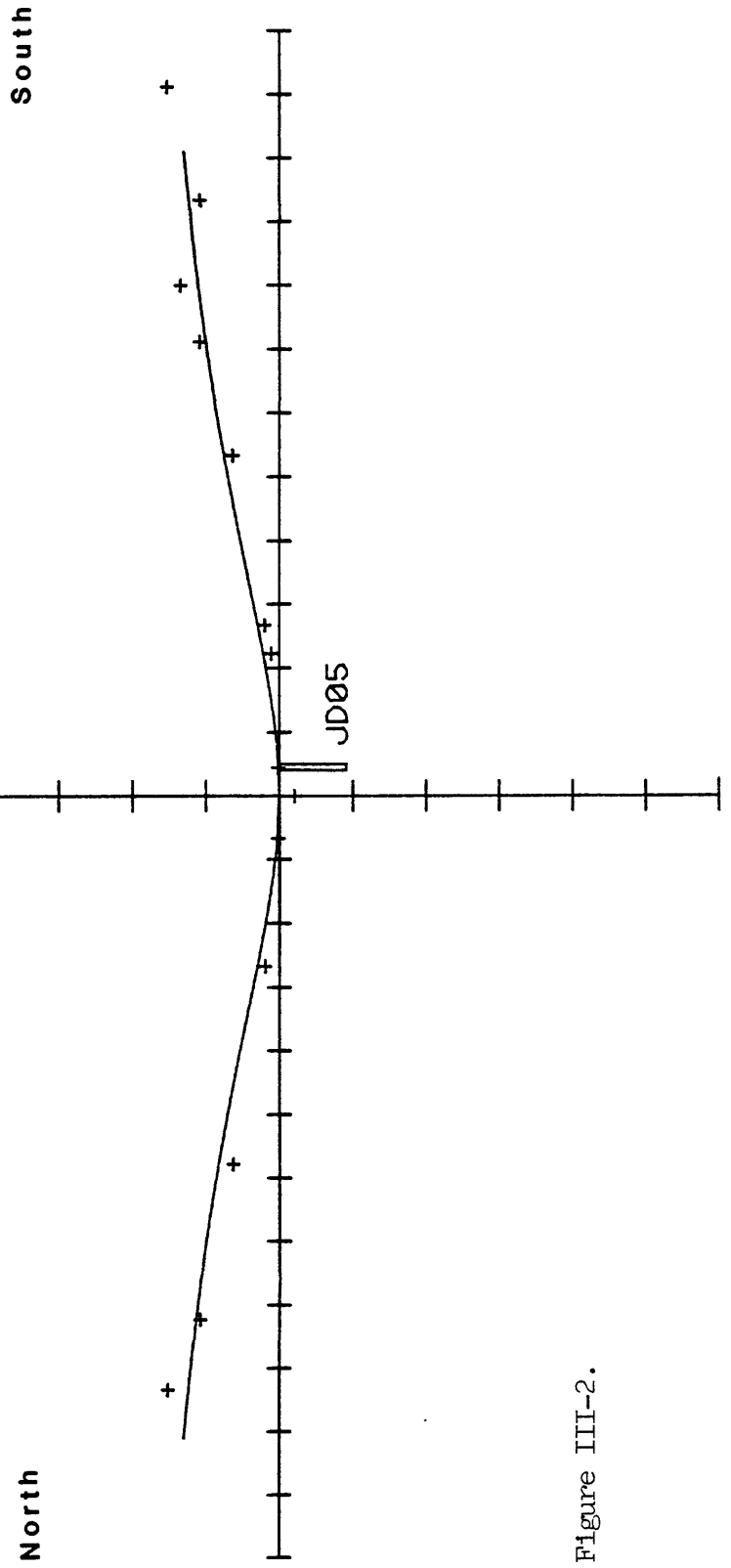
South

North

JD05

Figure III-2.

TABLE III-2.

JD05   DEPTH 210 m   BETA = -3.55   HT 450

BASE LEVEL = 257 m   COLLAR ELEV = 260 m

SCALE: 1 TIC MARK = 225 m   X OFFSET = 2100

GRADIENT = 72.8   LAPSE RATE= 5 deg C/km

Depth,m   dG, DEG C/km

```
0                       -18.57
10                      -18.35
20                      -18.13
30                      -17.91
40                      -17.7
50                      -17.49
60                      -17.28
70                      -17.08
80                      -16.88
90                      -16.69
100                     -16.5
110                     -16.31
120                     -16.12
130                     -15.94
140                     -15.76
150                     -15.59
160                     -15.41
170                     -15.24
180                     -15.08
190                     -14.91
200                     -14.75
210                     -14.59
```

HOLE JD06   DEPTH 155 m   BETA = -3   HT 800

BASE LEVEL = 180 m   COLLAR ELEV = 210 m

SCALE: 1 TIC MARK = 400 m   X OFFSET = 1900

GRADIENT = 88.6   LAPSE RATE= 5 deg C/km
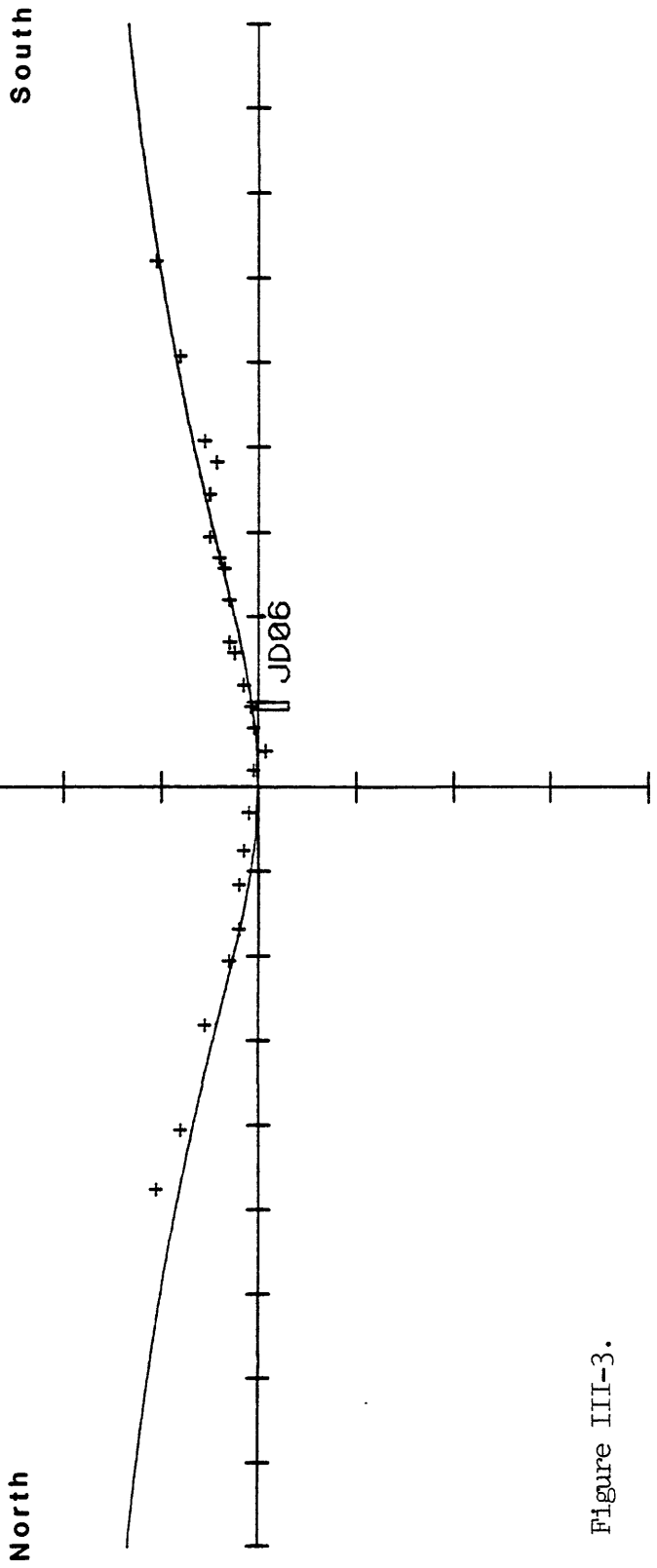
South

North

JD06

Figure III-3.

TABLE III-3.

JD06   DEPTH 155 m   BETA = -3   HT 800

BASE LEVEL = 180 m   COLLAR ELEV = 210 m

SCALE: 1 TIC MARK = 400 m   X OFFSET = 1900

GRADIENT = 88.6   LAPSE RATE= 5 deg C/km

Depth,m   dG, DEG C/km

Depth,m	dG, DEG C/km
0	-24.79
10	-24.61
20	-24.43
30	-24.25
40	-24.07
50	-23.89
60	-23.72
70	-23.54
80	-23.37
90	-23.2
100	-23.04
110	-22.87
120	-22.71
130	-22.54
140	-22.38
150	-22.22
160	-22.07

HOLE JD08   DEPTH 215 m   BETA = -1.45   HT 600

BASE LEVEL = -45 m   COLLAR ELEV = 230 m

SCALE: 1 TIC MARK = 300 m   X OFFSET = 1905

GRADIENT = 84.46   LAPSE RATE= 5 deg C/km

North

South

JD08

Figure III-4a, Close-in relief.

TABLE III-4a, Correction for close-in relief.

JD08   DEPTH 215 m   BETA = -1.45   HT 600

BASE LEVEL = -45 m   COLLAR ELEV = 230 m

SCALE: 1 TIC MARK = 300 m   X OFFSET = 1905
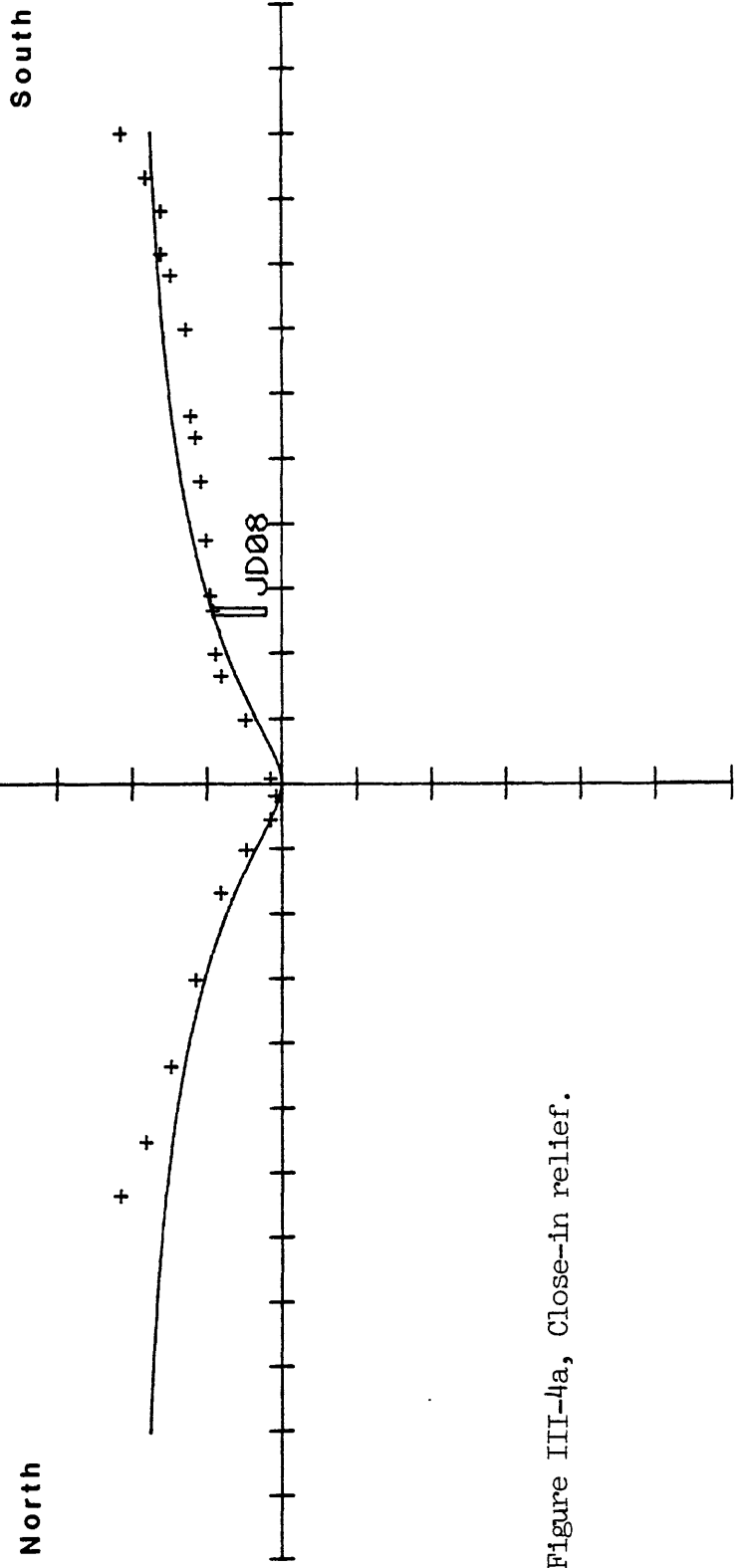
GRADIENT = 84.46   LAPSE RATE= 5 deg C/km

Depth,m	dG, DEG C/km
0	-8.79
10	-8.84
20	-8.88
30	-8.92
40	-8.95
50	-8.98
60	-9.01
70	-9.03
80	-9.05
90	-9.07
100	-9.08
110	-9.09
120	-9.1
130	-9.11
140	-9.11
150	-9.11
160	-9.11
170	-9.1
180	-9.1
190	-9.09
200	-9.08
210	-9.07
220	-9.06

HOLE JD08   DEPTH 215 m   Alpha = 1.65   HT 700

BASE LEVEL = -443.5 m   COLLAR ELEV = 230 m

SCALE: 1 TIC MARK = 350 m   X OFFSET = 1675

GRADIENT = 84.46   LAPSE RATE= 5 deg C/km
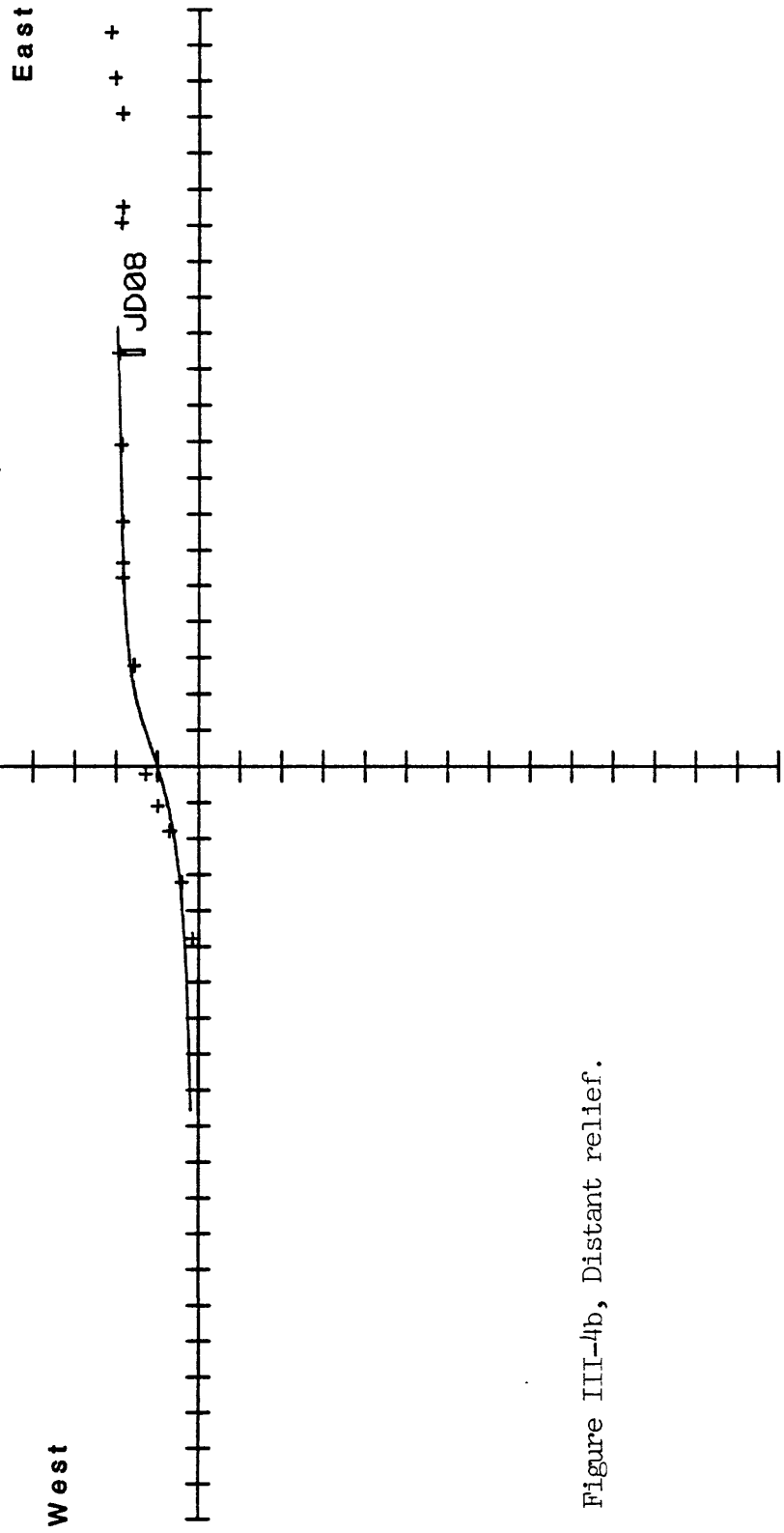
West

East

JD08

Figure III-4b, Distant relief.

TABLE III-4b, Correction for distant relief.

JD08   DEPTH 215 m   Alpha = 1.65   HT 700

BASE LEVEL = -443.5 m   COLLAR ELEV = 230 m

SCALE: 1 TIC MARK = 350 m   X OFFSET = 1675

GRADIENT = 84.46   LAPSE RATE= 5 deg C/km

Depth,m   dG, DEG C/km

Depth,m	dG, DEG C/km
0	4.33
10	4.33
20	4.33
30	4.32
40	4.32
50	4.32
60	4.32
70	4.31
80	4.31
90	4.31
100	4.3
110	4.3
120	4.3
130	4.3
140	4.29
150	4.29
160	4.29
170	4.29
180	4.29
190	4.28
200	4.27

HOLE JD09   DEPTH 217 m   BETA = -2.45   HT 800

BASE LEVEL = -8 m   COLLAR ELEV = 210 m

SCALE: 1 TIC MARK = 400 m   X OFFSET = 1530

GRADIENT = 94   LAPSE RATE= 5 deg C/km

South

North

JD09

Figure III-5a, Close-in relief.

TABLE III-5a, Correction for close-in relief.

JD09   DEPTH 217 m   BETA = -2.45   HT 800

BASE LEVEL = -8 m   COLLAR ELEV = 210 m

SCALE: 1 TIC MARK = 400 m   X OFFSET = 1530
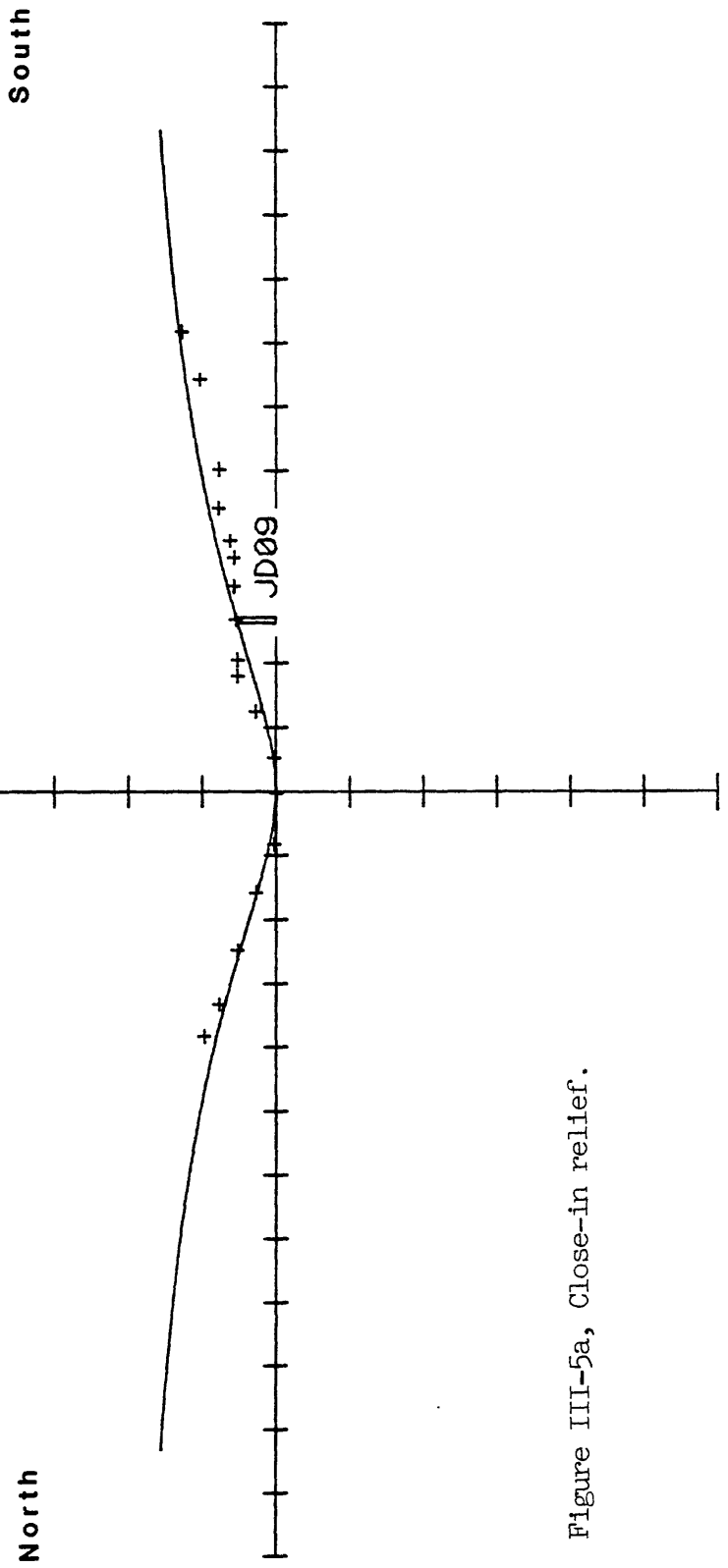
GRADIENT = 94   LAPSE RATE= 5 deg C/km

Depth,m	dG, DEG C/km
0	-14.33
10	-14.29
20	-14.25
30	-14.21
40	-14.17
50	-14.13
60	-14.09
70	-14.04
80	-14
90	-13.96
100	-13.92
110	-13.87
120	-13.83
130	-13.78
140	-13.74
150	-13.7
160	-13.65
170	-13.61
180	-13.56
190	-13.52
200	-13.47
210	-13.42
220	-13.38

HOLE JD09   DEPTH 217 m   Alpha = 1.65   HT 690

BASE LEVEL = -446 m   COLLAR ELEV = 210 m

SCALE: 1 TIC MARK = 345 m   X OFFSET = 1675

GRADIENT = 94   LAPSE RATE= 5 deg C/km
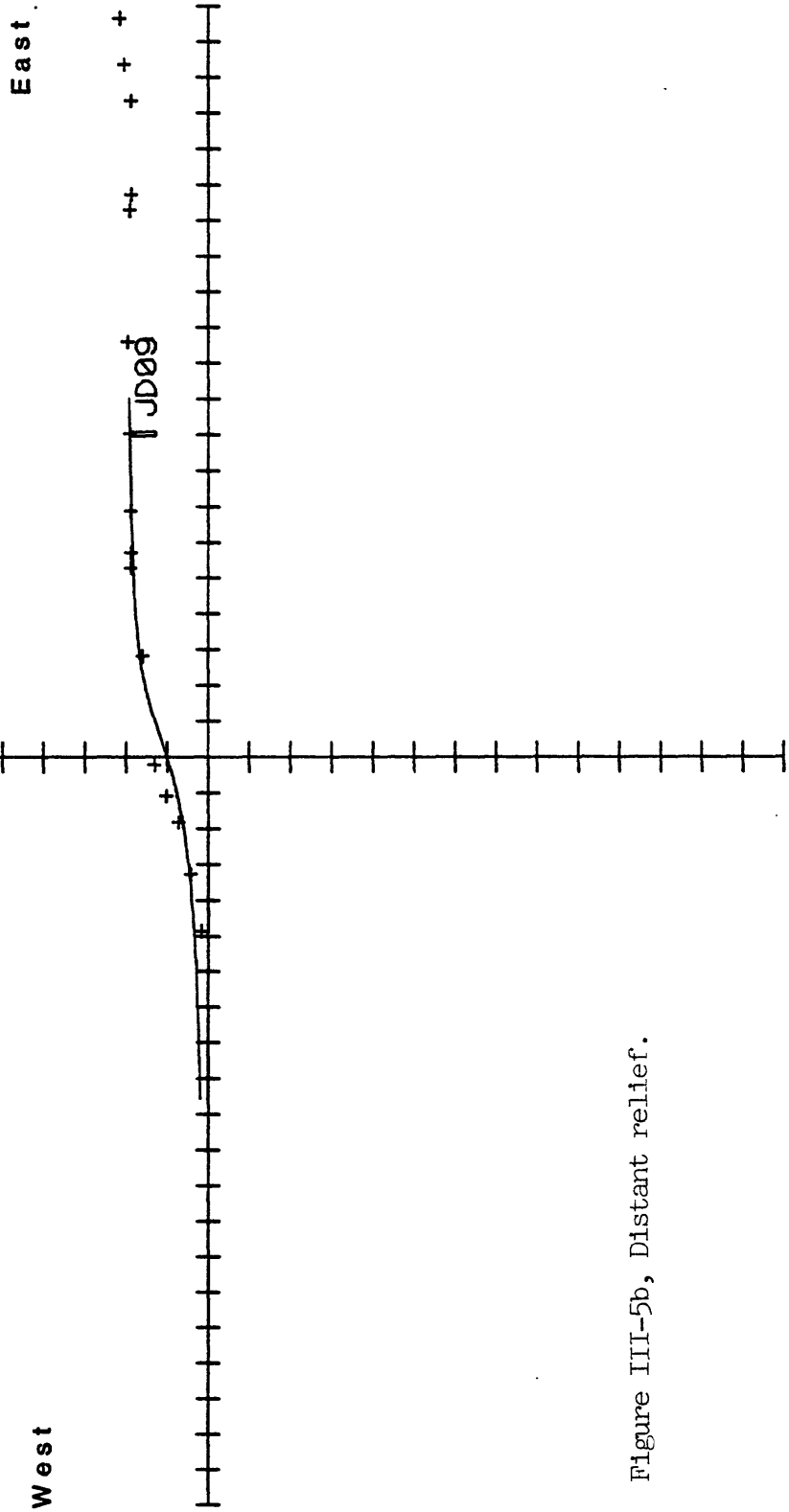
West

East

JD09

Figure III-5b, Distant relief.

TABLE III-5b, Correction for distant relief.

JD09 DEPTH 217 m Alpha = 1.65 HT 690

BASE LEVEL = -446 m COLLAR ELEV = 210 m

SCALE: 1 TIC MARK = 345 m X OFFSET = 1675

GRADIENT = 94 LAPSE RATE= 5 deg C/km

Depth,m dG, DEG C/km

Depth,m	dG, DEG C/km
0	6.17
10	6.17
20	6.16
30	6.15
40	6.15
50	6.14
60	6.13
70	6.13
80	6.12
90	6.11
100	6.11
110	6.1
120	6.09
130	6.08
140	6.08
150	6.07
160	6.06
170	6.05
180	6.04
190	6.04
200	6.03

APPENDIX IV. Tabulations of solid-grain thermal conductivity of drill cuttings

from boreholes at Zerqa Ma'in and Zara (Table IVA)

and other areas of Jordan (Table IVB)

TABLE IVA. Summary of grain thermal conductivities for 7 boreholes near the Zerqa Ma'in and Zara Geothermal Areas, Jordan

Borehole	Depth interval m	K_s mcal cm^{-1} sec^{-1} °C^{-1}	W m^{-1} K^{-1}
JD04	20-25	14.96	6.26
	40-45	13.63	5.70
	60-65	16.53	6.92
	80-85	14.66	6.14
	100-105	17.61	7.37
	120-125	16.87	7.06
	140-145	12.44	5.21
	160-165	12.58	5.27
	165-170	10.09	4.22
	170-175	6.11	2.56
	175-180	8.55	3.58
	180-185	9.82	4.11
	185-190	7.02	2.94
	190-195	8.67	3.63
	195-200	7.23	3.02
	200-205	8.50	3.56
	220-225	13.13	5.50
JD05	55-60	6.38	2.67
	90-95	8.28	3.46
	155-160	4.69	1.96
	160-165	4.22	1.76
	165-170	4.39	1.84
	170-175	4.10	1.72
	175-180	4.56	1.91
	180-185	4.78	2.00
	185-190	3.87	1.62
	190-195	4.41	1.85
	195-200	4.07	1.70
	200-205	4.14	1.74
	205-210	4.13	1.73
	215-220	4.31	1.80
JD06	65-70	6.27	2.63
	75-80	5.75	2.41
	85-90	5.44	2.28
	95-100	5.44	2.28
	100-105	4.28	1.79
	110-115	3.94	1.65
	120-125	5.35	2.24
	130-135	6.27	2.62
	140-145	4.84	2.03
	150-155	5.10	2.13

TABLE IVA. Summary of grain thermal conductivities for 7 boreholes
near the Zerqa Ma'in and Zara Geothermal Areas, Jordan (continued)

Borehole	Depth interval m	K_s	
		$mcal\ cm^{-1}\ sec^{-1}\ °C^{-1}$	$W\ m^{-1}\ K^{-1}$
JD08	60-70	5.66	2.37
	80-90	4.65	1.95
	100-110	6.61	2.77
	120-130	5.73	2.40
	140-150	8.08	3.38
	160-170	5.40	2.26
	170-180	5.84	2.45
	190-200	7.02	2.94
	200-210	6.23	2.61
	210-220	4.68	1.96
JD09	30-35	4.59	1.92
	45-50	4.75	1.99
	60-65	4.40	1.84
	75-80	4.40	1.84
	90-95	4.04	1.69
	105-110	5.81	2.43
	120-125	7.01	2.93
	135-140	4.67	1.96
JD10	A*	6.18	2.59
	B	6.72	2.81
	C	6.52	2.73
	D	5.26	2.20
	E	5.91	2.47
JD11	A*	6.22	2.60
	B	6.31	2.64
	C	6.50	2.72
	D	6.56	2.75
	E	6.25	2.62

*Drill cuttings of unknown depth (collected from drilling-waste
piles at borehole).

TABLE IVB. Summary of grain thermal conductivities for 4 boreholes in Jordan

Borehole	Sample*	K_s	
		mcal cm^{-1} sec^{-1} °C^{-1}	W m^{-1} K^{-1}
JD14	A	5.02	2.10
	B	6.68	2.80
	C	6.03	2.52
	D	4.89	2.05
	E	7.16	3.00
	F	6.16	2.58
	G	5.44	2.28
JD16	A	6.39	2.68
	B	6.24	2.61
	C	6.11	2.56
	D	5.92	2.48
	E	6.28	2.63
	F	6.15	2.57
	G	6.23	2.61
JD21	A	6.45	2.70
	B	6.27	2.62
	C	7.11	2.98
	D	7.48	3.13
	E	6.66	2.79
JD26	A	7.43	3.11
	B	7.15	2.99
	C	7.82	3.28

*Drill cuttings of unknown depth (collected from
   drilling-waste piles at borehole).